NASA Contractor Report 2828

Thermal Design for Areas of Interference Heating On Actively Cooled Hypersonic Aircraft

R. L. Herring and J. E. Stone

CONTRACT NAS1-14140
JANUARY 1978

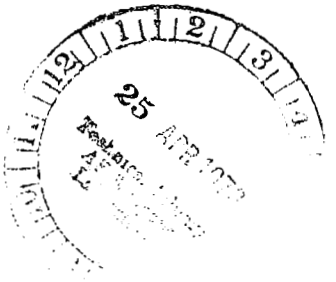

NASA

NASA Contractor Report 2828

Thermal Design for Areas of Interference Heating On Actively Cooled Hypersonic Aircraft

R. L. Herring and J. E. Stone
McDonnell Douglas Corporation
St. Louis, Missouri

Prepared for
Langley Research Center
under Contract NAS1-14140

NASA
National Aeronautics
and Space Administration

**Scientific and Technical
Information Office**

1978

FOREWORD

The overall objective of this study was to select, from numerous design alternatives, actively cooled panel design concepts for application in regions on high speed aircraft that are subject to interference heating effects. The study was conducted in accordance with the requirements and instructions of NASA RFP 1-15-5625 and McDonnell Technical Proposal Report MDC A3499 with minor revisions mutually agreed upon by NASA and MCAIR. The study was conducted using customary units for the principal measurements and calculations. Results were converted to the International System of Units (S.I.) for the final report.

Mr. Ralph L. Herring was the MCAIR Program Manager with Mr. James E. Stone as Principal Investigator. Overall management was provided by Mr. John W. Anderson, Chief Technology Engineer - Thermodynamics. Assistance was provided by Mr. Leland C. Koch and Mr. David W. Peterson.

TABLE OF CONTENTS

LIST OF FIGURES

LIST OF FIGURES (Continued)

LIST OF FIGURES (Continued)

LIST OF FIGURES (Continued)

LIST OF FIGURES (Continued)

LIST OF ABBREVIATIONS AND SYMBOLS

ABBREVIATIONS

ACPOP	Mechanical stress computer program
ACS	Active cooling system
CASD	Finite element, structural design computer program
KBDR	General heat transfer computer program
KBEB	Thermal stress computer program
NDE	Nondestructive evaluation
TPS	Thermal Protection System

SYMBOLS

B	Thermal model dimensional constant
b	Length of loaded panel edge
Btu	British thermal unit
C	Correlating constant in heat transfer equations, Dimensional constant in mass correlations
D	Diameter, Panel bending stiffness
e	Mean roughness projection
E	Young's modulus of elasticity
E'	Effective modulus of elasticity
F	Allowable stress, Mass weighing factor
f	Friction factor
°F	Degrees Fahrenheit
ft	Feet
G	Grade
H	Height
h	Heat transfer coefficient
HP	Horsepower
hr	Hour
in	Inch
K	Panel buckling constant
k	Thermal conductivity
L	Length

SYMBOLS

lbf	Pounds force
lbm	Pounds mass
M	Mass
$\dot{m}$	Coolant flow rate per panel
N	Load per unit width
NM	Nautical Mile
Nu	Nusselt number
P	Pressure
p	Pitch
PR	Prandtl number
$\dot{Q}$	Integrated heating rate
$\dot{q}$	Heating rate per unit area
R	Stress ratio (min. tension stress/max. tension stress)
Re	Reynolds number
S	Honeycomb core size (diameter of inscribed circle)
s, sec	Second
St	Stanton number
t	Thickness
V	Velocity
W	Width
Wt	Mass
Y	Twist ratio (inside diameters per 180° tape twist)

GREEK SYMBOLS

Δ	Difference
δ	Initial deflection
ψ	Stress
Θ	Angle
μ	Viscosity, Poisson's ratio
ρ	Density
ϕ	Dimensionless ratio

S.I. UNITS

g	Gram
K	Kelvin
m	Meter
N	Newton
Pa	Pascal
W	Watt

S.I. PREFIXES

c	Centi (10^{-2})
k	Kilo (10^{3})
m	Milli (10^{-3})
M	Mega (10^{6})

SUBSCRIPTS

avg	Average
b	Bond, Bulk, Baseline
c	Core
C,L	Coolant in distribution lines
c,p	Coolant in panel
comp.	Compression
cr	Critical
H-X	Heat exchanger
i	Inner, Initial
I/M	Inspectability and Maintainability
L	Laminar
o	Due to normal load only
P	Producibility
pp	Pumping power
R	Reservoir, Reliability
s	Skin
so	Outer skin

SUBSCRIPTS

si	Inner skin
s,m	Skin, midway between tubes
s,t	Skin, above tube
T	Turbulent
t	Tube
W	Mass
w	Face sheet wrinkling, Wall

1. SUMMARY

Actively cooled panel concepts, configured specifically for use in regions on high speed aircraft which are subject to interference heating effects, have been identified. Figure 1 indicates the many potential design solutions, each compatible with an aircraft actively cooled structural arrangement, that were considered. Each of these structural and cooling system design alternatives offered potentially favorable characteristics for certain design heating conditions.

A wide range of design heating conditions was considered. Uniform surface heating rates ($\dot{q}$ uniform), over the entire panel, of up to 113.5 kW/m^2 (10 $Btu/sec\ ft^2$) were considered. Local heating rate increases ($\dot{q}$ peak/$\dot{q}$ uniform), attributable to interference heating effects on a portion of the panel surface, up to a factor of 5 were examined.

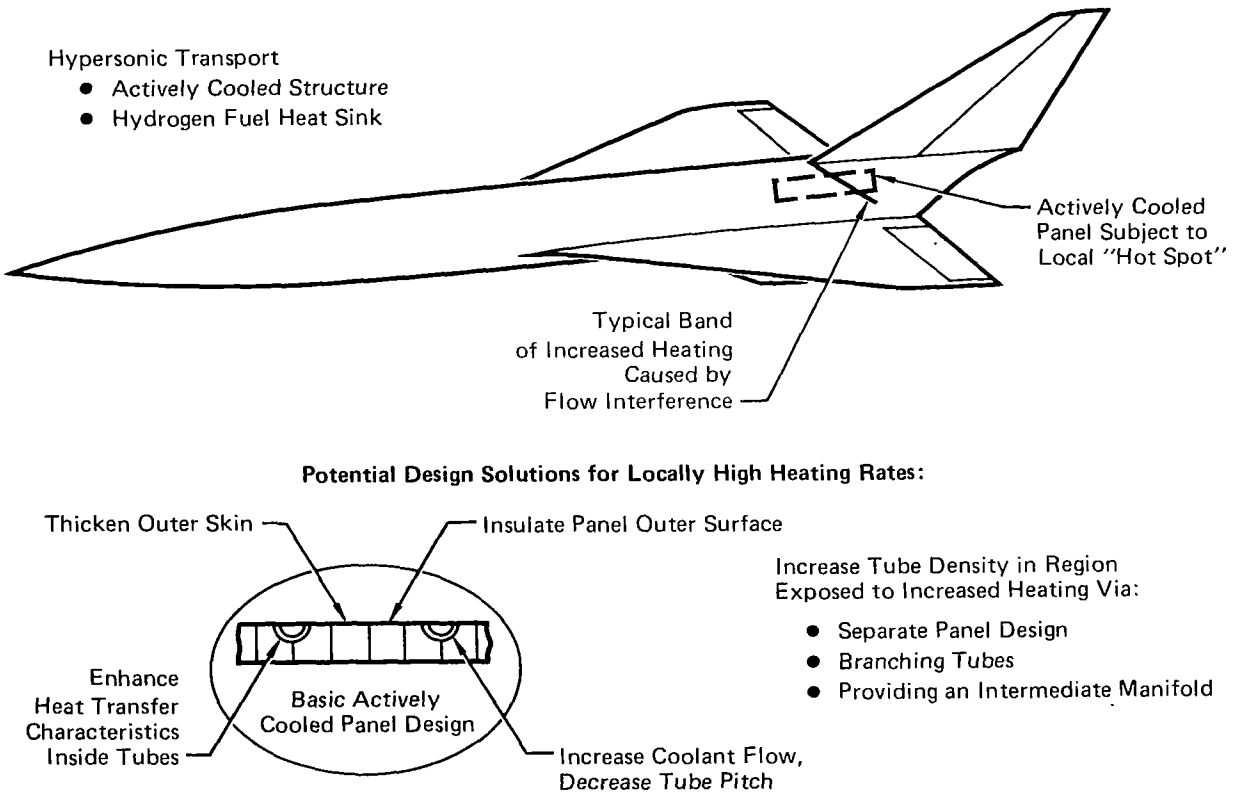

FIGURE 1
ACTIVELY COOLED PANEL DESIGN ALTERNATIVES

The design alternatives were compared using four figures of merit: mass, producibility, reliability and inspectability/maintainability. It was concluded that three design approaches were superior over various portions of the matrix of potential design conditions. Figure 2 identifies the regime of applicability established for the three selected design concepts.

For regions that experience mild uniform surface heating and minor interference heating effects, it is not necessary to significantly alter the basic cooled panel design approach. These design conditions are best satisfied by providing slight modifications to the basic design that is optimized for uniform heating such as reducing the coolant tube spacing and/or increasing the coolant flow. A Modified Baseline Panel Concept, suitable for this application, is defined.

Under moderate design heating rate conditions, a Finned Tube Concept is recommended. The only significant difference between this concept and the basic cooled panel design is that the coolant tubes are internally finned. The internal heat transfer enhancement afforded by these tubes helps minimize the mass chargeable to the panel. As indicated in Figure 2, this design approach is attractive over a broad band of potential design heating conditions.

At very high uniform heating rates and/or peak heating rates, an Insulated Panel Concept is required. This configuration uses a thermal protection system (TPS), consisting of a metallic shingle and insulation, over the basic cooled panel. Other studies found that insulated systems are necessary, to some extent, to reduce the absorbed heat load to a level compatible with the available fuel heat sink. This design aspect was not considered in establishing the regime of applicability shown in Figure 2.

Panel design was found to be primarily influenced by the peak heating rate experienced. The specific location of the interference heating pattern on the panel surface was not a driving factor. In addition, it was concluded that a three dimensional heating pattern did not impose a significant problem to panels already configured for two dimensional interference heating.

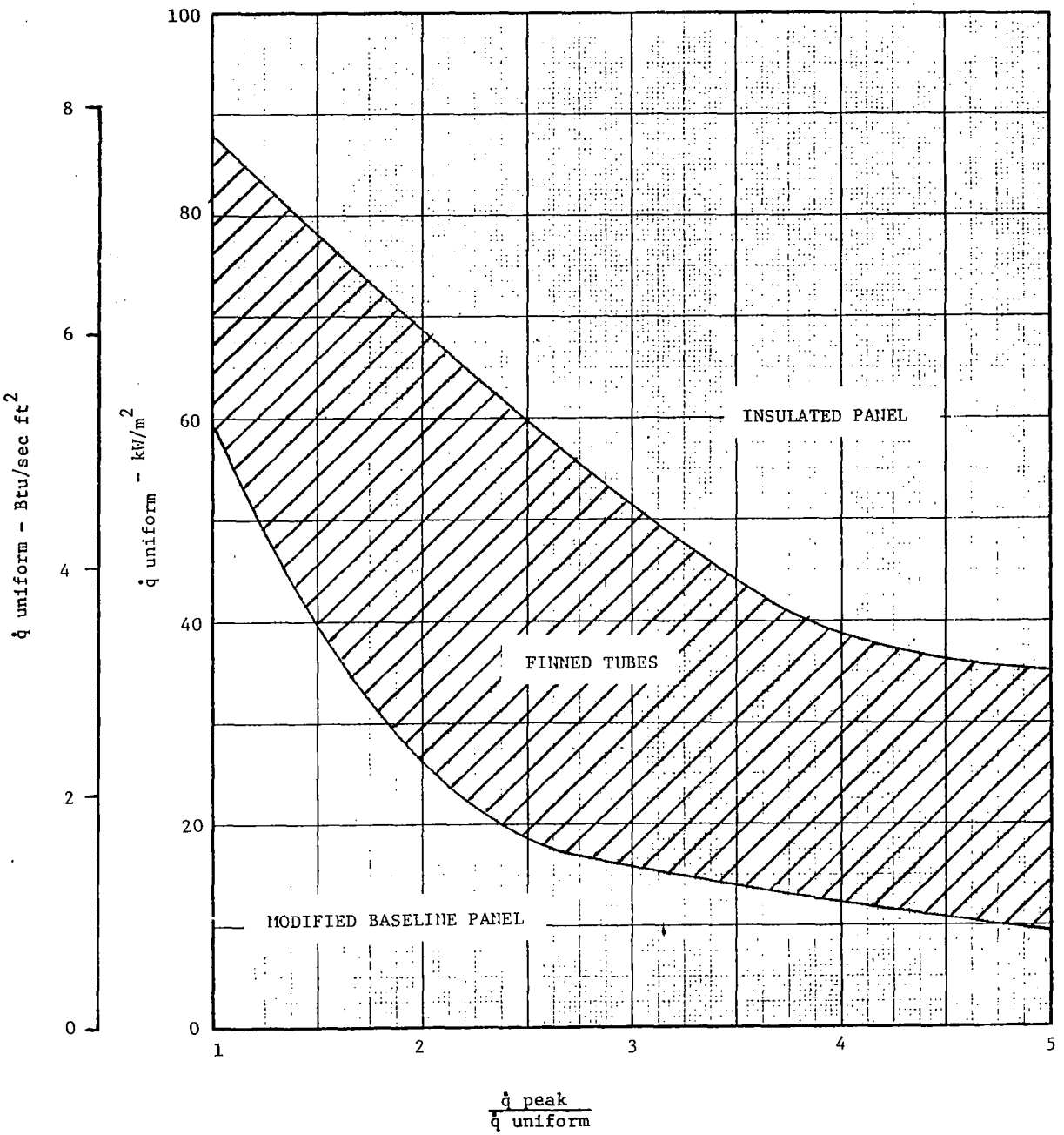

FIGURE 2
DESIGN RECOMMENDATIONS

2. INTRODUCTION

Aerodynamic heating encountered during high speed flight imposes design complexities, and in the local regions of the aircraft subject to interference heating these complexities are compounded. While the exact nature of interference heating in hypersonic flight is not firmly established, numerous conditions can result that cause order of magnitude increases in local surface aerodynamic heating rates. These include the intersection of a shock wave (e.g., induced by a protuberance) with a downstream flow field, convergence of boundary layers in corners, and reattachment of a separated boundary layer.

This study is a step in the evolution of actively cooled structure for high speed aircraft. Past investigations acknowledged the potential advantages of cooled structure and addressed specific considerations requiring resolution of feasibility. Studies, such as Reference 1, provided an understanding of the airframe heat loads associated with hypersonic transports and provided insight into active cooling system design. Another study, Reference 2, demonstrated that such systems can incorporate fail-safe provisions to provide abort mode operation in case of cooling system failure. In addition, studies are currently being conducted in which test specimens of various actively cooled structural concepts are being fabricated and tested. These studies are discussed in Reference 3.

The intent of the study reported herein was to identify the effect of interference heating on actively cooled panel design. The following study objectives were established:

- Define cooled panel conceptual designs for application in regions subject to large local increases in surface heating rate.
- Evaluate these concepts and compare their design requirements with those cooled panels designed for exposure to uniform surface heating.
- Select panel designs for three specific interference heating conditions. These conditions considered a uniform surface heating rate ($\dot{q}_{uniform}$) over the entire panel and a band of increased heating, caused by local flow disturbance effects, superimposed over the uniform heating level near one end of the panel. These increased heating bands reflected bell-shaped heating rate distributions with a designated locus of peak heating ($\dot{q}_{peak}$). The three specified design conditions considered the following heating rate levels:

Design Condition	$\dot{q}_{uniform}$	$\dot{q}_{peak}$
1	22.7 kW/m^2 (2 Btu/sec ft^2)	45.4 kW/m^2 (4 Btu/sec ft^2)
2	22.7 kW/m^2 (2 Btu/sec ft^2)	113.5 kW/m^2 (10 Btu/sec ft^2)
3	56.7 kW/m^2 (5 Btu/sec ft^2)	170.2 kW/m^2 (15 Btu/sec ft^2)

- o Investigate both two and three dimensional heating patterns to determine whether the more complex three dimensional pattern imposes any unique design requirements.
- o Prepare parametric data providing "cross-over" information identifying the optimum design concept for any specific heating condition within a wide range of potential conditions. These conditions considered heating rates from 5.7 kW/m^2 (0.5 Btu/sec ft^2) to 567 kW/m^2 (50 Btu/sec ft^2).

In addition to these primary objectives, supplementary goals were established. The significance of variations in the location, extent, and shape of the interference heating pattern was to be identified. A secondary trade study comparing coolant tube heat transfer augmentation techniques was to be accomplished prior to comparing candidate cooled panel concepts. Finally, trends were to be consistently scrutinized to determine if any improvements in the presently accepted cooled panel design philosophy could be identified.

Section 3 provides the background information regarding the study bases and analytical techniques used. It also defines the baseline cooled panel designs that were used in subsequent analyses.

Detailed concept definitions are provided in Section 4 along with discussions of the analyses used to size the concepts for the three specified two-dimensional heating pattern design conditions. This section also describes the ranking system that was used for concept comparisons. Ranking criteria included producibility, reliability, and inspectability/maintainability.

The three dimensional heating pattern analyses are discussed in Section 5. Section 6 discusses the parametric evaluations conducted to expand the usefulness of the study results. Conclusions and observations derived from the study are presented in Section 7.

3. DESIGN BASES AND TECHNIQUES

Many variables, in addition to the specified design requirements, affect the design of actively cooled structural panels. Some assumptions had to be made to hold the number of these variables to a manageable level for this study. These assumptions were based on the experience afforded by earlier cooled panel studies including those summarized in References 1 and 2. Analytical techniques developed during these previous studies were used wherever possible. The analyses conducted to size the baseline panel configurations formed procedural bases which were modified only when necessary during subsequent analyses.

3.1 General Design Guidelines

In order to capitalize on the data available from the earlier studies, it was assumed that the subject panel design is intended for installation on a Mach 6 hypersonic transport aircraft. The system design assumed was that considered in the Reference 1 and 2 studies. As indicated in Figure 3, coolant is pumped to the aircraft external surface panels to absorb the aerodynamic heat, and is returned to a heat exchanger. Heat is rejected to the hydrogen fuel and the coolant recirculated.

As reported in Reference 3, at least three distinctly different structural concepts have been developed to meet the basic cooled panel requirements:

- o A skin stringer structure with dual counterflow cooling passages.
- o A honeycomb sandwich structure with single pass tubes imbedded in the honeycomb core.
- o A stringer-stiffened, brazed plate-fin sandwich structure using the rectangular fin core as coolant passages.

Each of these concepts has unique advantages and, at this time, none can be judged to be superior.

The honeycomb sandwich panel structural concept, shown in Figure 4, was selected as the baseline configuration for this study, primarily to take advantage of available information. Although it was beyond the scope of this study to analyze all viable structural concepts, it is nevertheless expected that the trends developed are relatively independent of the baseline structural arrangement.

A methanol/water solution was initially considered for use as the study's heat transport fluid. Results of mass optimization studies previously conducted at MCAIR showed that mass is minimized with methanol based coolants with ethylene glycol/water solutions the second most attractive candidate. However, there is

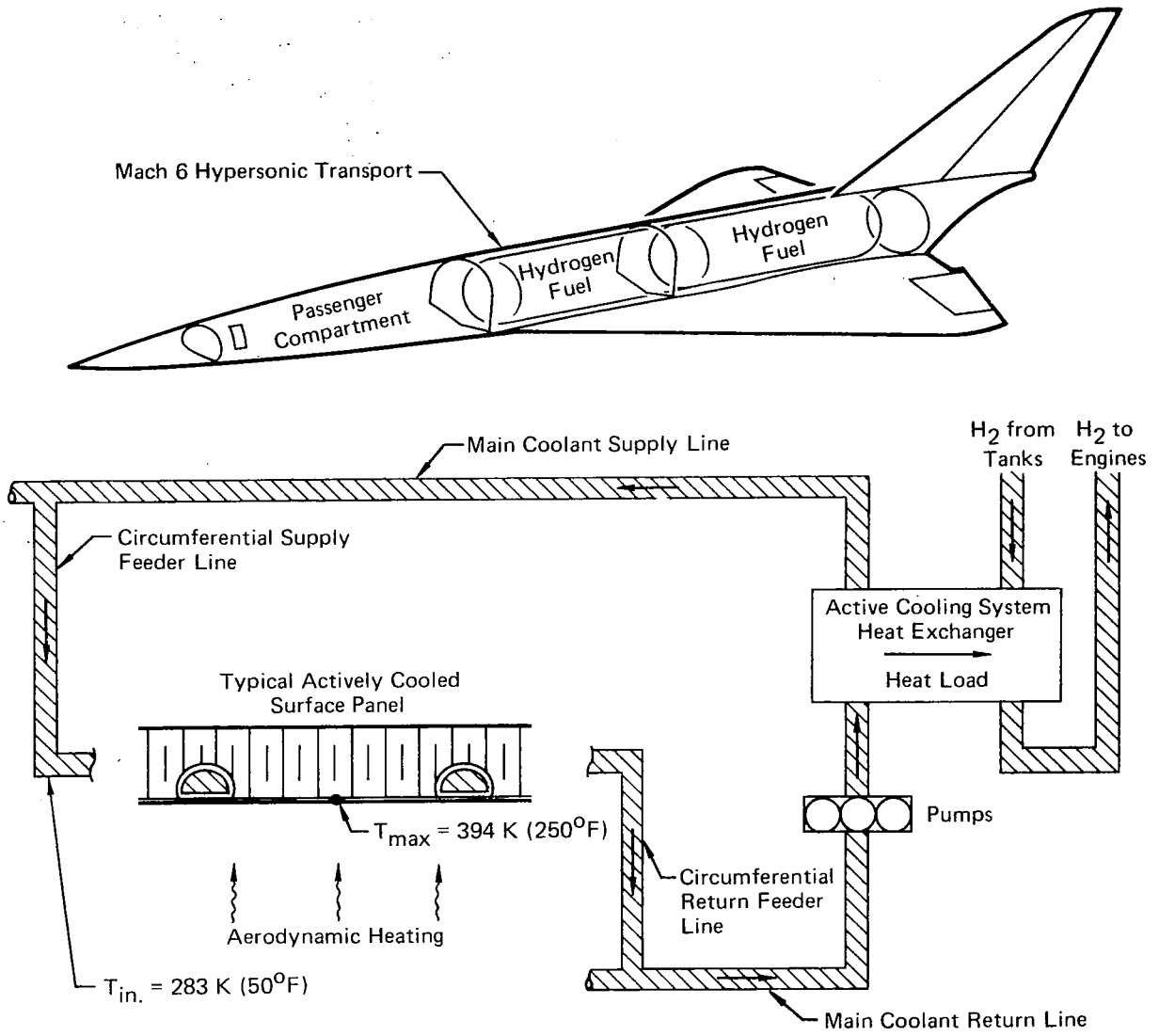

FIGURE 3
AIRFRAME ACTIVE COOLING SYSTEM

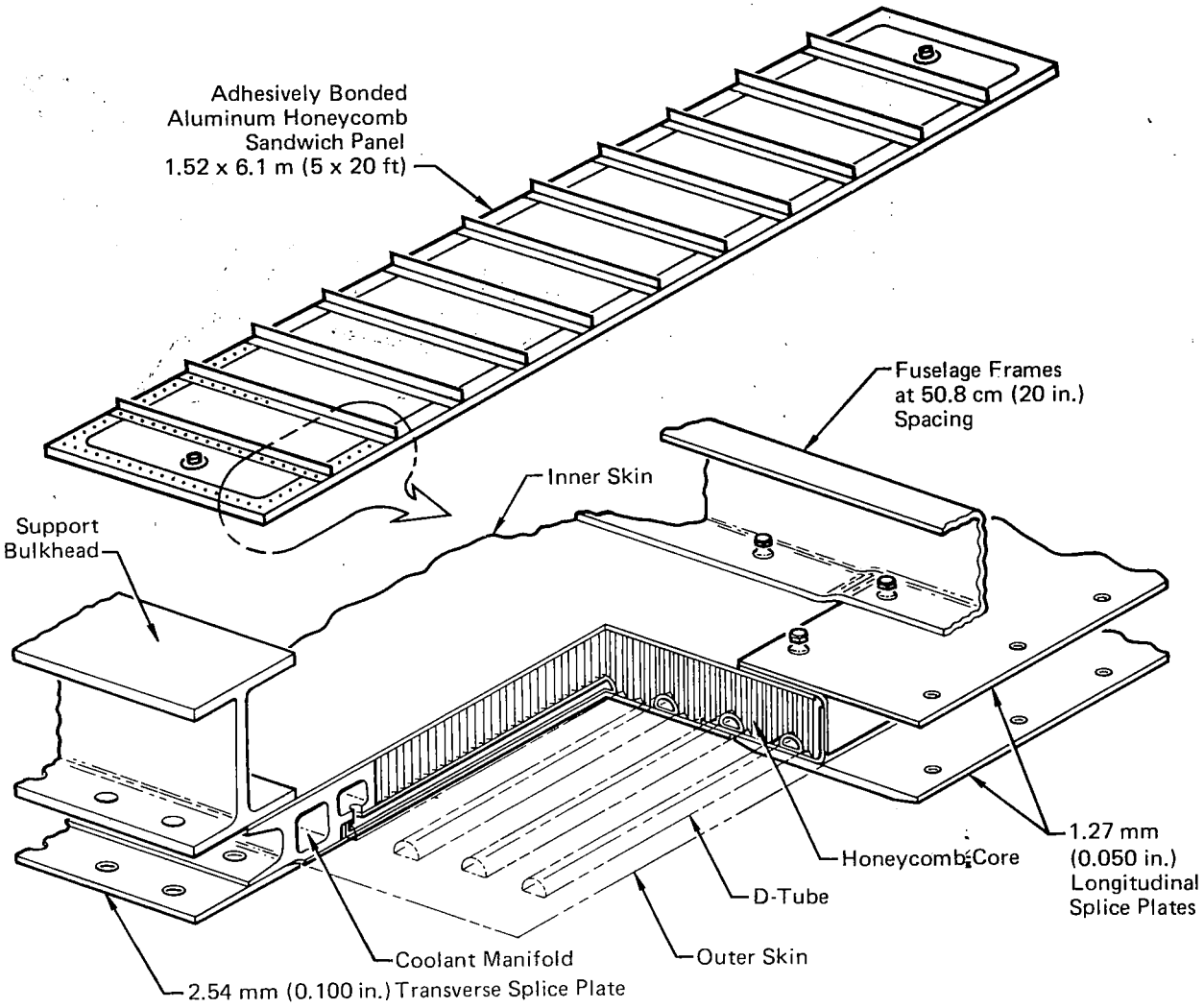

FIGURE 4
HONEYCOMB SANDWICH STRUCTURAL CONCEPT

concern regarding the use of methanol due to its low flash point. Ethylene glycol/water, which has a higher flash point, is specified as the coolant to be used in the hardware test program discussed in Reference 3. For this reason, it was decided to base this study on the use of an ethylene glycol/water (40 percent water by weight) solution. An inlet temperature of 283 K (50°F) was considered to be optimum for ethylene glycol/water solutions.

Figure 5 summarizes the design guidelines used. The following comments supplement the information contained in Figure 5.

a. The tube-to-skin joint thermal conductance value is representative of a good thermal contact, significantly better than obtainable with current adhesive bonding materials. This value is more representative of a solder joint and is felt to be achievable through normal development procedures.

b. The coolant tube wall thickness is midway in the range of thicknesses, 0.51 to 0.89 mm (0.020 to 0.035 in), available in aluminum tubing of the diameters considered.

c. The coolant tube diameter is defined as the outside diameter of a round aluminum tube prior to shaping into the D-tube configuration.

d. The minimum allowable panel outer skin thickness is established by installed maintenance considerations.

e. Coolant properties are based on vendor data as presented in Figures 6 and 7.

3.2 Thermodynamic Analyses

The cooled panel configurations were analyzed in sufficient depth to determine:

a. The coolant flow required to limit the maximum outer skin temperature to 394 K (250°F). When the flow rate and pressure drop through the panel are known, the effect of these requirements on active cooling system components can be determined.

b. Temperature distributions throughout the structure. This information is required for the structural analysis of panel designs as discussed in Section 3.3.

A cooled panel thermal model was set up using MCAIR's General Heat Transfer Computer Program, KBDR. This program provides for three-dimensional detail, has transient temperature capabilities, and includes locally increased thermal node density to permit detailed analysis of the region exposed to increased heating. The model (Figure 8) represents a cooled panel section one pitch wide and 6.1 m

PHYSICAL CHARACTERISTICS

Panel Size; 6.10 m (20 ft) by 1.52 m (5 ft)

Panel Construction; honeycomb sandwich

Cover Skin, Edging Member, and Splice Plate Material; 2024-T81 Aluminum

Coolant Tube and Manifold Material; 6061-T6 Aluminum

Honeycomb Core Material; 5056-H39 Aluminum

Honeycomb Core Density; 49.7 kg/m^3(3.1 lbm/ft^3)

Panel Tube and Header System Arrangement; non-redundant

Panel Assembly; adhesively bonded except for tube-to-skin joint

Tube-to-Skin Joint Thermal Conductance; 45.4 $kW/m^2 \cdot K$ (8000 Btu/hr ft^2 °F)

Coolant Tube Shape; D-shape

Coolant Tube Wall Thickness; 0.71 mm (0.028 in)

Minimum Practical Tube Spacing; 2.54 cm (1.0 in)

Minimum Practical Coolant Tube Inside Diameter; 0.48 cm (3/16 in)

Minimum Allowable Panel Outer Skin Thickness; 0.64 mm (0.025 in)

Minimum Practical Panel Inner Skin Thickness; 0.41 mm (0.016 in)

STRUCTURAL CHARACTERISTICS

Panel Support; simple support provided on 50.8 cm (20 in) centers in panel length

Panel In-Plane Axial Static Loading; $\pm$175.1 kN/m ($\pm$1000 lbf/in) limit load

Panel Normal Pressure; $\pm$6.895 kPa ($\pm$1.0 lbf/in^2) pressure limit at design heat flux

Factor of Safety for Ultimate Strength; 1.5 x limit for mechanical loads and 1.0 x limit for thermal effects

Panel Fatigue Loading Requirements; 20000 cycles (5000 cycles with a scatter factor of 4.0) with in-plane loading from +175.1 kN/m (-1000 lbf/in) to -175.1 kN/m (-1000 lbf/in)

THERMAL CHARACTERISTICS

Panel Outer Skin Maximum Temperature; 394 K (250°F)

Coolant Pressure at Panel Exit; in excess of 345 kPa (50 lbf/in^2) absolute

Coolant; Ethylene-Glycol/Water solution (60%/40% by weight)

Coolant Temperature at Panel Inlet; 283 K (50°F)

Coolant Distribution Line Pressure Drop; 896 kPa (130 lbf/in^2)

Heat Exchanger Pressure Drop; 138 kPa (20 lbf/in^2)

Pumping Power Penalty Factor; 0.338 g/kW·s (2 lbm/HP hr)

FIGURE 5
BASIC DESIGN GUIDELINES

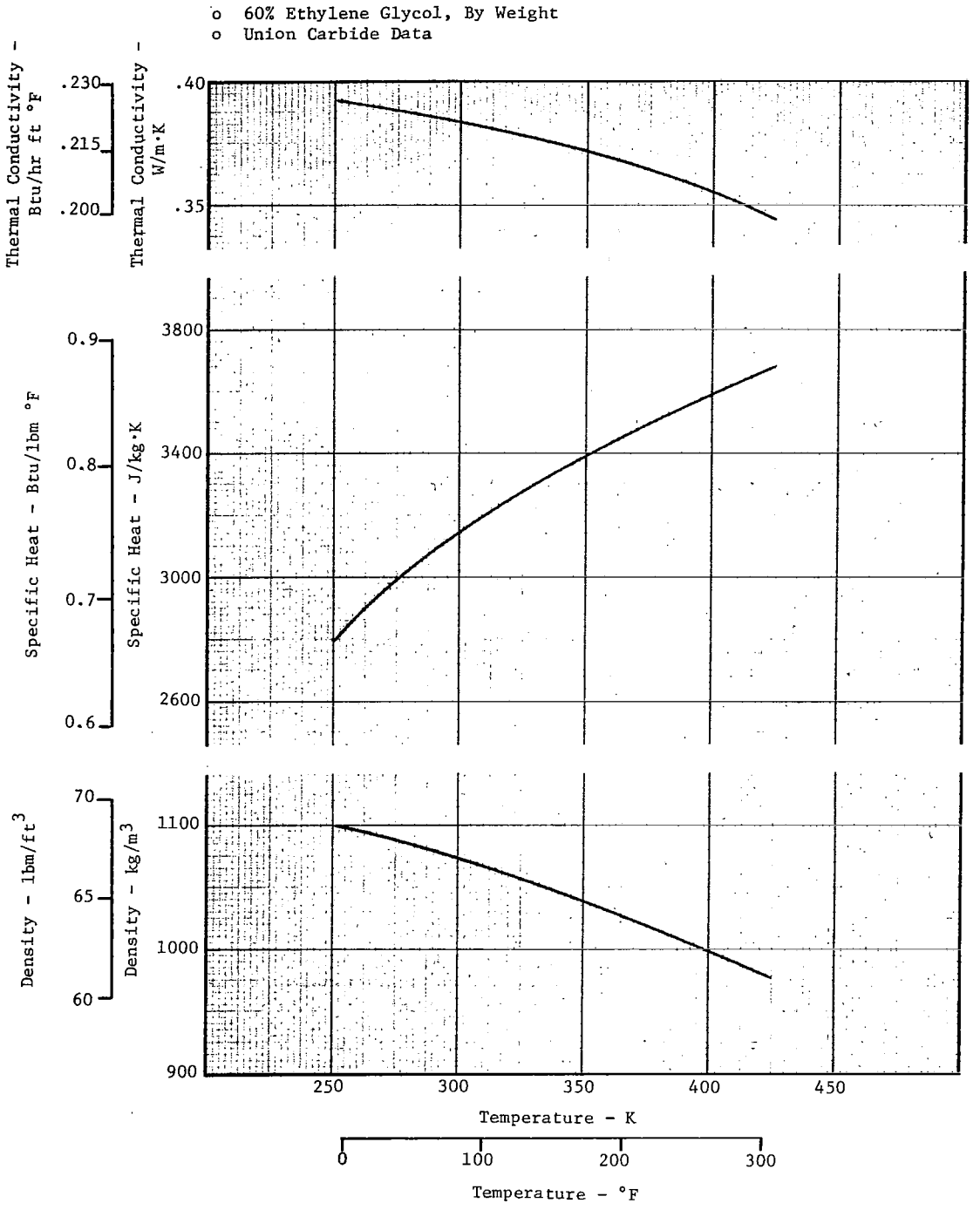

FIGURE 6
COOLANT DENSITY, SPECIFIC HEAT, AND THERMAL CONDUCTIVITY

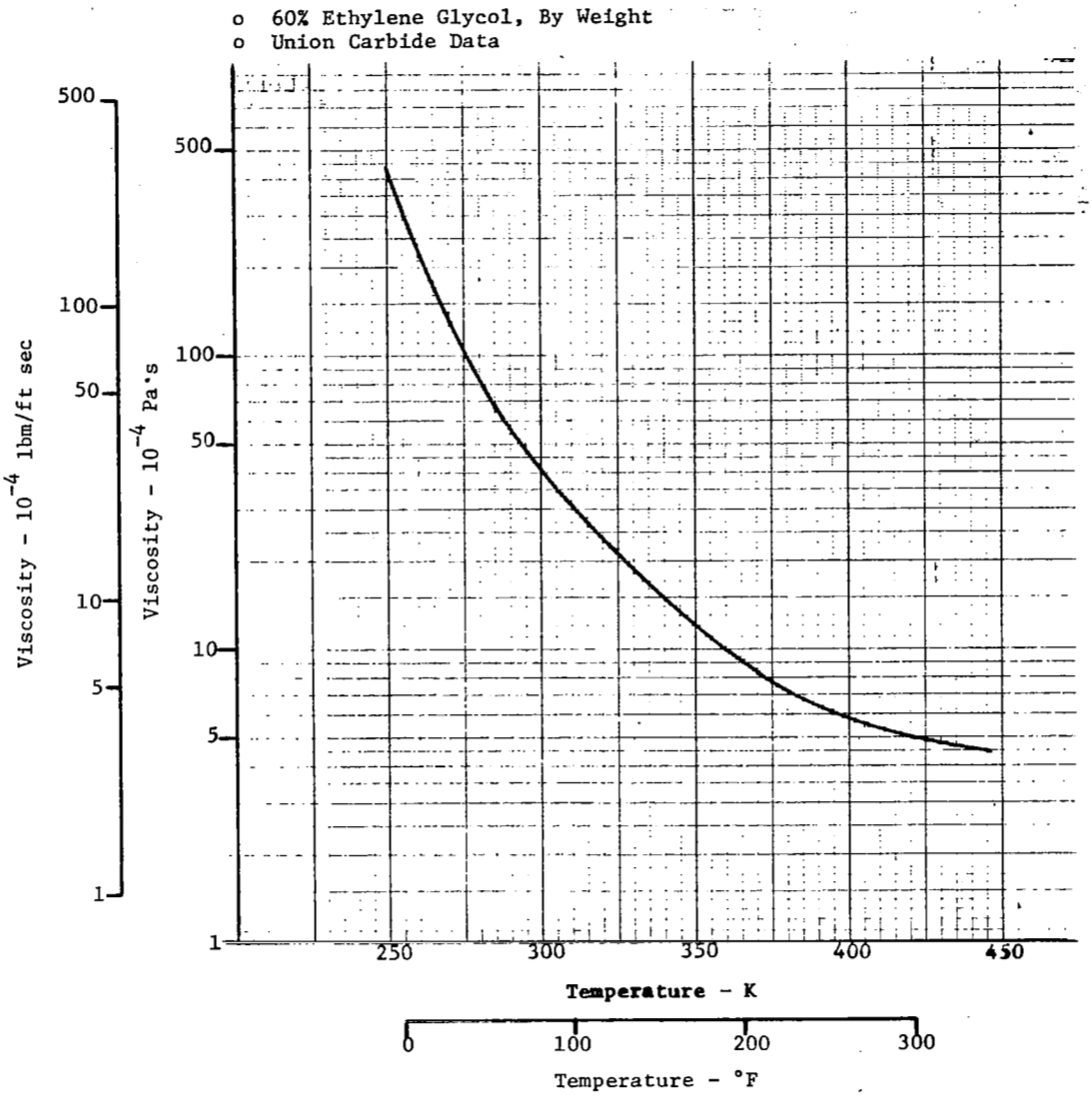

FIGURE 7
COOLANT VISCOSITY

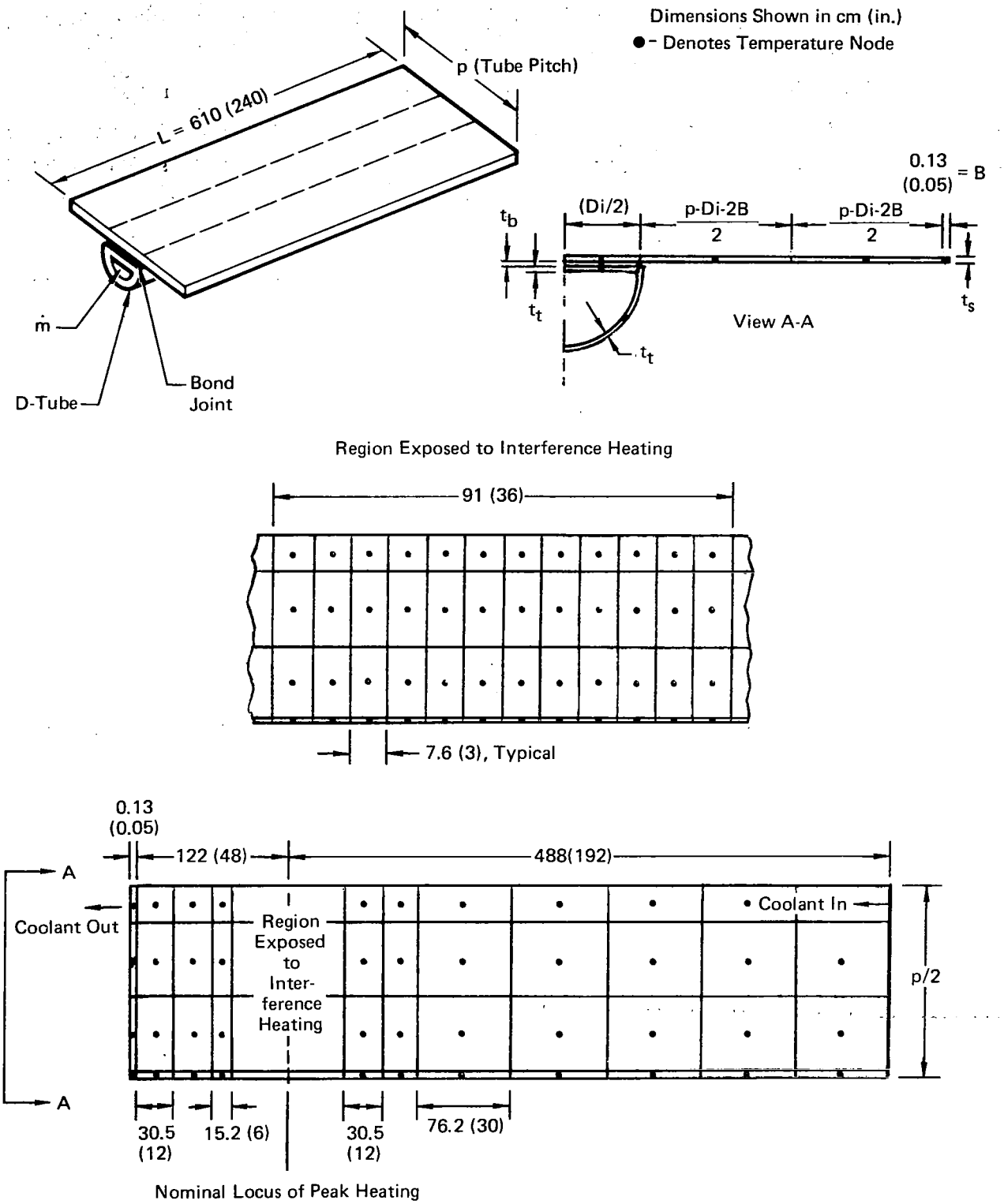

FIGURE 8
BASIC COOLED PANEL THERMAL MODEL

(20 ft) long. (One pitch is the distance between tube centers.) The model consists of 24 fluid nodes and 161 structural nodes, to encompass both lengthwise and spanwise temperature gradients. The coolant tubes are assumed to be D-shaped and soldered to the skin. The model was programmed to easily accommodate variations in tube spacing and geometry, skin thickness, surface heating rate and coolant flow. The honeycomb core backup material is not simulated since check cases confirmed that this simplification is acceptable for establishing coolant flow requirements. Only steady state heat transfer conditions were considered. It is reasonable to expect that the flow disturbances causing interference heating are nearly stable during cruise.

Coolant heat transfer coefficients for most configurations were computed with conventional smooth pipe flow correlations:

$$\text{Laminar flow,} \qquad h = C_L \frac{k}{D} \left[(Re)(Pr) \frac{D}{L}\right]^{1/3} \left(\frac{\mu}{\mu_w}\right)^{0.14}$$

where $C_L = 10.55$ (1.86)

$$\text{Turbulent flow,} \quad h = C_T \frac{k}{D} (Re)^{0.8} (Pr)^{1/3} \left(\frac{\mu}{\mu_w}\right)^{0.36}$$

where $C_T = 0.1305$ (0.023)

The Reynolds number at each fluid node was determined using fluid properties evaluated at the local bulk fluid temperature unless specified otherwise. An equivalent (hydraulic) diameter was used when analyzing noncircular coolant tubes. For D-shaped tubes the hydraulic diameter was assumed to be 61.1 percent of the equivalent round tube inside diameter. (This factor was derived at MCAIR by correlating measurements of tube samples shaped from round to "D".) When the calculated Reynolds number was less than a specified critical value, the laminar expression was used. When the Reynolds number was greater than another specified critical value, the turbulent expression was used. A Reynolds number between the critical values indicates transitional flow. Transitional heat transfer coefficients were determined by logarithmically interpolating between the laminar heat transfer coefficient, determined using the laminar critical Reynolds number, and the turbulent heat transfer coefficient determined with the turbulent critical Reynolds number. For smooth tubes, the critical Reynolds numbers used were 2100 maximum for laminar flow and 10,000 minimum for turbulent flow.

Coolant pressure drops (ΔP) were determined using the standard pressure drop relation for straight sections found in Reference 4:

$$\Delta P = C \left(\frac{fL}{D}\right) (\rho V^2), \text{ where } C = 2 \times 10^{-3} \ (4.32 \times 10^{-4})$$

The friction factor (f) was determined from the following conventional smooth pipe relationships:

$$f = \frac{16}{R_e} \quad \text{for laminar flow}$$

$$f = \frac{0.0791}{(R_e)^{0.25}} \quad \text{for transitional flow}$$

$$f = \frac{0.046}{(R_e)^{0.2}} \quad \text{for turbulent flow}$$

With the panel geometry and surface heating rates defined, the thermal model was used to determine coolant flow requirements by iterating on the flow until the maximum allowable skin temperature was obtained. Coolant pressure drop and temperature increase information was obtained simultaneously. Structural temperature distributions obtained with this model permitted a preliminary structural evaluation of the panel. In many instances, a more detailed structural analysis of the configurations was warranted. A detailed structural temperature model, illustrated in Figure 9, was used to provide the necessary information. This model consists of 15 structural temperature nodes and two (inlet/outlet) coolant nodes. As indicated, temperatures of both the honeycomb core and inner skin structure are provided for the detailed structural analysis. The detailed structural temperature model requires, as input, results from the converged conditions derived using the cooled panel thermal model. The local coolant flow and temperature are forced to known values (for the specified geometry and heating rate) and the resultant structural temperature distribution obtained. This two-dimensional model can be used to simulate any location along the panel length. Justification for the use of this simple two-dimensional analysis rather than a three-dimensional analysis is provided in Section 3.3.

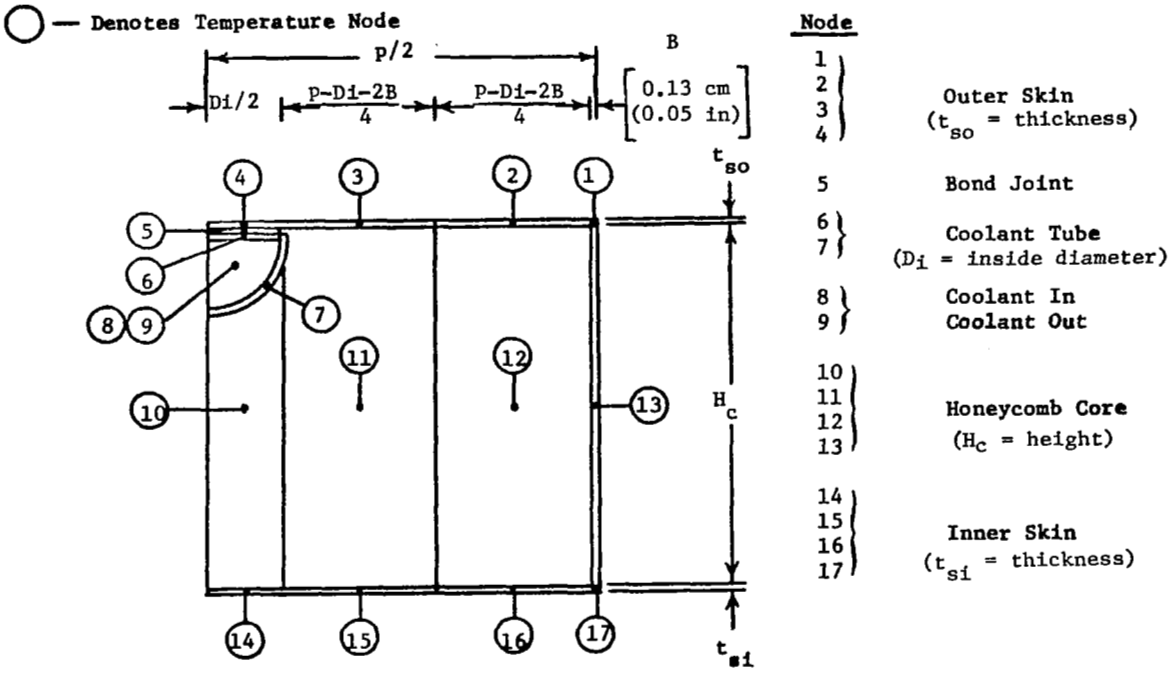

FIGURE 9
DETAILED STRUCTURAL TEMPERATURE MODEL

The panel inner surface was assumed to be adiabatic. The internal thermal environment would vary from regions near cryogenic tankage to regions near the engines. However, all regions would be thermally designed to eliminate temperature extremes and result in an internal environmental temperature reasonably close to the level attained by the inner skin.

It was also necessary to consider the active cooling system (ACS) components. Reference 1 showed that ACS components can be heavy enough to significantly affect aircraft performance. In light of those results, a concerted effort was expended during the study summarized in Reference 2 to minimize ACS component mass. In the present study, relationships developed in Reference 2 were used to establish the effect of the panel designs on ACS component mass.

Figure 10 presents the relationships used to estimate the ACS component mass attributable to a 9.29 m^2 (100 ft^2) panel. Seven items were identified as ACS components:

Component Masses expressed in kg (S.I. units)
" " " " lbm (customary units)

Coolant in Panel; $Wt_{c,p} = C_1 \left(\frac{D_i^2 \cdot \rho_i}{p}\right)$

$C_1 = 4.341 \times 10^{-2}$ (S.I.) = 3.894 (customary)

Coolant in Distribution Lines; $Wt_{C,L} = C_2 (\dot{m})^{0.75} (\mu avg)^{0.0833} (\rho avg)^{0.5833}$

$C_2 = 0.2554$ (S.I.) = 1.622 (customary)

Coolant Distribution Lines; $Wt_L = (0.238 + C_3 \cdot \Delta Ppanel)\, Wt_{C,L}$

$C_3 = 1.814 \times 10^{-4}$ (S.I.) = 1.251×10^{-3} (customary)

Heat Exchanger; $Wt_{H-X} = C_4 (\dot{Q}panel)$

$C_4 = 1.05 \times 10^{-2}$ (S.I.) = 2.441×10^{-2} (customary)

Pumps; $Wt_{pumps} = C_5 \left(\frac{\dot{m} \cdot \Delta Ppump}{\rho avg}\right)$

$C_5 = 0.4414$ (S.I.) = 0.19 (customary)

Pumping Power Penalty; $Wt_{pp} = C_6 \left(\frac{\dot{m} \cdot \Delta Ppump}{\rho avg}\right)$

$C_6 = 1.485$ (S.I.) = 0.639 (customary)

Reservoir; $Wt_R = 0.06\ (Wt_{c,p} + Wt_{C,L} + 0.4\ Wt_{H-X})$

Symbol	Definition	S.I. Units	Customary Units
Di	Coolant D-tube inside diameter	cm	in
ρi	Coolant density at initial temperature	kg/m^3	lbm/ft^3
p	Coolant tube pitch, distance between tubes	cm	in
$\dot{m}$	Coolant flow rate/panel	kg/s	lbm/sec
μavg	Coolant viscosity at average temperature	Pa·s	lbm/ft sec
ρavg	Coolant density at average temperature	kg/m^3	lbm/ft^3
ΔPpanel	Coolant pressure drop through panel	kPa	lbf/in^2
$\dot{Q}$panel	Heat absorbed/panel	kW	Btu/sec
ΔPpump	Coolant pressure rise across pumps	kPa	lbf/in^2

Assumptions Forming Bases for Expressions

Coolant Distribution Line Pressure Drop (ΔP_{lines}) = 896 kPa(130 lbf/in^2)

Heat Exchanger Pressure Drop (ΔP_{H-X}) = 138 kPa(20 lbf/in^2)

Pressure Rise Across Pumps (ΔPpump) = $\Delta P_{lines} + \Delta P_{H-X} + \Delta Ppanel$

Pump Inlet Pressure (Pinlet) = 276 kPa(40 lbf/in^2)

Maximum System Pressure (Psystem) = ΔPpump + Pinlet

Pumping Power Penalty Factor = 0.338 $\frac{g(fuel)}{kW \cdot s}$ = 2 $\frac{lbm(fuel)}{HP\ hr}$

Effective Flight Time = 1.22 hr

Panel Size = 6.10 m(20 ft) by 1.52 m(5ft)

FIGURE 10
ACTIVE COOLING SYSTEM COMPONENTS MASS CORRELATIONS

Coolant in Panel - This relationship simply reflects the mass of coolant required to initially fill the coolant tubes and manifolds of the panel. In most instances the tube volume is based on D-shaped tubes and a factor of 1.19 is applied to account for the manifold. A coolant density of 1.073 Mg/m^3 (67 lbm/ft^3), representative of a typical fill temperature of 300 K (80°F), was assumed.

Coolant in Distribution Lines - This relationship was derived by correlating information from References 1 and 2. The coolant distribution system layout and line lengths contribute significantly to the relationship. Another primary factor was the assumed overall maximum coolant distribution line pressure drop (ΔP lines) of 896 kPa (130 lbf/in^2). This assumption was shown in Reference 2 to be consistent with the goal of minimizing the ACS mass penalty. The correlation uses coolant properties evaluated at the average temperature from panel inlet to outlet.

Coolant Distribution Lines - Data correlations from References 1 and 2 also provided the basis for this relationship which accounts for the effects of total system pressure on coolant line wall thickness and of coolant flow on line size. The indicated assumptions for distribution line and heat exchanger pressure drops and pump inlet pressure result in a total system pressure level of 1.31 MPa (190 lbf/in^2) plus the panel pressure drop requirement.

Heat Exchanger - Heat exchanger total mass (including contained coolant) was assumed to vary linearly with heat load. This expression is the same as that used in the Reference 2 study.

Pumps - This relationship was derived from data from Reference 5 which has been used as the basis for pump masses in References 1 and 2. A dual pump configuration was assumed.

Pumping Power Penalty - This penalty was expressed, consistent with previous studies, as the equivalent mass of fuel that would be required to power the coolant pumps. A conversion factor of 0.338 g/kW.s (2.0 lbm/HP hr) was used based on analyses conducted during the Reference 2 study. The effective flight time of 1.22 hr (estimated for the baseline aircraft) also contributes to this relationship.

Reservoir - This relationship was derived from Reference 2 and accounts for the dry mass of the reservoir as well as the coolant mass. Reservoir sizing is influenced by the total aircraft coolant load and must accommodate expansion and contraction caused by changes in coolant density.

The summation of the seven ACS component masses yields a total which, when added to the panel structural mass, can be used to compare panel designs.

3.3 Structural Analysis

This section defines the design loads, ultimate factors of safety, strength analysis methods and programs, material properties, and bases for structural mass analysis.

3.3.1 Design Loads and Factors of Safety - The applied loads, shown in Figure 11, include an in-plane design limit column loading of 175 kN/m (1000 lbf/in). To be consistent with conditions used for the design of actively cooled panels at MCAIR in previous studies, such as the Reference 2 program, normal airloads were included and all loads were considered fully reversible. The normal airload on the uniformly heated portion of the panel was a pressure differential of 6.9 kPa (1.0 lbf/in^2) limit. Peak external normal pressures in flow interference regions were estimated using the expression:

$$\frac{\dot{q}_{peak}}{\dot{q}_{uniform}} = \left(\frac{p_{disturbed}}{p_{undisturbed}}\right)^{0.85}$$

This expression relates conditions in the disturbed flow, peak heating, region with those in the adjacent undisturbed flow, uniform heating, region and is a common expression for defining pressures in regions of interference heating. Its application in this study resulted in the pressure differentials shown in Figure 11.

The panels were designed to withstand any combination of limit loads and temperature conditions without yielding and to withstand any combination of ultimate loads and temperature conditions without failure. The factors of safety shown in Figure 12 were consistent with those used in Reference 2 and were based on the recommendations of Reference 6.

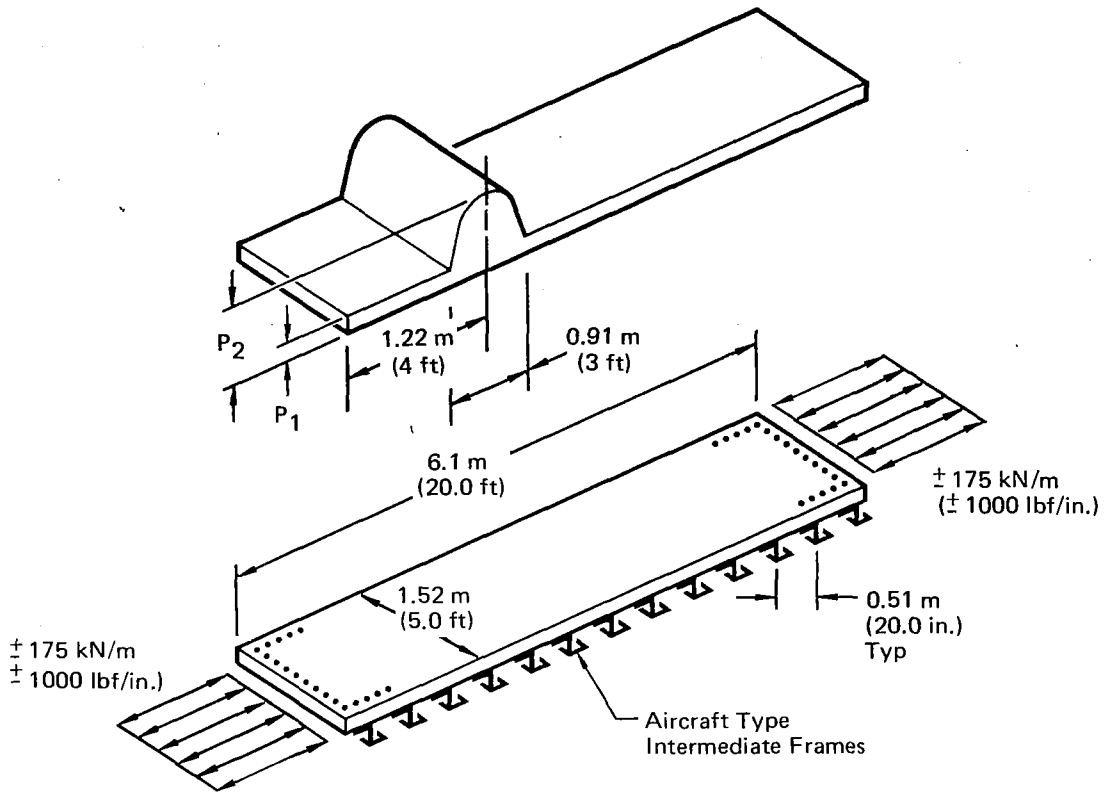

Design Condition	Pressure			
	P_1		P_2	
	kPa	(lbf/in.^{2})	kPa	(lbf/in.^{2})
1	6.9	(1.0)	19.9	(2.89)
2	6.9	(1.0)	65.2	(9.46)
3	6.9	(1.0)	34.2	(4.96)

FIGURE 11
DESIGN LIMIT LOADS

Static Strength Design Conditions	Factor of Safety	
	Limit	Ultimate
In-Plane Axial Load	1.0	1.5
Lateral Pressure	1.0	1.5
Thermal Stress	1.0	1.0
Temperature	1.0	1.0
Temperature Gradient	1.0	1.0
Coolant Pressures	1.0	1.5(1)

(1) Burst pressure (acting alone) factor of safety for coolant passages, manifolds and fittings is 4.0.

FIGURE 12
FACTORS OF SAFETY

3.3.2 Strength Analysis Methods - The structural analysis and optimization of the honeycomb panels made use of three computer programs: A thermal stress program, KBEB, (Thermal Stresses in a Beam Cross Section), a mechanical stress program, ACPOP (Actively Cooled Panel Optimization Program) and a finite element program, CASD (Computer Aided Structural Design) which computes thermal and mechanical stresses. KBEB and ACPOP were used to analyze the panels with two dimensional heating. All three programs were used to analyze the panels with three dimensional heating.

The KBEB program computes the thermal stresses in beams with symmetrical or unsymmetrical cross sections for any combination of end restraints, with up to five different materials, and with temperature gradients across the width of the beam. It is based on the methods and equations of References 7 and 8. The required inputs are the coordinates, area and moment of inertia of each element of the beam cross section, rotational and axial fixity of the beam ends, coefficient of thermal expansion and modulus of elasticity

of each material at several arbitrarily chosen temperatures over the range to be considered, and the temperature of each element. The temperatures for each element were obtained from thermodynamic analysis using the model described in Figure 9. The program outputs include the coefficient of thermal expansion and modulus of elasticity for each element at its temperature and the effective area, axial thermal stress and load for each element. Edge restraints were determined by considering the adjacent panels. Because the adjacent panels were heated to temperatures similar to those for the subject panel, the entire structure was assumed to be free to expand thermally. The panels have bending continuity both at the support frames and at the splices to adjacent panels. Therefore, the panel edges were considered to be free axially and fixed rotationally.

The ACPOP mechanical stress program, developed at MCAIR, is described in Reference 9. It analyzes and sizes honeycomb panels with or without integral D-tubes for any combination of in-plane and normal loads with any of several edge restraints. It analyzes them for the following failure modes from Reference 10:

Face Sheet Wrinkling:

$$F_w = \frac{.82\sqrt{\frac{E_c E' t_s}{t_c}}}{1. + .64\left(\frac{\delta E_c}{t_c F_c}\right)}$$

Face Sheet Dimpling:

$$S = \sqrt{\frac{t}{\frac{F_c\,(1 - \mu^2)}{2E'}}}$$

Panel Buckling:

$$N_{cr} = K\frac{\pi^2 D}{b^2}$$

Beam Column Effects:

$$\psi = \frac{\psi o}{1 - N/N_{cr}}$$

Inputs to the ACPOP program are the panel length and width; the cross-sectional area and bending stiffness of the panel edge supports; the edge restraint; in-plane and normal applied loads; allowable working stresses of the inner and outer face sheets and of the D-tube and core; moduli of elasticity associated with the allowable working stresses; density of the core; densities of the D-tube and face sheet materials; the D-tube diameter, thickness and pitch; and the outer and inner face sheet (skin) thicknesses. For each inside face sheet thickness input the program iterates on panel height until all failure mode criteria are satisfied. Program output includes panel height, unit mass (structural mass per unit area), applied and allowable stress levels and margins of safety. The unit masses for several inner face sheet thickness were compared and the thickness resulting in the minimum mass was selected. An example of this comparison is shown in Figure 13, a plot of panel unit mass versus the heights that resulted from inputting various inner face sheet thicknesses for some typical cases. The edge restraints were selected by consideration of adjacent panels. Because the long edges of the panel were attached to similar panels which would have similar loading and would, therefore, not offer any support, these edges were assumed to be free. Since the panel had bending continuity at the ends and at the intermediate supports, it acted as a continuous beam column on multiple supports. For a uniformly distributed load, a uniform, continuous beam has zero slope at the supports and each span can be analyzed as a fixed end beam. Therefore, the spans not exposed to the effects of interference heating were analyzed as if they were fixed in bending at both ends. However, locally high pressures are associated with regions experiencing interference heating. This increased load would not be uniformly distributed and would be most critical when centered at the midspan of a single span of the panel. The span thus loaded would not have zero slope at the ends but would have rotation approaching that of a simply supported beam. Therefore, the panel regions exposed to interference heating were conservatively analyzed as having no fixity (rotational restraint) at the ends.

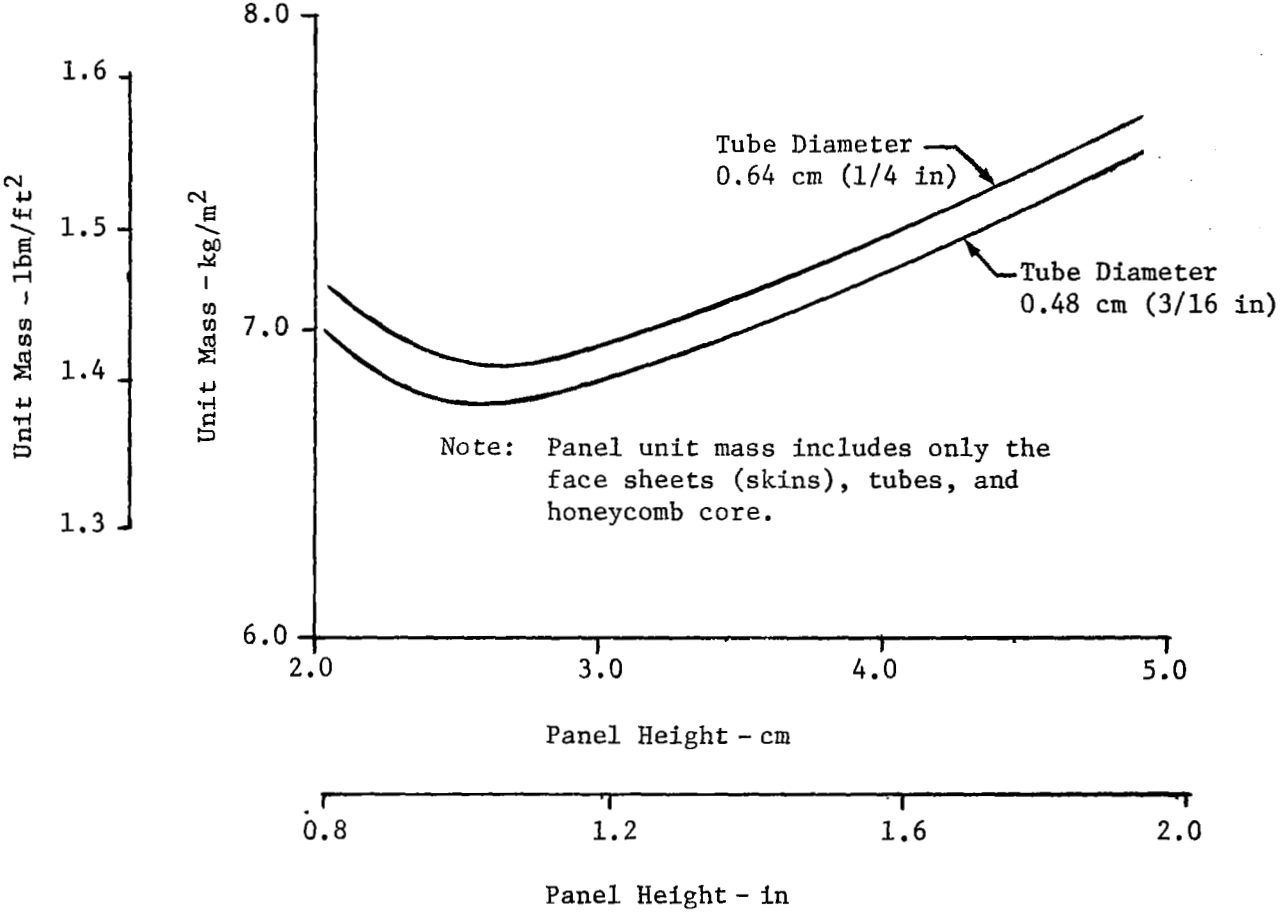

FIGURE 13
TYPICAL PANEL UNIT MASS TRENDS

In order to determine the panel geometry that resulted in the minimum panel mass while maintaining a positive margin of safety, it was necessary to iterate between the ACPOP and KBEB programs. The panels were first sized for mechanical stresses alone by the use of ACPOP. Thermal stresses were then calculated for the resulting configuration using KBEB. The thermal stresses were superimposed algebraically with the mechanical stresses and, if a negative margin of safety resulted, the allowable stress input for the critical element was reduced and the procedure was repeated until a positive margin of safety was obtained. Where thermal and mechanical stresses were relieving, the smaller of the two was neglected. Algebraic superposition of mechanical and thermal stresses was justified because the allowable stresses for fatigue and buckling were always within the elastic range. This procedure was used to size the panel for both the uniformly heated region and the region exposed to interference heating.

The CASD program was used in the three dimensional heating pattern analysis to determine additional thermal stresses and external reactions caused by the unsymmetrical heating patterns and the different heating patterns in adjacent panels. This program analyzes structures consisting of bar and shear panel elements for mechanical and thermal loads. It uses a combination of the equations for the equilibrium of forces and those for the compatibility of deformation. Special features of the program include the ability to present a complete structure by describing only one half of a symmetrical or nearly symmetrical structure. Inputs to the CASD program are the structural geometry; the area, modulus of elasticity and coefficient of thermal expansion of each bar; the thickness and modulus of rigidity of each shear panel; the temperature at each node, the applied loads; and the restraints at each reaction. Program output options include internal loads and stresses, external reactions, and deflections.

3.3.3 Material Properties - The basic strength data (compression, coefficient of thermal expansion, and modulus of elasticity) used for the 2024-T81 skins and for the 6061-T6 aluminum coolant passages were obtained from Reference 11. The material properties used were based on 10,000 hour exposure at elevated temperature. The compressive yield stress (elastic limit) of the 2024-T81 was calculated to be 351.9 MPa (51,000 lbf/in^2).

Allowable tension stress levels for the skins and coolant passages were developed such that a "safe life" design could be achieved. This involved establishing operating stress levels for the skins such that an initial flaw in the skins would not grow to a critical length which would result in catastrophic failure within the life of the panel (defined as 20,000 cycles of mechanical and thermal loads including a scatter-factor of 4). It also required the establishment of operating stress levels in the tubes such that an initial surface flaw would not propagate through the tube wall within the life of the panel.

The allowable for the 2024-T81 skin material was developed by addressing cracks propagating from one side of a fastener hole. The initial flaw sizes used when establishing the allowable operating stress levels for the skins were based on the results of Reference 12, addressing probable flaw sizes in fastener holes. It was determined, as shown in Figure 14, that given a stress ratio of minus one (R = -1) and an initial flaw size of 0.013 cm (.005 in), a flaw would not grow to the critical length within the 20,000 cycle life provided the maximum operating stress level was less than 106.9 MPa (15500 lbf/in^2).

The allowable operating stress level in the D-tubes was determined by addressing surface flaws at the point of maximum stress in the tube. Tube surface flaw sizes were established as those which could reasonably be detected using conventional NDE (nondestructive evaluation) methods. The analysis indicated, as shown in Figure 14, that an initial flaw .033 cm (.013 in) long and .013 cm (.005 in) deep will not grow through the thickness of the .071 cm (.028 in) wall tube within the life of the panel, provided the operating stress level is less than 158.6 MPa (23,000 lbf/in^2).

The allowable ultimate tension stresses are the permissable operating stresses times an ultimate factor of 1.5. These are 160.3 MPa (23,250 lbf/in^2) for the 2024-T81 skin and 237.9 MPa (34,500 lbf/in^2) for the 6061-T6 D-tubes.

3.3.4 Structural Mass Analysis - The panel structural mass was calculated for each configuration and loading condition. The total structural mass was the sum of the mass of the honeycomb sandwich structure (skins, tubes and honeycomb core) and the mass of the manifolds and joint materials.

The mass of the honeycomb sandwich structure was determined from the unit structural mass (mass per unit area) output of the ACPOP computer program explained in Section 3.3.2. The unit masses for the interference heating portion and the uniform heating portion were multiplied by their respective areas and summed.

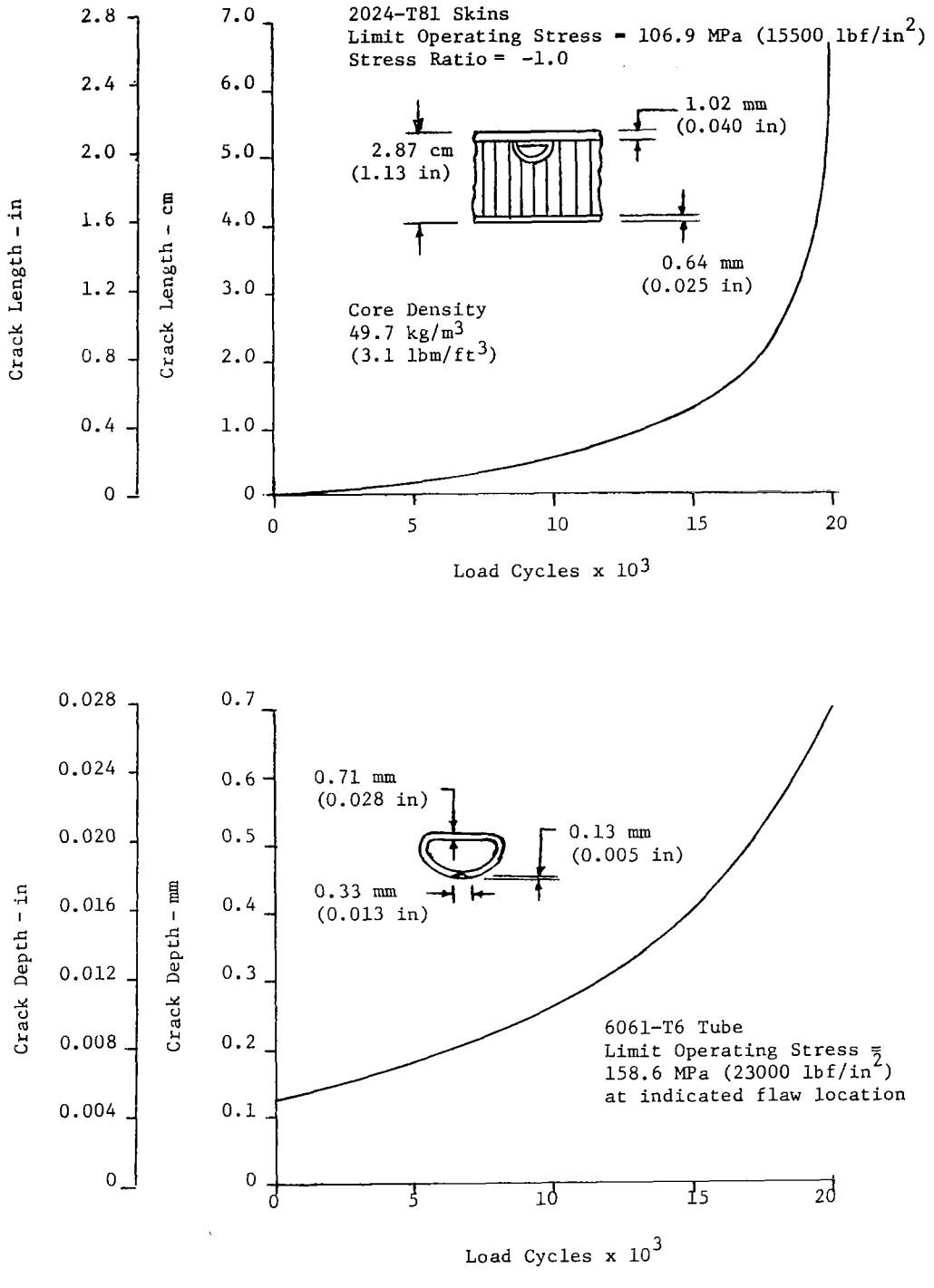

FIGURE 14
ALUMINUM CRACK PROPAGATION RATES

To maintain structural continuity, and avoid unnecessary fabrication difficulties, it was desirable for the panel height to be the same in both the uniformly and interference heated regions. This was accomplished by determining the unit mass for each of several panel heights and selecting the height that resulted in the minimum total structural mass.

The mass of the manifolds and joint materials was based on previous MCAIR designs. Details of these items are illustrated in Figure 4. Figure 15 presents the mass of each item and the total manifold and joint material mass for a typical panel of 2.87 cm (1.13 in) height with manifolds at the two ends. These details and masses had to be modified to be compatible with some of the configurations studied herein. Where this was done, the mass of each item affected was ratioed on the basis of required size or quantity changes. This is explained, where required, in the discussions of the studied concepts. The mass of the closure angles, manifolds, bushings and fasteners will change slightly for different panel heights, but the total mass change will be small and has been neglected.

Component	Mass	
	Kg	(lbm)
Closure Angles	3.2	(7.0)
Manifolds and Bellmouth	5.4	(11.8)
Splice Plates	3.5	(7.8)
Adhesives	19.4	(42.7)
Connectors	0.1	(0.1)
Bushings/Fasteners	2.1	(4.6)
Total	33.7	(74.0)

FIGURE 15
BASIC MASS OF PANEL MANIFOLDS AND JOINT MATERIALS

3.4 Baseline Panel Sizing

In order to assess the effects of designing cooled panels to accommodate interference heating, it is necessary to know the mass charged to cooled panels designed for uniform heating rates. Two cooled panel configurations were, therefore, sized for uniform heating rates of 22.7 kW/m^2 (2 Btu/sec ft^2) and 56.7 kW/m^2 (5 Btu/sec ft^2), which are the uniform heating rates that were used in subsequent analyses of the specific interference heating pattern design conditions. These heating rates are typical of these encountered at Mach 6 cruise.

The primary objective of these baseline panel sizing studies was to establish the minimum mass levels associated with the design heating rates. Thermodynamic and structural analyses were conducted to determine the masses of panels with variations in the panel geometric parameters of tube pitch, tube diameter, and outer skin thickness. The minimum values considered for these parameters were established by the guidelines discussed in Section 3.1. Figures 16 and 17 provide pertinent information on each of the panels analyzed for the two uniform heating rates. These data are for the coolant flow required to maintain a 394 K (250°F) maximum structural temperature. The total mass presented is the summation of the structural and ACS component masses charged to a given panel design.

Figures 18 and 19 provide the individual ACS component masses calculated for these panel geometries. The 394 K (250°F) maximum structural temperature can be maintained over the entire range of parameters considered for the $\dot{q}$ = 22.7 kW/m^2 (2 Btu/sec ft^2) condition. However, for tube pitches above 3.81 cm (1.5 in) and for thin panel outer skins at a pitch of 3.81 cm (1.5 in), heat cannot be removed from the panel fast enough to keep from exceeding this permissible maximum temperature for the $\dot{q}$ = 56.7 kW/m^2 (5 Btu/sec ft^2) condition. At the lower design heating rate the ACS component masses are shown to be relatively insensitive to tube pitch over the range of 2.54 to 3.81 cm (1.0 to 1.5 in). At the more severe heating condition ACS component masses increase sharply with increasing tube pitch.

To understand the overall significance of panel geometry variations, the total mass charged to a panel (Figures 16 and 17) must be examined. For the lower heating rate significant mass penalties are encountered only at pitches in excess of 3.81 cm (1.5 in) or with tube diameters greater than 0.64 cm (1/4 in). In general, mass is minimized with the thin outer skin configurations. There are thermal advantages, for abort considerations, in having

Configuration	Tube Pitch cm (in)	Tube Diameter cm (in)	Outer Skin Thickness mm (in)	Coolant Flow/Tube g/s (lbm/hr)	Panel ΔP kPa (lbf/in²)	Panel Structural Mass kg (lbm)	ACS Components Mass kg (lbm)	Total Mass kg (lbm)
2-1	2.54(1.00)	0.48(3/16)	0.64(.025)	14.5 (115)	241 (35)	94 (207)	19 (41)	112 (248)
2-2 *			1.02(.040)	13.4 (106)	207 (30)	95 (210)	18 (39)	113 (249)
2-3			1.27(.050)	12.6 (100)	193 (28)	98 (216)	17 (37)	115 (253)
2-4		0.64(1/4)	0.64(.025)	18.7 (148)	63 (9.2)	94 (207)	25 (55)	119 (262)
2-5			1.02(.040)	17.0 (135)	54 (7.8)	96 (212)	24 (52)	120 (264)
2-6			1.27(.050)	16.5 (131)	52 (7.5)	100 (220)	23 (51)	123 (271)
2-7		0.95(3/8)	0.64(.025)	24.5 (194)	12 (1.8)	95 (210)	41 (91)	137 (301)
2-8			1.02(.040)	22.7 (180)	11 (1.6)	100 (221)	40 (88)	140 (309)
2-9			1.27(.050)	22.1 (175)	10 (1.5)	105 (232)	39 (87)	145 (319)
2-10	3.18(1.25)	0.48(3/16)	0.64(.025)	20.2 (160)	414 (60)	94 (207)	20 (43)	113 (250)
2-11			1.02(.040)	17.3 (137)	310 (45)	95 (209)	18 (39)	112 (248)
2-12			1.27(.050)	16.6 (132)	290 (42)	97 (214)	17 (38)	114 (252)
2-13		0.64(1/4)	0.64(.025)	25.3 (201)	103 (15)	94 (207)	25 (55)	119 (262)
2-14			1.02(.040)	21.9 (174)	83 (12)	96 (211)	23 (50)	118 (261)
2-15			1.27(.050)	20.8 (165)	76 (11)	98 (217)	22 (49)	121 (266)
2-16		0.95(3/8)	0.64(.025)	41.5 (329)	24 (3.5)	94 (208)	43 (94)	137 (302)
2-17			1.02(.040)	35.7 (283)	20 (2.9)	98 (216)	40 (88)	138 (304)
2-18			1.27(.050)	34.3 (272)	19 (2.7)	102 (225)	39 (86)	141 (311)
2-19	3.81(1.50)	0.48(3/16)	0.64(.025)	31.3 (248)	931 (135)	94 (207)	25 (55)	119 (262)
2-20			1.02(.040)	23.2 (184)	538 (78)	94 (208)	19 (42)	113 (250)
2-21			1.27(.050)	21.4 (170)	469 (68)	97 (213)	18 (40)	115 (253)
2-22		0.64(1/4)	0.64(.025)	37.8 (300)	207 (30)	94 (207)	28 (61)	122 (268)
2-23			1.02(.040)	28.0 (222)	124 (18)	95 (209)	23 (50)	117 (259)
2-24			1.27(.050)	26.0 (206)	103 (15)	98 (215)	22 (48)	119 (263)
2-25	5.08(2.00)	0.48(3/16)	1.02(.040)	46.7 (370)	2035 (295)	94 (208)	32 (70)	126 (278)
2-26			1.27(.050)	38.5 (305)	1380 (200)	96 (211)	25 (55)	121 (266)
2-27		0.64(1/4)	1.02(.040)	53.0 (420)	386 (56)	94 (208)	28 (62)	122 (270
2-28			1.27(.050)	43.9 (348)	269 (39)	97 (213)	24 (54)	121 (267)

* Selected

FIGURE 16
BASELINE PANELS DESIGNED FOR UNIFORM HEATING OF 22.7 kW/m² (2 BTU/SEC FT²)

Configuration	Tube Pitch cm	(in)	Tube Diameter cm	(in)	Outer Skin Thickness mm	(in)	Coolant Flow/Tube g/s	(lbm/hr)	Panel ΔP kPa	(lbf/in^2)	Panel Structural Mass kg	(lbm)	ACS Components Mass kg	(lbm)	Total Mass kg	(lbm)
5-1	2.54	(1.00)	0.48	(3/16)	0.64	(.025)	53.6	(425)	2620	(380)	94	(207)	70	(154)	164	(361)
5-2					1.02	(.040)	40.6	(322)	1460	(212)	95	(210)	48	(105)	143	(315)
5-3					1.27	(.050)	37.8	(300)	1295	(188)	98	(216)	44	(97)	142	(313)
5-4			0.64	(1/4)	0.64	(.025)	56.7	(450)	434	(63)	94	(207)	54	(119)	148	(326)
5-5 *					1.02	(.040)	43.5	(345)	255	(37)	96	(212)	44	(97)	140	(309)
5-6					1.27	(.050)	40.4	(320)	221	(32)	100	(220)	42	(92)	142	(312)
5-7			0.95	(3/8)	0.64	(.025)	80.7	(640)	76	(11)	95	(210)	76	(167)	171	(377)
5-8					1.02	(.040)	67.5	(535)	55	(8)	100	(221)	68	(151)	169	(372)
5-9					1.27	(.050)	62.8	(498)	48	(7)	105	(232)	66	(145)	171	(377)
5-10	3.18	(1.25)	0.48	(3/16)	1.02	(.040)	72.5	(575)	4310	(625)	95	(209)	91	(201)	186	(410)
5-11					1.27	(.050)	60.5	(480)	3070	(445)	97	(214)	68	(149)	165	(363)
5-12			0.64	(1/4)	0.64	(.025)	134.3	(1065)	2150	(312)	94	(207)	114	(252)	208	(459)
5-13					1.02	(.040)	72.5	(575)	689	(100)	96	(211)	56	(124)	152	(335)
5-14					1.27	(.050)	61.2	(485)	496	(72)	98	(217)	49	(107)	147	(324)
5-15			0.95	(3/8)	0.64	(.025)	145.0	(1150)	234	(34)	94	(208)	92	(202)	186	(410)
5-16					1.02	(.040)	95.2	(755)	103	(15)	98	(216)	70	(154)	168	(370)
5-17					1.27	(.050)	88.3	(700)	90	(13)	102	(225)	67	(147)	169	(372)
5-18	3.81	(1.50)	0.64	(1/4)	1.02	(.040)	156.4	(1240)	2745	(398)	95	(209)	121	(266)	215	(475)
5-19					1.27	(.050)	105.3	(835)	1325	(192)	98	(215)	71	(156)	168	(371)
5-20			0.95	(3/8)	1.02	(.040)	163.9	(1300)	276	(40)	97	(213)	88	(193)	184	(406)
5-21					1.27	(.050)	132.4	(1050)	193	(28)	100	(221)	75	(165)	175	(386)

* Selected

FIGURE 17
BASELINE PANELS DESIGNED FOR UNIFORM HEATING OF 56.7 kW/m^2 (5 BTU/SEC FT^2)

Configuration	Coolant in Panel kg	(lbm)	Coolant in Distribution Lines kg	(lbm)	Coolant Distribution Lines kg	(lbm)	Heat Exchanger kg	(lbm)	Pumps kg	(lbm)	Pumping Power Penalty kg	(lbm)	Reservoir kg	(lbm)	Total ACS Components Mass kg	(lbm)
2-1	3.2	(7.1)	8.1	(17.8)	2.3	(5.0)	2.2	(4.9)	0.5	(1.0)	1.5	(3.4)	0.7	(1.6)	19	(41)
2-2 *			7.5	(16.6)	2.1	(4.6)			0.4	(0.9)	1.4	(3.1)	0.7	(1.5)	18	(39)
2-3			7.2	(15.8)	2.0	(4.3)			0.4	(0.9)	1.3	(2.9)	0.7	(1.5)	17	(37)
2-4	6.9	(15.3)	10.0	(22.0)	2.5	(5.5)			0.5	(1.1)	1.7	(3.8)	1.1	(2.4)	25	(55)
2-5			9.2	(20.3)	2.3	(5.0)			0.5	(1.0)	1.5	(3.4)	1.0	(2.3)	24	(52)
2-6			9.0	(19.8)	2.2	(4.9)			0.5	(1.0)	1.5	(3.3)	1.0	(2.2)	23	(51)
2-7	18.8	(41.5)	12.4	(27.4)	3.0	(6.6)			0.6	(1.4)	2.1	(4.7)	2.0	(4.3)	41	(91)
2-8			11.7	(25.8)	2.8	(6.2)			0.6	(1.3)	2.0	(4.4)	1.9	(4.2)	40	(88)
2-9			11.4	(25.2)	2.7	(6.0)			0.6	(1.3)	1.9	(4.2)	1.9	(4.1)	39	(87)
2-10	2.5	(5.6)	8.8	(19.4)	2.8	(6.1)			0.6	(1.3)	2.0	(4.3)	0.7	(1.6)	20	(43)
2-11			7.8	(17.1)	2.3	(5.0)			0.5	(1.0)	1.6	(3.5)	0.7	(1.5)	18	(39)
2-12			7.5	(16.5)	2.2	(4.8)			0.5	(1.0)	1.5	(3.3)	0.7	(1.5)	17	(38)
2-13	5.6	(12.3)	10.7	(23.5)	2.7	(6.0)			0.6	(1.3)	1.9	(4.2)	1.0	(2.3)	25	(55)
2-14			9.4	(20.8)	2.4	(5.3)			0.5	(1.1)	1.6	(3.6)	1.0	(2.1)	23	(50)
2-15			9.0	(19.9)	2.3	(5.0)			0.5	(1.0)	1.5	(3.4)	1.0	(2.1)	22	(49)
2-16	15.1	(33.2)	15.9	(35.1)	3.9	(8.5)			0.9	(1.9)	2.9	(6.4)	1.9	(4.2)	43	(94)
2-17			14.1	(31.0)	3.4	(7.5)			0.7	(1.6)	2.5	(5.5)	1.8	(4.0)	40	(88)
2-18			13.7	(30.1)	3.3	(7.3)			0.7	(1.6)	2.4	(5.3)	1.8	(3.9)	39	(86)
2-19	2.1	(4.7)	10.9	(24.1)	4.4	(9.8)			1.0	(2.2)	3.4	(7.6)	0.8	(1.8)	25	(55)
2-20			8.5	(18.7)	2.9	(6.3)			0.6	(1.3)	2.0	(4.5)	0.7	(1.5)	19	(42)
2-21			8.0	(17.6)	2.6	(5.7)			0.5	(1.2)	1.8	(4.0)	0.7	(1.5)	18	(40)
2-22	4.6	(10.2)	12.7	(28.0)	3.5	(7.7)			0.8	(1.7)	2.6	(5.7)	1.1	(2.4)	28	(61)
2-23			10.0	(22.0)	2.6	(5.7)			0.5	(1.2)	1.8	(4.0)	1.0	(2.1)	23	(50)
2-24			9.3	(20.6)	2.4	(5.3)			0.5	(1.1)	1.6	(3.6)	0.9	(2.0)	22	(48)
2-25	1.6	(3.5)	11.9	(26.3)	7.3	(16.0)			1.8	(3.9)	5.9	(13.1)	0.9	(1.9)	32	(70)
2-26			10.2	(22.5)	5.0	(11.0)			1.1	(2.5)	3.9	(8.5)	0.8	(1.7)	25	(55)
2-27	3.5	(7.7)	13.2	(29.2)	4.1	(9.0)			1.0	(2.1)	3.1	(6.9)	1.0	(2.3)	28	(62)
2-28			11.3	(25.0)	3.3	(7.2)			0.7	(1.6)	2.4	(5.2)	1.0	(2.1)	24	(54)

* Selected

FIGURE 18
ACS COMPONENT MASSES, 22.7 kW/m^2 (2 BTU/SEC FT^2)

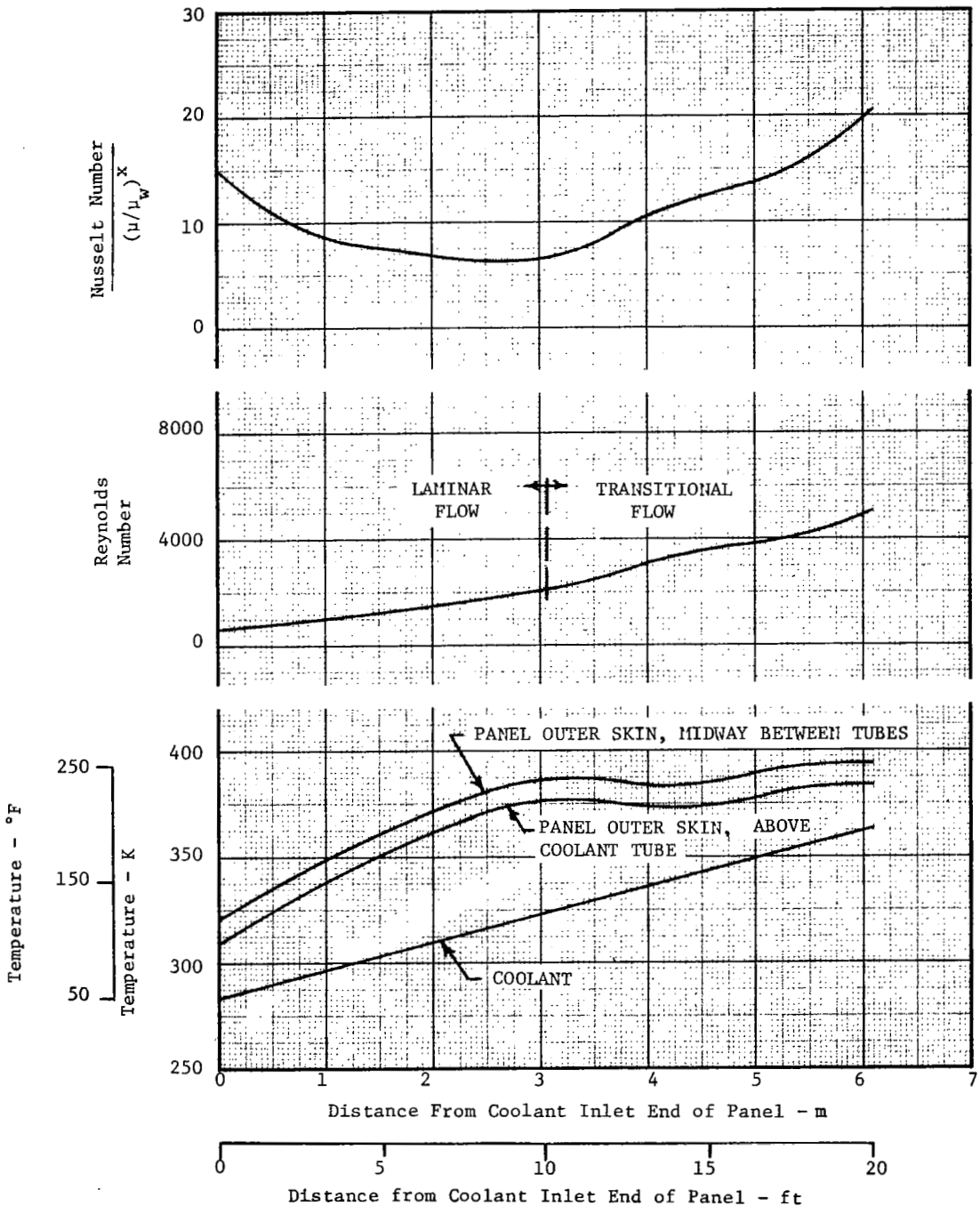

FIGURE 20
THERMAL CHARACTERISTICS, PANEL DESIGNED FOR 22.7 kW/m^2 (2 BTU/SEC FT^2)

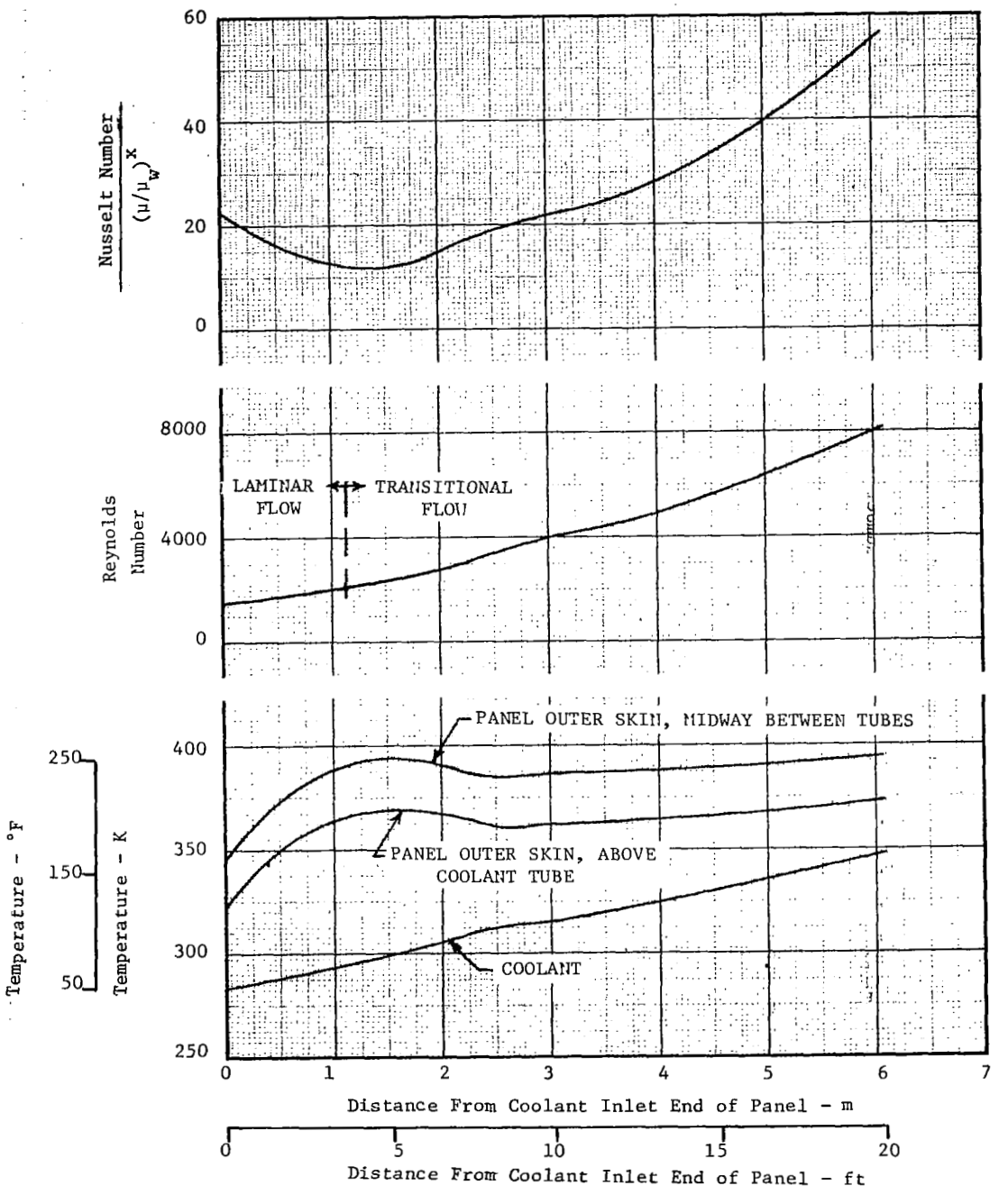

FIGURE 21
THERMAL CHARACTERISTICS, PANEL DESIGNED FOR 56.7 kW/m^2 (5 BTU/SEC FT^2)

These characteristics imply that forcing the coolant flow to be more turbulent by increasing flow rate, hence increasing internal heat transfer, would be advantageous. However, for a specified panel geometry, only one coolant flow will exactly satisfy the structural temperature criteria. Forcing the flow to become more turbulent simply by increasing the flow rate will overcool the panel and produce higher pressure drops. This will increase ACS component masses. If tube pitch were increased to reduce panel structural mass, the higher flow-per-tube requirement would increase flow turbulence. Total mass charged to the panel would also be increased with this approach, as shown by data from Figures 16 and 17:

Constants: Maximum Panel Temperature = 394 K (250°F)
Outer Skin Thickness = 1.02 mm (0.040 in)
Coolant Tube Diameter = 0.48 cm (3/16 in)

Tube Pitch		Heating Rate		Flow/Tube		Reynolds	Panel Mass	
cm	(in)	kW/m^2	($Btu/sec\ ft^2$)	g/s	(lbm/hr)	Number	kg	(lbm)
2.54	(1.0)	22.7	(2)	13.4	(106)	5200	113	(249)
3.81	(1.5)	22.7	(2)	23.2	(184)	7100	113	(250)
5.08	(2.0)	22.7	(2)	46.7	(370)	9000	126	(278)
2.54	(1.0)	56.7	(5)	40.6	(322)	12000	143	(315)
3.18	(1.25)	56.7	(5)	72.5	(575)	14000	186	(410)
3.81	(1.5)	56.7	(5)	171.5	(1360)	20000	330	(727)

These trends show that the "brute force" method of increasing coolant flow to improve the panel's heat transfer characteristics can produce a significant mass penalty. Therefore, more sophisticated techniques must be used to design panels to accommodate higher levels of heating at an acceptable penalty.

The uniform surface heating rates for the baseline panels produced small thermal gradients, as shown in Figures 20 and 21, and the resulting thermal stresses were small in comparison to the mechanical stresses. For all cases, thermal stresses were compression in the inner and outer cover skins and tensile in the tubes. The established criteria was that thermal and mechanical stresses would be superimposed only when they were additive. Consequently, the maximum skin compression stresses occurred when thermal stresses were combined with mechanical stresses resulting from in-plane compression load. The maximum skin tension stress occurred with in-plane tension load acting alone. The maximum tube tension stress occurred in the tubes when thermal stresses were combined with panel tensile in-plane loading and outward acting normal pressure.

Skin margins of safety were based on face sheet wrinkling and face sheet dimpling allowables when addressing compression stresses and on tension allowables associated with growth of cracks from fastener holes when addressing tension stresses. Since the skin tension stress allowables were always less than the compression allowables, tension stresses were always critical for sizing the baseline panel skins.

The tubes were always critical in tension when thermal and mechanical stresses were superimposed. However, for the .071 mm (0.028 in) tube wall thickness used in the study a positive margin of safety was always obtained in the tubes. Hence, the skins were the critical panel elements and they were critical for fatigue crack propagation under cyclical stresses ranging from maximum compression to those resulting from mechanical tension loading. As a result, thermal stresses did not impact panel mass with the range of parameters and groundrules specified for this study.

The calculated stresses for configuration 2-2 (the selected configuration at the lower heating rate) were as follows:

Item	Outer Skin		Inner Skin		Tube	
	MPa	(lbf/in^2)	MPa	(lbf/in^2)	MPa	(lbf/in^2)
Thermal Stress	-8.4	(-1220)	-0.8	(-120)	10.5	(1530)
Mechanical Stress	±143.1	(±20760)	±156.4	(±22680)	±136.6	(±19810)
Max. Total Stress	-151.5	(-21980)	-157.2	(-22800)	147.1	(21340)

The most critical stress was the mechanical tension stress alone in the inner skin with a margin of safety equal to $\left(\frac{\text{allowable stress}}{\text{ultimate stress}}\right) - 1.0 = \left(\frac{160.3}{156.4}\right) - 1.0 = \left(\frac{23250}{22800}\right) - 1.0 = +0.02$. The calculated stresses for configuration 5-5 (the selected configuration at the higher heating rate) were as follows:

Item	Outer Skin		Inner Skin		Tube	
	MPa	(lbf/in^2)	MPa	(lbf/in^2)	MPa,	(lbf/in^2)
Thermal Stress	-28.8	(-4180)	-14.5	(-2110)	28.5	(4130)
Mechanical Stress	±141.3	(±20500)	±159.3	(±23110)	±134.9	(±19560)
Max. Total Stress	-170.1	(-24680)	-173.8	(-25220)	163.4	(23690)

Again, the most critical stress was the mechanical tension stress alone in the inner skin with a margin of safety of $\left(\frac{160.3}{159.3}\right) - 1.0 = \left(\frac{23250}{23110}\right) - 1.0 = +0.01$.

Each of the baseline configurations were analyzed as described above to determine the combination of inner skin thickness and panel height that resulted in minimum mass. Figure 22 presents those results.

Figure 13 presents a plot of unit structural mass (mass per unit area) versus panel height for the combination of a 1.02 mm (.040 in) outer skin thickness, 2.54 cm (1.0 in) tube pitch and both 0.48 cm (3/16 in) and 0.64 (1/4 in) tube diameters, the combinations selected for the baseline panel designs. The other combinations of outer skin thickness, tube pitch and tube diameter produced similar results. Figure 13 shows that, although for a given configuration, a single combination of panel height and inner skin thickness yields the minimum mass, reasonably small deviations from that panel height cause only very small increases in mass.

The total panel structural mass for each configuration, shown in Figures 16 and 17, includes the mass of the manifolds and joint materials defined in Figure 15. This mass was 33.7 kg (74.0 lbm) for all baseline cases. As shown in Figures 16 and 17, the structural mass differences between various configurations was significant but not as great as the ACS component mass differences.

Configuration	Outer Skin Thickness		Inner Skin Thickness		Panel Height		Unit Mass	
	mm	(in)	mm	(in)	mm	(in)	kg/m^2	(lbm/ft^2)
2-1, 5-1	0.64	(0.025)	0.89	(.035)	2.97	(1.17)	6.49	(1.33)
2-2*, 5-2	1.02	(0.040)	0.64	(.025)	2.57	(1.01)	6.64	(1.36)
2-3, 5-3	1.27	(0.050)	0.46	(.018)	2.72	(1.07)	6.93	(1.42)
2-4, 5-4	0.64	(0.025)	0.79	(.031)	3.65	(1.11)	6.49	(1.33)
2-5, 5-5*	1.02	(0.040)	0.51	(.020)	2.77	(1.09)	6.74	(1.38)
2-6, 5-6	1.27	(0.050)	0.41	(.016)	2.72	(1.07)	7.13	(1.46)
2-7, 5-7	0.64	(0.025)	0.58	(.023)	2.74	(1.08)	6.64	(1.36)
2-8, 5-8	1.02	(0.040)	0.41	(.016)	2.72	(1.07)	7.18	(1.47)
2-9, 5-9	1.27	(0.050)	0.41	(.016)	2.44	(0.96)	7.71	(1.58)
2-10	0.64	(0.025)	0.99	(.039)	2.77	(1.09)	6.49	(1.33)
2-11, 5-10	1.02	(0.040)	0.66	(.026)	2.67	(1.05)	6.59	(1.35)
2-12, 5-11	1.27	(0.050)	0.48	(.019)	2.62	(1.03)	6.84	(1.40)
2-13, 5-12	0.64	(0.025)	0.89	(.035)	2.72	(1.07)	6.49	(1.33)
2-14, 5-13	1.02	(0.040)	0.58	(.023)	2.67	(1.05)	6.69	(1.37)
2-15, 5-14	1.27	(0.050)	0.46	(.018)	2.62	(1.03)	6.98	(1.43)
2-16, 5-15	0.64	(0.025)	0.71	(.028)	2.67	(1.05)	6.54	(1.34)
2-17, 5-16	1.02	(0.040)	0.48	(.019)	2.62	(1.03)	6.93	(1.42)
2-18, 5-17	1.27	(0.050)	0.41	(.016)	2.57	(1.01)	7.37	(1.51)
2-19	0.64	(0.025)	1.04	(.041)	2.72	(1.07)	6.49	(1.33)
2-20, 5-18	1.02	(0.040)	0.69	(.027)	2.72	(1.07)	6.54	(1.34)
2-21, 5-19	1.27	(0.050)	0.53	(.021)	2.62	(1.03)	6.79	(1.39)
2-22	0.64	(0.025)	0.97	(.038)	2.67	(1.05)	6.49	(1.33)
2-23, 5-20	1.02	(0.040)	0.64	(.025)	2.62	(1.03)	6.59	(1.35)
2-24, 5-21	1.27	(0.050)	0.48	(.019)	2.62	(1.03)	6.88	(1.41)
2-25	1.02	(0.040)	0.74	(.029)	2.67	(1.05)	6.54	(1.34)
2-26	1.27	(0.050)	0.56	(.022)	2.62	(1.03)	6.69	(1.37)
2-27	1.02	(0.040)	0.71	(.028)	2.51	(0.99)	6.54	(1.34)
2-28	1.27	(0.050)	0.53	(.021)	2.57	(1.01)	6.79	(1.39)

*SELECTED

FIGURE 22
BASELINE PANEL GEOMETRIES AND UNIT MASSES

4. TWO-DIMENSIONAL INTERFERENCE HEATING PATTERNS

Three typical interference heating patterns that could be experienced on high speed aircraft were considered. These design conditions, illustrated by Figure 23, are two-dimensional, in that the local heating rate varies with the panel lengthwise location but not widthwise. In each case the total panel is exposed to a uniform surface heating rate, with an additional heat load being superimposed over a portion of the panel. The heating rate distributions are bell-shaped (sinusoidal, $\phi = 0$ to π). The superimposed distributions extend 0.91 m (3 ft) along the panel length and cover the full 1.52 m (5 ft) width. The nominal location of the peak heating is 1.22 m (4 ft) from one end of the panel. A potential 0.3 m (1 ft) lengthwise shift in the pattern was acknowledged during design studies.

A primary study objective was to identify practical cooled panel concepts that could maintain the maximum structural temperature at 394 K (250°F) when exposed to these heating patterns with minimal mass penalty. A preliminary understanding was obtained by analyzing the effects of the specified heating patterns on the baseline cooled panels.

The results are summarized in Figure 24. The baseline panel configurations, described in Section 3.4, would experience excessive surface temperatures near the locus of peak interference heating, which was assumed to be 1.22 m (4 ft) from the panel coolant inlet end. Imposing Design Conditions 1 and 2 on the baseline panel designed for a uniform 22.7 kW/m^2 (2 Btu/sec ft^2) heating rate produced maximum temperatures of 411 K (280°F) and 547 K (525°F) respectively. If the Design Condition 3 heating pattern would cross a panel designed for a constant 56.7 kW/m^2 (5 Btu/sec ft^2), a maximum surface temperature of 522 K (480°F) would be experienced.

These results verify that interference heating can impose severe design requirements on aircraft configured with actively cooled structure. The analyses conducted to determine which cooled panel design modifications provide the best solutions to this design challenge are discussed in this section.

4.1 Candidate Panel Design Concepts

The candidate design concepts for regions exposed to interference heating are described in this section. Analytical evaluations are presented in Section 4.3.

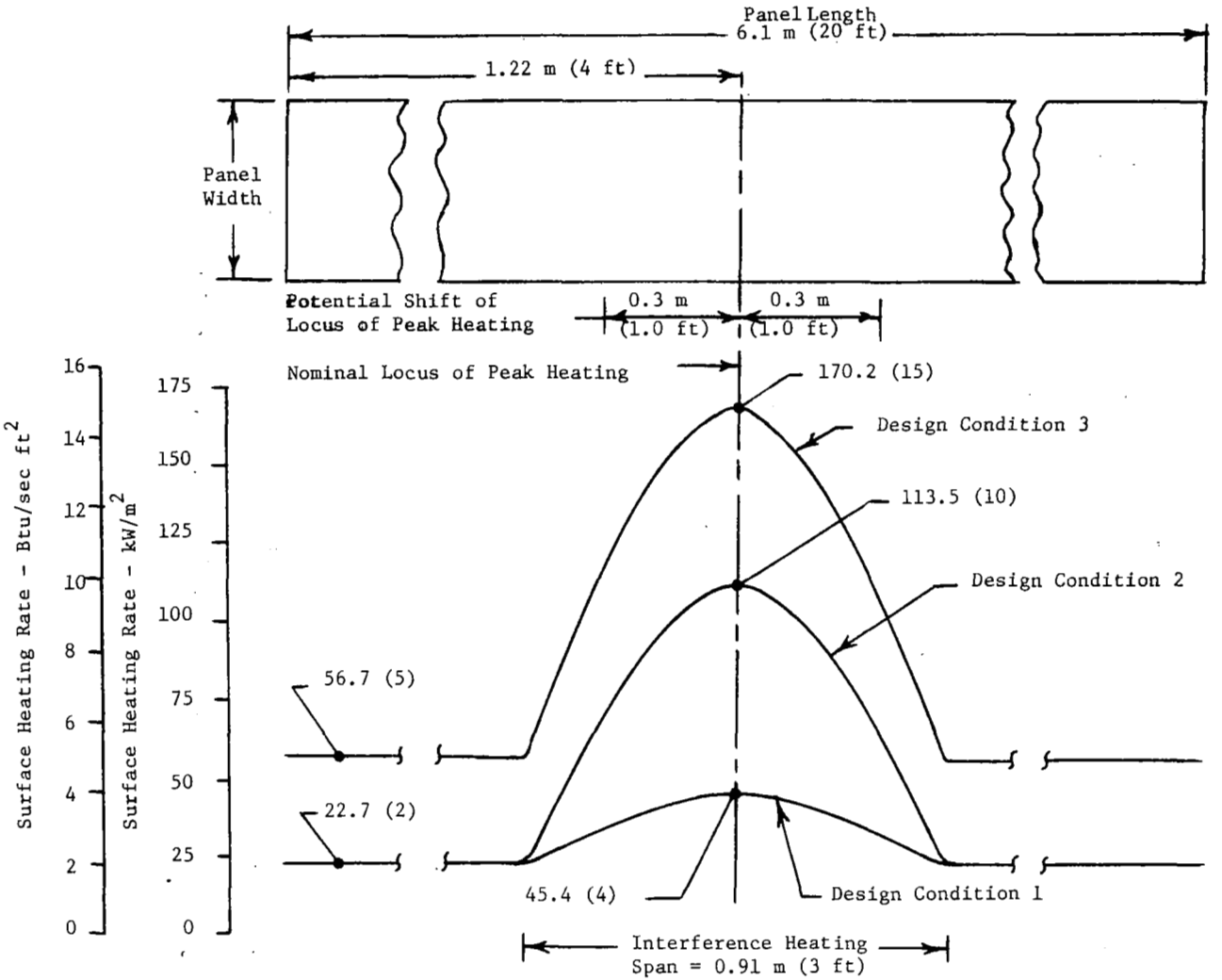

FIGURE 23
TWO DIMENSIONAL INTERFERENCE HEATING DESIGN CONDITIONS

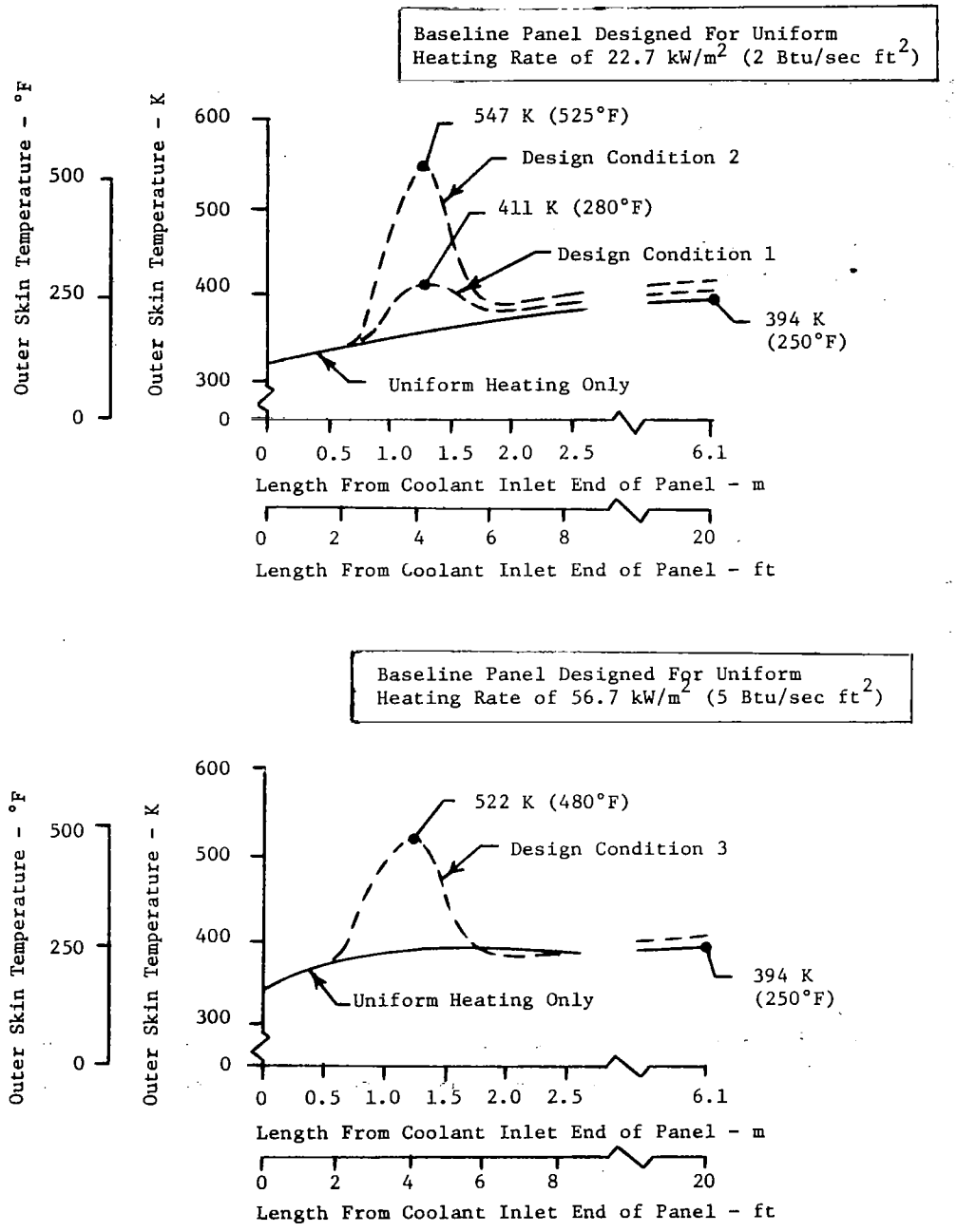

FIGURE 24
EFFECT OF INTERFERENCE HEATING ON BASELINE PANEL DESIGNS

A logical solution for a modestly increased heat load is a Modified Baseline Panel Concept. The baseline panel analyses, Section 3.4, revealed that two minor modifications to the basic configuration could improve heat transfer characteristics. First, simply increasing the coolant flow is beneficial up to the point that the pressure drop penalties outweigh the improved heat transfer. Secondly, tube pitch restricted to 2.54 cm (1.0 in), because of panel assembly conditions, could be decreased to 1.91 cm (0.75 in) when smaller coolant tubes of 0.48 cm (3/16 in) were used. Reducing the pitch effectively minimizes panel mass.

The thickness of the outer skin has a strong influence on the thermal efficiency. Peak structural temperatures occur in the outer skin midway between coolant tubes. Heat is conducted laterally through the skin to the coolant tubes, with the thermal resistance being inversely proportional to skin thickness. Thus, a Thickened Skin Concept was studied to determine the benefit of varying this parameter. This concept, Figure 25, was configured with the skin thickened only in the region exposed to interference heating, to avoid an unnecessary mass penalty.

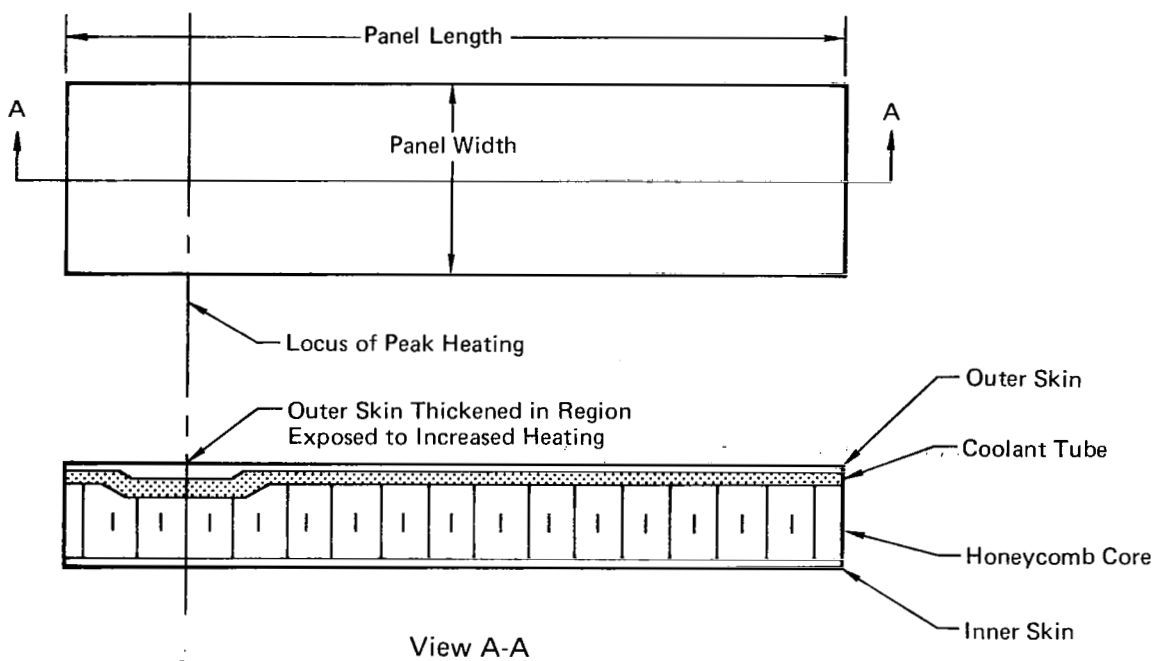

FIGURE 25
THICKENED SKIN CONCEPT

Three concepts were studied to evaluate the potential benefits of closer tube spacing on the end of the panel exposed to interference heating. These were the Intermediate Manifold Concept, the Branched Tubes Concept, and the Separate Panels Concept, shown in Figure 26. In the first concept, an intermediate manifold is used to redistribute the coolant to an increased number of tubes in the region of the panel exposed to interference heating. Since the flow boundary layer origin is re-established, the local heat transfer coefficient is higher.

The Branched Tubes Concept was studied to evaluate the benefits of dividing the upstream flow into two closely spaced downstream tubes. The upstream tube spacing is thus dictated by the minimum allowable downstream tube spacing.

The Separate Panels Concept provides an independent panel, configured specifically for the small section affected by interference heating without influencing the remainder of the panel region. As indicated in Figure 26, two tube orientations were investigated for the separate panel.

Another generalized design concept, High Heat Transfer Tubes, was investigated. Techniques to augment the convective heat transfer inside the tubes were analyzed following library research. As indicated in Figure 27, numerous techniques based on promoting flow turbulence were examined. The increased heat transfer benefits had to be traded off against the penalties associated with increased pressure drop.

Other studies, such as those summarized in References 1 and 2, have acknowledged that cooled hypersonic aircraft will require some degree of shielding to make the total heat load absorbed compatible with the available fuel heat sink. Reference 2 also revealed the additional fail-safe capability afforded by the external surface protection. A current MCAIR study (NAS1-13939) is being conducted to evaluate, both analytically and via testing, a Radiative Actively Cooled Panel design. This design approach also merits consideration for regions exposed to interference heating. Numerous surface protection techniques are possible, ranging from simple surface coating materials to external heat shields backed up by insulation. The Insulated Panel Concept, shown in Figure 28 was selected to typify this approach, since it has been judged to be superior to other concepts in the concurrent MCAIR study and the results of that study were readily accessible.

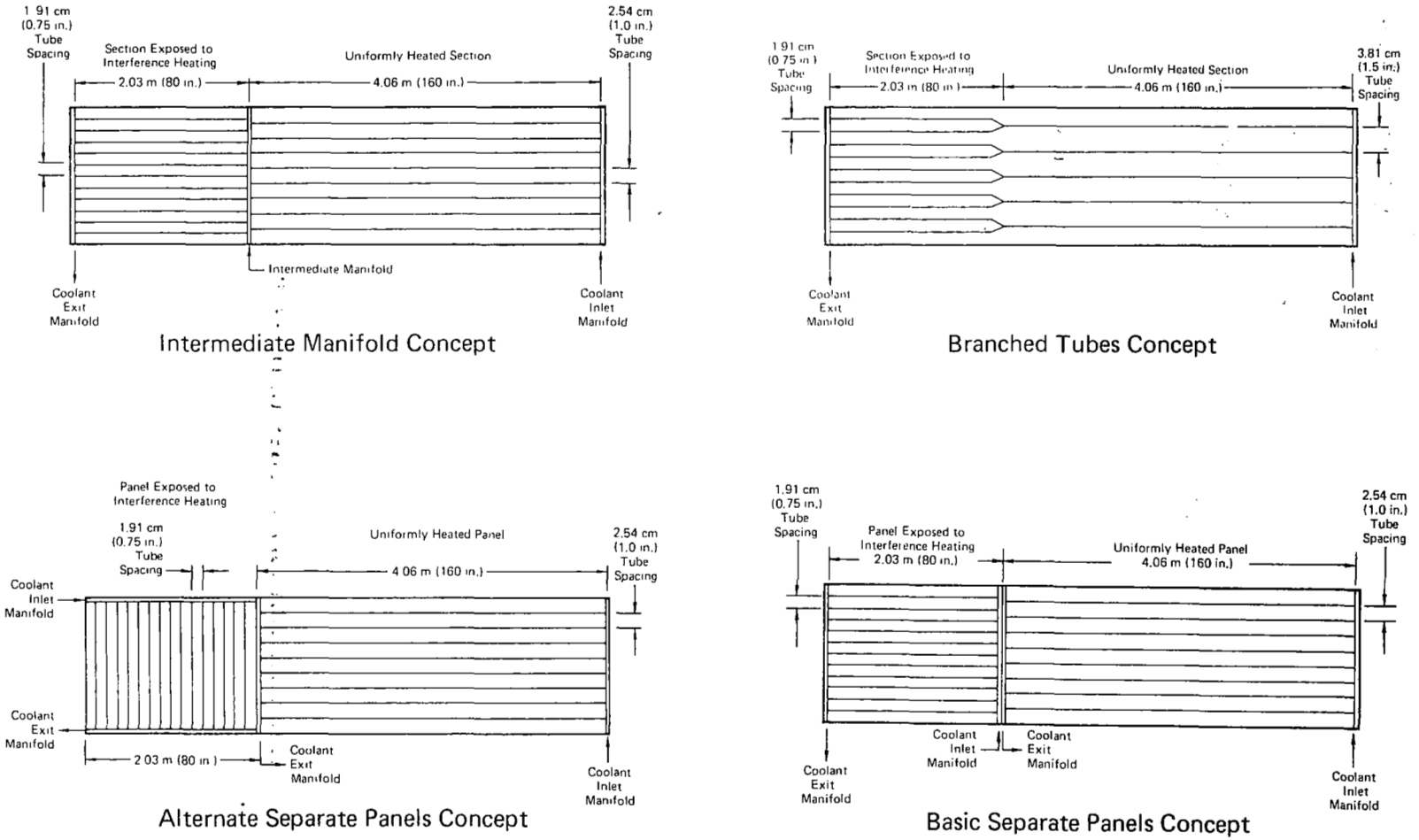

FIGURE 26
INTERMEDIATE MANIFOLD, BRANCHED TUBES, AND SEPARATE PANELS CONCEPTS

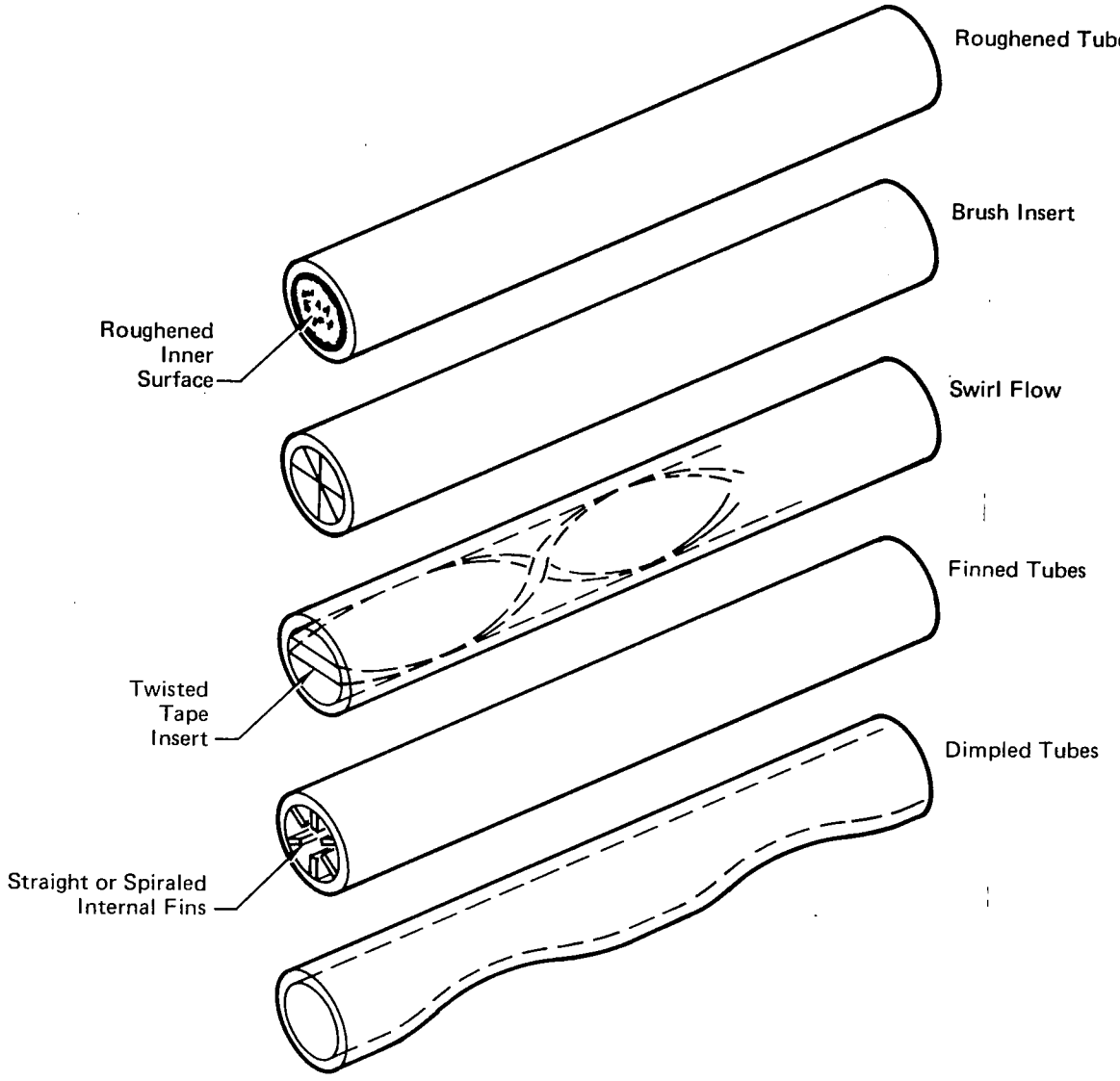

FIGURE 27
HIGH HEAT TRANSFER TUBES CONCEPTS

If only thermodynamic considerations were involved, heating near the coolant exit would be more critical, since the coolant temperature is higher at that point and the rate of heat removal is lower. However, at the inlet end, structural mass requirements could be higher to accommodate more severe stresses caused by the larger temperature gradients.

Analyses were conducted with the baseline panel concepts modified to limit the maximum structural temperature to 394 K (250°F) when exposed to the three specified interference heating design conditions. At each condition, the heating pattern was assumed to be located first at the inlet and then at the exit end of the panel. Figure 30 summarizes the configurations analyzed. ACS component mass requirements were found to be greater, as expected, when the heating pattern is located near the panel coolant exit for all three design conditions. Thermal stresses were found to be sufficiently low such that structural requirements were not affected.

Figure 31 illustrates the conclusion that, thermodynamically, heating at the coolant exit end is more demanding, using Design Condition 1 as an example. When the peak heating is at the exit end, the maximum panel outer skin temperatues exceed 394 K (250°F). To reduce maximum temperatures to 394 K (250°F) coolant flow must be increased. This increases the mass of ACS components.

As a result of these analyses, it was concluded that the exit location was more demanding and subsequent concept evaluations considered only that location.

Another conclusion, apparent from Figure 30, is that a small shift in the heating pattern location, such as the $\pm$0.3 m (1 ft) shift examined, would not significantly impact panel mass. Even extreme shifts would produce mass differences of 10 percent and less. Therefore, subsequent concepts were designed to recognize the possibility of a $\pm$ 0.3 m (1 ft) shift in the heating pattern by structural arrangement concessions, but ACS component requirements were assumed to be insensitive to that effect.

4.3 Concept Evaluation

Each candidate concept was analyzed to determine a minimum mass configuration for each of the three design conditions. These analyses are described below.

Interference Heating Location	Design Condition	Tube Pitch cm (in)	Tube Diameter cm (in)	Coolant Flow/Tube g/s (lbm/hr)	Panel ΔP kPa (lbf/in^2)	Panel Structural Mass kg (lbm)	ACS Components Mass kg (lbm)	Total Mass kg (lbm)
NEAR INLET	1	2.54 (1.00)	0.48 (3/16)	18.9 (150)	379 (55)	98 (216)	22 (49)	120 (265)
NEAR EXIT	1	2.54 (1.00)	0.48 (3/16)	23.3 (185)	558 (81)	98 (216)	26 (58)	124 (274)
NEAR INLET	2	1.91 (0.75)	0.48 (3/16)	47.3 (375)	2200 (319)	103 (228)	74 (163)	177 (391)
NEAR EXIT	2	1.91 (0.75)	0.48 (3/16)	50.4 (400)	2585 (375)	103 (228)	82 (181)	186 (409)
NEAR INLET	3	1.91 (0.75)	0.48 (3/16)	88.3 (700)	6205 (900)	99 (219)	203 (448)	303 (667)
NEAR EXIT	3	1.91 (0.75)	0.48 (3/16)	92.7 (735)	7240 (1050)	99 (219)	234 (516)	333 (735)

FIGURE 30
CONFIGURATIONS ANALYZED TO ESTABLISH CRITICAL HEATING PATTERN LOCATION

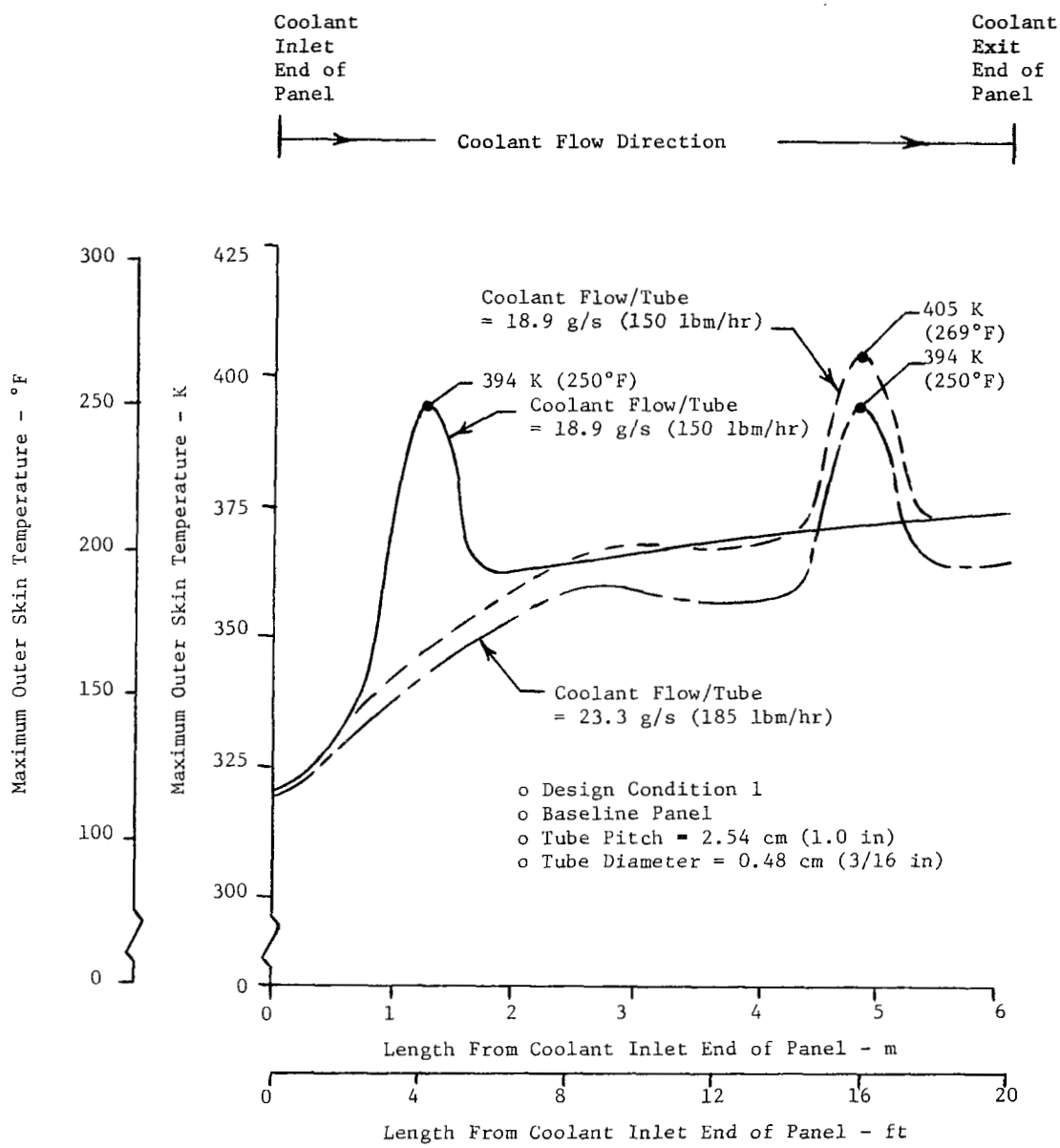

FIGURE 31
HEATING PATTERN LOCATED NEAR COOLANT EXIT END OF PANEL REQUIRES INCREASED COOLANT FLOW

4.3.1 Modified Baseline Panel Concept - The configurations studied to establish the critical heating pattern location, as discussed in Section 4.2, were Modified Baseline Panel Concepts. Figure 32 summarizes the Modified Baseline Panel Concepts sized for heating patterns located near the coolant exit end of the panel. For Design Condition 1 the baseline panel sized for a uniform heating rate of 22.7 kW/m^2 (2 $Btu/sec\ ft^2$), modified only by increasing the coolant flow per tube from 13.4 g/s (106 lbm/hr) to 23.3 g/s (185 lbm/hr), was examined (Configuration 2). This nonstructural modification resulted in an 11.3 kg (25 lbm), or 10 percent, panel mass increase. By reducing the coolant tube pitch to 1.91 cm (0.75 in) to require a smaller increase in coolant flow per tube, Configuration 1, the change in the mass of ACS components was negligible. In fact, reducing the tube pitch produced a slight increase in overall panel mass, since the structural mass increased about 0.91 kg (2 lbm).

At Design Condition 2, coolant flow requirements for the Modified Baseline Panel Concept with 0.48 cm (3/16 in) tubes at 2.54 cm (1.0 in) spacing were very large. This resulted in excessive pressure drops. Therefore, as shown in Figure 32, only alternate concepts, with either reduced tube pitch or increased tube diameter, were considered. The concept with a pitch reduction to 1.91 cm (0.75 in), Configuration 3, resulted in a significantly lower mass. Even though the pressure drops are not as critical with the larger tubes, the coolant flow requirements increase the mass of ACS components severely.

At Design Condition 3, only one configuration was found to satisfy the maximum structural temperature criterion without excessive flow or pressure drop. Even in this case, the total panel mass of 333 kg (735 lbm) was nearly 2.4 times that of the baseline panel sized for a uniform heating rate of 56.7 kW/m^2 (5 $Btu/sec\ ft^2$).

The panel geometry and unit structural masses are shown in Figure 33. Selected maximum mechanical, thermal, and total stresses and margins of safety are summarized in Figure 34. In all cases, the thermal stresses were found to be compressive in the skins and tensile in the tubes. The mechanical stresses were reversible, as explained in Section 3.3, and therefore, additive to the thermal stresses when of the same sign. Where thermal stresses would relieve mechanical stresses, the relief was neglected. Figure 34 shows that the maximum combined compression stresses in the outer and inner skin were -197.0 MPa (-28,570 lbf/in^2) and -169.8 MPa (-24,640 lbf/in^2),

Configuration	Design Condition	Tube Pitch cm (in)	Tube Diameter cm (in)	Coolant Flow/Tube g/s (lbm/hr)	Panel ΔP kPa (lbf/in^2)	Panel Structural Mass kg (lbm)	ACS Components Mass kg (lbm)	Total Mass kg (lbm)
MOD. BASE. 1	1	1.91 (0.75)	0.48 (3/16)	17.1 (136)	331 (48)	99 (218)	26 (58)	125 (276)
MOD. BASE. 2	1	2.54 (1.00)	0.48 (3/16)	23.3 (185)	558 (81)	98 (216)	26 (58)	124 (274)
MOD. BASE. 3	2	1.91 (0.75)	0.48 (3/16)	50.4 (400)	2585 (375)	103 (228)	82 (181)	186 (409)
MOD. BASE. 4	2	2.54 (1.00)	0.64 (1/4)	128.6 (1020)	2140 (310)	106 (234)	131 (288)	237 (522)
MOD. BASE. 5	2	2.54 (1.00)	0.95 (3/8)	180.3 (1430)	359 (52)	110 (243)	192 (423)	302 (666)
MOD. BASE. 6	3	1.91 (0.75)	0.48 (3/16)	92.7 (735)	7240 (1050)	99 (219)	234 (516)	333 (735)

Note: All configurations have outer skin thickness = 1.02 mm (0.040 in)

Configuration	Coolant In Panel kg (lbm)	Coolant in Distribution Lines kg (lbm)	Coolant Distribution Lines kg (lbm)	Heat Exchanger kg (lbm)	Pumps kg (lbm)	Pumping Power Penalty kg (lbm)	Reservoir kg (lbm)	Total ACS Components Mass kg (lbm)
MOD. BASE. 1	4.3 (9.4)	11.7 (25.7)	3.5 (7.7)	2.4 (5.3)	0.8 (1.7)	2.6 (5.7)	1.1 (2.4)	26 (58)
MOD. BASE. 2	3.2 (7.1)	11.9 (26.2)	4.0 (8.9)	↓	0.9 (2.0)	3.1 (6.8)	1.0 (2.1)	26 (58)
MOD. BASE. 3	4.3 (9.4)	27.4 (60.4)	19.4 (42.7)	3.0 (6.7)	6.0 (13.2)	20.1 (44.4)	2.1 (4.6)	82 (181)
MOD. BASE. 4	6.9 (15.3)	45.3 (99.9)	28.3 (62.5)	↓	10.0 (22.1)	33.7 (74.2)	3.2 (7.1)	131 (288)
MOD. BASE. 5	18.8 (41.5)	104.3(229.9)	31.6 (69.7)	↓	6.2 (13.6)	20.7 (45.6)	7.4(16.4)	192 (423)
MOD. BASE. 6	4.3 (9.4)	43.1 (95.0)	66.9 (147.4)	6.6 (14.5)	25.2 (55.5)	84.6 (186.6)	3.2 (7.1)	234 (516)

FIGURE 32
SUMMARY OF MODIFIED BASELINE PANEL CONCEPT CONFIGURATIONS

Configuration	Panel Height		Interference Heating Area						Uniform Heating Area			
			Ultimate Pressure		Inner Skin Thickness		Structural Unit Mass		Inner Skin Thickness		Structural Unit Mass	
	cm	(in)	kPa	(lbf/in^2)	mm	(in)	kg/m^2	(lbm/ft^2)	mm	(in)	kg/m^2	(lbm/ft^2)
MOD. BASE. 1	2.59	(1.02)	29.9	(4.34)	0.86	(.034)	7.57	(1.55)	0.56	(.022)	6.74	(1.38)
MOD. BASE. 2	2.62	(1.03)	29.9	(4.34)	0.91	(.036)	7.42	(1.52)	0.64	(.025)	6.64	(1.36)
MOD. BASE. 3	3.58	(1.41)	97.9	(14.20)	1.52	(.060)	9.42	(1.93)	0.46	(.018)	6.59	(1.35)
MOD. BASE. 4	3.28	(1.29)	97.9	(14.20)	1.52	(.060)	9.76	(2.00)	0.48	(.019)	6.79	(1.39)
MOD. BASE. 5	2.82	(1.11)	97.9	(14.20)	1.52	(.060)	10.25	(2.10)	0.41	(.016)	7.18	(1.47)
MOD. BASE. 6	2.95	(1.16)	51.3	(7.44)	1.07	(.042)	8.10	(1.66)	0.51	(.020)	6.59	(1.35)

FIGURE 33
MODIFIED BASELINE PANEL CONCEPT GEOMETRIES AND UNIT MASSES

Configuration and Item	Ultimate Stresses and Margins of Safety					
	Outer Skin		Inner Skin		Tube	
	MPa	(lbf/in^2)	MPa	(lbf/in^2)	MPa	(lbf/in^2)
MOD. BASE. 2						
Thermal Stress	-19.0	(-2760)	-3.8	(-550)	29.4	(4260)
Mechanical Stress	$\pm$147.2	($\pm$21350)	$\pm$159.5	($\pm$23130)	$\pm$138.4	($\pm$20080)
Max. Compression Stress	-166.2	(-24110)	-163.3	(-23680)	-138.4	(-20080)
Max. Tension Stress	147.2	(21350)	159.5	(23130)	167.8	(24340)
Allowable Tension Stress	160.3	(23250)	160.3	(23250)	237.9	(34500)
Min. Margin of Safety			+0.01 Tension			
MOD. BASE. 3						
Thermal Stress	-33.4	(-4850)	-5.9	(-860)	48.6	(7050)
Mechanical Stress	$\pm$158.6	($\pm$23010)	$\pm$149.3	($\pm$21660)	$\pm$145.6	($\pm$21120)
Max. Compression Stress	-192.1	(-27860)	-155.2	(-22520)	-145.6	(-21120)
Max. Tension Stress	158.6	(23010)	149.3	(21660)	194.2	(28170)
Allowable Tension Stress	160.3	(23250)	160.3	(23250)	237.9	(34500)
Min. Margin of Safety	+0.01 Tension					
MOD. BASE. 6						
Thermal Stress	-50.1	(-7260)	-10.3	(-1500)	73.8	(10700)
Mechanical Stress	$\pm$146.9	($\pm$21310)	$\pm$159.5	($\pm$23140)	$\pm$138.4	($\pm$20080)
Max. Compression Stress	-197.0	(-28570)	-169.8	(-24640)	-138.4	(-20080)
Max. Tension Stress	146.9	(21310)	159.5	(23140)	212.2	(30780)
Allowable Tension Stress	160.3	(23250)	160.3	(23250)	237.9	(34500)
Min. Margin of Safety			0.00 Tension			

FIGURE 34
MODIFIED BASELINE PANEL CONCEPT STRESSES AND MARGINS OF SAFETY

respectively. These stresses were not critical because in no case were the allowable face sheet wrinkling stresses and face sheet dimpling stresses less than the elastic limit of the material. Because of this and the fact that the skins had no thermal tension stresses in the longitudinal direction, the skins were critical in tension due to mechanical stresses alone and the margins of safety shown are based on this stress. Because the maximum total stresses in the tubes were tension and the allowable tension stresses are smaller than the allowable compression stress, the tubes are also critical in tension. When the thermal stresses were added to the mechanical stresses for panels sized for mechanical stresses only, no negative margins of safety were obtained. Transverse thermal stresses (i.e., acting perpendicular to the direction of the tubes) were determined by use of the KBEB program explained in Section 3.3. The support frames were assumed to be at the same temperature as the panel inner skin and were not included in the thermal stress analysis. Thermal stresses were found to be compressive in the outer and inner skins in the peak heating area and the immediately adjacent uniformly heated areas, graduating to tension in the areas of uniform heating farther from the peak heating. The maximum transverse thermal stresses were for Design Condition 2, a tube pitch of 1.91 cm (.75 in) and a tube diameter of 0.48 cm (3/16 in) and are shown in Figure 35. Because there are no mechanical stresses in the transverse direction, the total transverse stresses are these thermal stresses which are not large enough to be critical. In the peak heating area these transverse stresses were of the same sign (compression) and similar magnitude as

		Region Exposed to Interference Heating		Uniformly Heated Region	
		MPa	(lbf/in^2)	MPa	(lbf/in^2)
Outer Skin:	compression	-102.0	(-14800)	-37.5	(-5440)
	tension	0	(0)	19.9	(2890)
Inner Skin:	compression	- 93.8	(-13600)	-29.0	(-4210)
	tension	0	(0)	22.8	(3300)

FIGURE 35
MAXIMUM TRANSVERSE THERMAL STRESSES - MODIFIED BASELINE PANEL CONCEPT

the longitudinal thermal stresses. Therefore, when combined using the Mohr's Circle Method, the resulting maximum principal stresses were no greater than the larger of the two acting alone. In the uniform heating area, both the transverse and the longitudinal thermal stresses were small and their combination was not critical. The portions of the panels subjected only to uniform heating were sized for the same loads and in the same manner as the baseline panel except that the inner skin thicknesses and panel heights were modified where necessary, as explained in Section 3.3, to maintain a uniform panel height. Where this modification resulted in a mass increase, trade-off analysis was performed to determine the uniform height that produced the smallest total structural mass. The panel structural masses shown in Figure 32 were calculated for each case by multiplying the unit masses for the interference heating and uniform heating portions by their respective panel areas and adding the mass of the manifolds and joint materials. Because it was desirable for structural reasons to have the changes in skin thicknesses at support frames, the location for the changes between the areas designed for the two different heating rates was established at the first frame beyond the interference heating limit. This frame was 2.03 m (80 in) from the coolant outlet end of the panel, making the areas 3.10 m^2(33.33 ft^2) and 6.20 m^2(66.67 ft^2) for the interference heating and uniform heating design portions respectively. The masses of the manifolds and joint materials are the same as for the baseline panel, 33.7 kg (74.0 lbm).

4.3.2 Thickened Skin Concept - The potential benefits of thickening the outer skin in the region of increased heating were investigated. The thickness profile selected for thermal analysis is shown in Figure 36. Basically, the thickness was assumed to be maximum for 15.2 cm (6 in) either side of the locus of peak heating, tapering back to the baseline panel skin thickness of 1.02 mm (0.040 in) over a 30.5 cm (12 in) length on each side. The specified shift of $\pm$ 0.3 m (1 ft) in peak heating was acknowledged by increasing the total length of thickened skin an addition 30.5 cm (12 in) on each side, resulting in a 1.52 m (5 ft) span potentially exposed to interference heating effects.

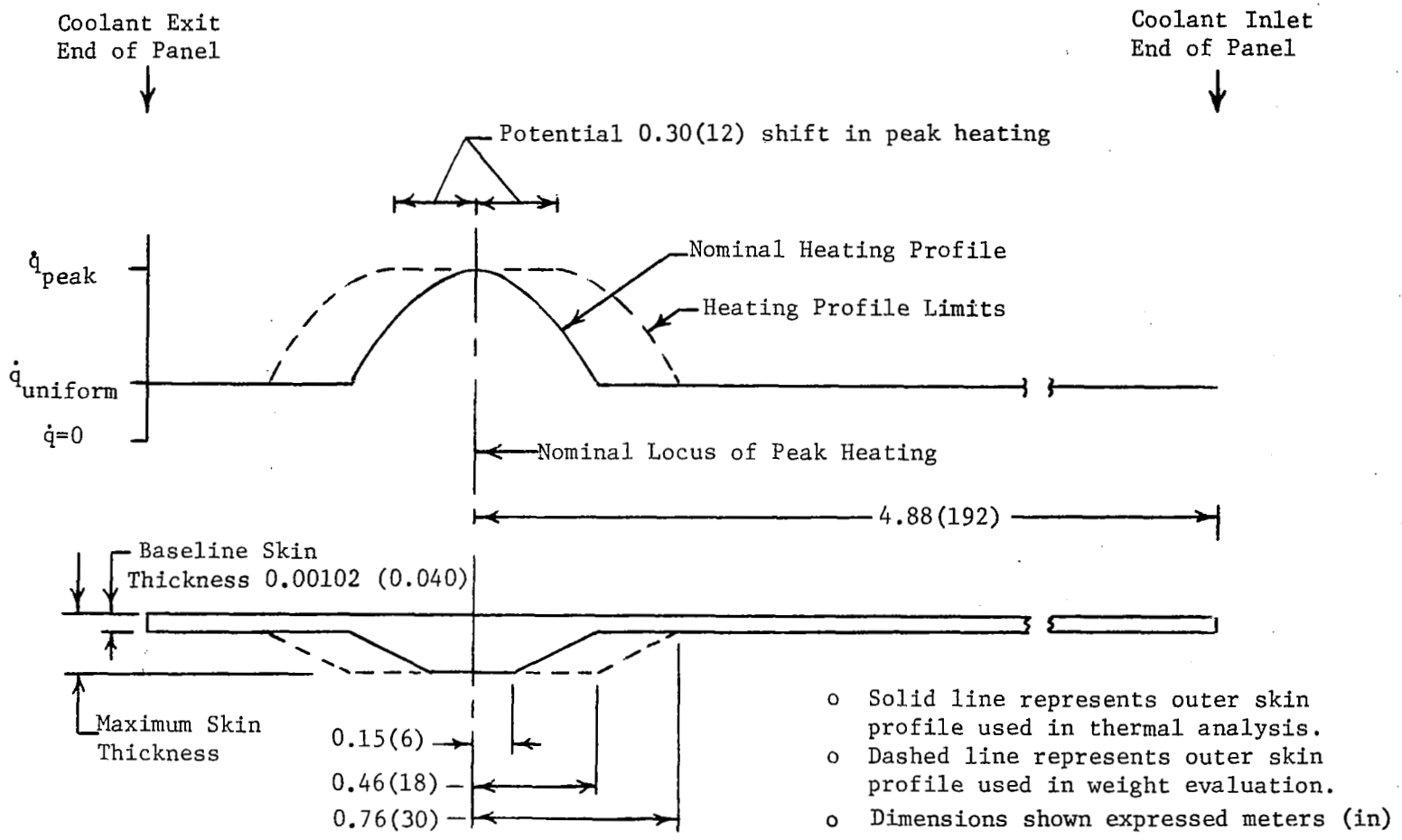

FIGURE 36
OUTER SKIN THICKNESS PROFILE - THICKENED SKIN CONCEPT

Although numerous other thickness profiles were considered, the mass differences were found to be negligible in respect to total panel mass, and the assumed profile would require less sophisticated manufacturing techniques than the alternatives. The tube bend radii are realistic (the angles involved are less severe than those implied by Figure 36) and the straight line skin tapering is achievable.

Since locally thickening the skin inwardly, into the honeycomb core, complicates manufacturing, the possibility of thickening the skin outwardly was considered. This approach would eliminate the necessity for tube bending, reduce the problems involved in bonding the tubes to the skin, and eliminate removal of honeycomb core material. However, this approach was not pursued in detail, since it would have required evaluation of the effects of local moldline protrusions on aircraft performance. This would have necessitated additional effort. This decision was further justified as subsequent producibility evaluation, presented in Section 4.4.2, revealed that the fabrication complexities did not strongly impact the overall ranking of the Thickened Skin Concept.

A parametric study was conducted involving variations in tube pitch and maximum outer skin thickness, up to 1.02 cm (0.4 in), for each of the three design conditions. A tube diameter of 0.48 cm (3/16 in) was used in the analysis, since previous results indicated the importance of maximizing the internal convective heat transfer characteristics. Coolant tube spacings (pitch) of 2.54 cm (1.0 in) and 1.91 cm (0.75 in) were considered.

The resultant converged designs that limit the maximum skin temperature to 394 K (250°F) are summarized in Figure 37. As shown, the coolant flow requirements and the associated pressure drops through the panel do not vary greatly for any of the configurations satisfying Design Condition 1. However, the significantly higher flow requirements and pressure drops experienced by panels with a 2.54 cm (1.0 in) tube pitch for Design Condition 2 and 3 reflect the advantages of minimizing tube pitch, thus reducing the mass of active cooling system components as summarized in Figure 38.

Figure 39 was prepared from the total panel masses presented in Figure 37 for the Thickened Skin Concepts and masses presented previously for the Modified Baseline Panel Concept (representative of a "non-thickened" skin concept).

Configuration	Design Condition	Tube Pitch cm (in)	Tube Diameter cm (in)	Outer Skin Thickness mm (in)	Coolant Flow/Tube g/s (lbm/hr)	Panel ΔP kPa (lbf/in^2)	Panel Structural Mass kg (lbm)	ACS Components Mass kg (lbm)	Total Mass kg (lbm)
THICK. SKIN 1	1	2.54(1.00)	0.48 (3/16)	2.54 (0.1)	18.8 (149)	386 (56)	103 (226)	23 (50)	125 (276)
THICK. SKIN 2	1	↓	↓	5.08 (0.2)	18.0 (143)	359 (52)	115 (253)	22 (48)	137 (301)
THICK. SKIN 3	1	↓	↓	10.16 (0.4)	19.0 (151)	393 (57)	141 (310)	23 (50)	163 (360)
THICK. SKIN 4	1	1.91(0.75)	↓	2.54 (0.1)	15.8 (125)	290 (42)	103 (228)	25 (55)	128 (283)
THICK. SKIN 5	1	↓	↓	10.16 (0.4)	16.1 (128)	303 (44)	142 (312)	25 (55)	166 (367)
THICK. SKIN 6	2	2.54(1.00)	0.48 (3/16)	5.08 (0.2)	54.9 (435)	2895 (420)	119 (263)	73 (160)	192 (423)
THICK. SKIN 7	2	1.91(0.75)	↓	2.54 (0.1)	41.0 (325)	1760 (255)	108 (239)	62 (136)	170 (375)
THICK. SKIN 8	2	↓	↓	10.16 (0.4)	44.1 (350)	2000 (290)	146 (321)	68 (150)	214 (471)
THICK. SKIN 9	3	2.54(1.00)	0.48 (3/16)	5.08 (0.2)	100.9 (800)	8065 (1170)	116 (256)	210 (463)	326 (719)
THICK. SKIN 10	3	1.91(0.75)	↓	2.54 (0.1)	54.2 (430)	2655 (385)	105 (231)	90 (199)	195 (430)
THICK. SKIN 11	3	↓	↓	5.08 (0.2)	53.0 (420)	2550 (370)	117 (258)	87 (192)	204 (450)
THICK. SKIN 12	3	↓	↓	10.16 (0.4)	61.8 (490)	3415 (495)	143 (315)	111 (244)	254 (559)

FIGURE 37
THICKENED SKIN CONCEPT CONFIGURATIONS

Configuration	Coolant In Panel kg	(lbm)	Coolant In Distribution Lines kg	(lbm)	Coolant Distribution Lines kg	(lbm)	Heat Exchanger kg	(lbm)	Pumps kg	(lbm)	Pumping Power Penalty kg	(lbm)	Reservoir kg	(lbm)	Total ACS Components Mass kg	(lbm)
THICK. SKIN 1	3.2	(7.1)	9.9	(21.9)	3.0	(6.7)	2.4	(5.3)	0.7	(1.5)	2.2	(4.9)	1.0	(2.1)	23	(50)
THICK. SKIN 2			9.6	(21.2)	2.9	(6.4)			0.6	(1.4)	2.1	(4.6)	0.9	(2.0)	22	(48)
THICK. SKIN 3			10.1	(22.2)	3.1	(6.9)			0.7	(1.5)	2.3	(5.0)	1.0	(2.1)	23	(50)
THICK. SKIN 4	4.3	(9.4)	10.9	(24.0)	3.2	(7.0)			0.7	(1.5)	2.3	(5.1)	1.0	(2.3)	25	(55)
THICK. SKIN 5			11.1	(24.4)	3.2	(7.1)			0.7	(1.6)	2.4	(5.3)	1.0	(2.3)	25	(55)
THICK. SKIN 6	3.2	(7.1)	23.4	(51.5)	17.8	(39.3)	3.0	(6.7)	5.3	(11.7)	17.9	(39.4)	1.8	(3.9)	73	(160)
THICK. SKIN 7	4.3	(9.4)	23.3	(51.3)	13.0	(28.6)			3.8	(8.3)	12.7	(27.9)	1.8	(4.0)	62	(136)
THICK. SKIN 8			24.7	(54.5)	14.8	(32.7)			4.4	(9.7)	14.8	(32.6)	1.9	(4.2)	68	(150)
THICK. SKIN 9	3.2	(7.1)	36.6	(80.7)	62.3	(137.3)	6.6	(14.5)	22.6	(49.9)	76.1	(167.8)	2.8	(6.1)	210	(463)
THICK. SKIN 10	4.3	(9.4)	28.0	(61.8)	20.2	(44.5)			6.6	(14.6)	22.2	(49.0)	2.3	(5.1)	90	(199)
THICK. SKIN 11			27.5	(60.6)	19.3	(42.5)			6.3	(13.8)	21.1	(46.5)	2.3	(5.1)	87	(192)
THICK. SKIN 12			31.1	(68.6)	26.7	(58.8)			9.1	(20.0)	30.5	(67.2)	2.5	(5.6)	111	(244)

FIGURE 38
ACS COMPONENT MASSES - THICKENED SKIN CONCEPT

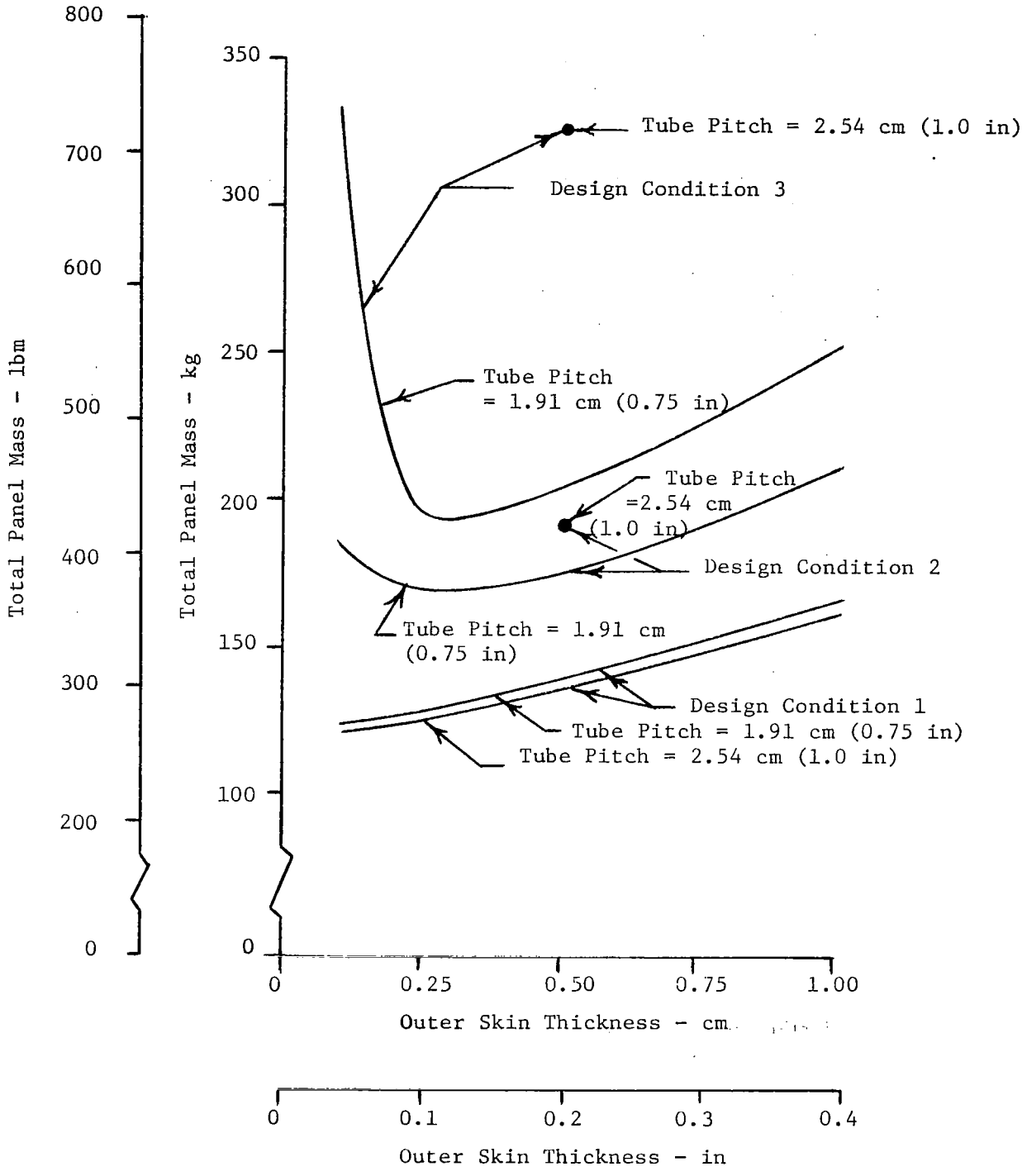

FIGURE 39
BENEFITS DERIVED BY THICKENING SKIN ARE LIMITED

It indicates that configurations with a tube pitch of 1.91 cm (0.75 in) are considerably lighter than those with a tube pitch of 2.54 cm (1.0 in) for Design Conditions 2 and 3. The effect of tube pitch at Design Condition 1 was found to be reversed, but the difference was small.

Another trend revealed by Figure 39 is the effect of skin thickness. In Design Condition 1, increasing the skin thickness above the 1.02 mm (0.04 in) associated with the Modified Baseline Panel Concept increases total panel mass. On the other hand, for Design Conditions 2 and 3, total panel mass will be reduced by thicker skins, up to about 2.54 mm (0.1 in). Beyond this point, structural mass increases will be greater than any reductions in the mass of ACS components.

The consistently evident trend in Figure 39 that an optimum skin thickness will exist for Design Conditions 2 and 3 is explained by Figure 40. The temperature differences shown were based on correlations derived from the computer analyses conducted for these concepts.

As the skin thickness increases, the temperature differential in the outer skin (from a point midway between coolant tubes to one immediately above the coolant tube) decreases. Conversely, the temperature differential between the tube wall and the outer skin directly above the tube wall increases. When the summation of these temperature differences is minimized, coolant tube wall temperatures are maximized. This enhances the potential for convective heat transfer and minimizes requirement for coolant flow.

Since panel structural mass increases with increasing skin thickness, as illustrated by Figure 41, it becomes apparent that an optimum panel total mass skin thickness limitation is reached quickly and benefits to be gained by skin thickening are limited. Figure 41 also shows that surface pressure has a significant effect on panel mass but that panel height has little effect.

The Thickened Skin Concept panel geometry and unit structural masses are shown in Figure 42. Selected maximum mechanical, thermal, and total stresses and margins of safety are summarized in Figure 43.

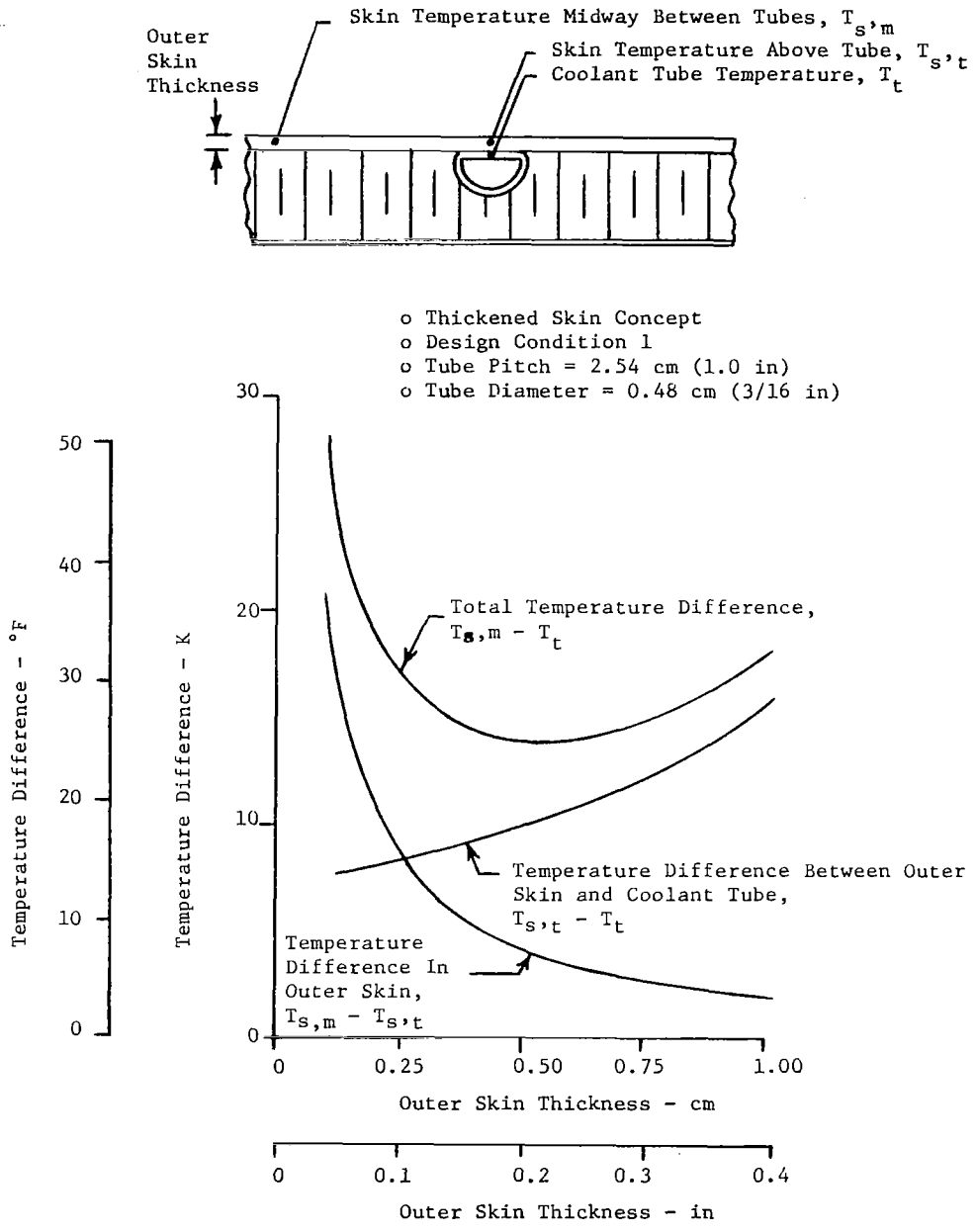

FIGURE 40
THERMALLY OPTIMUM SKIN THICKNESS

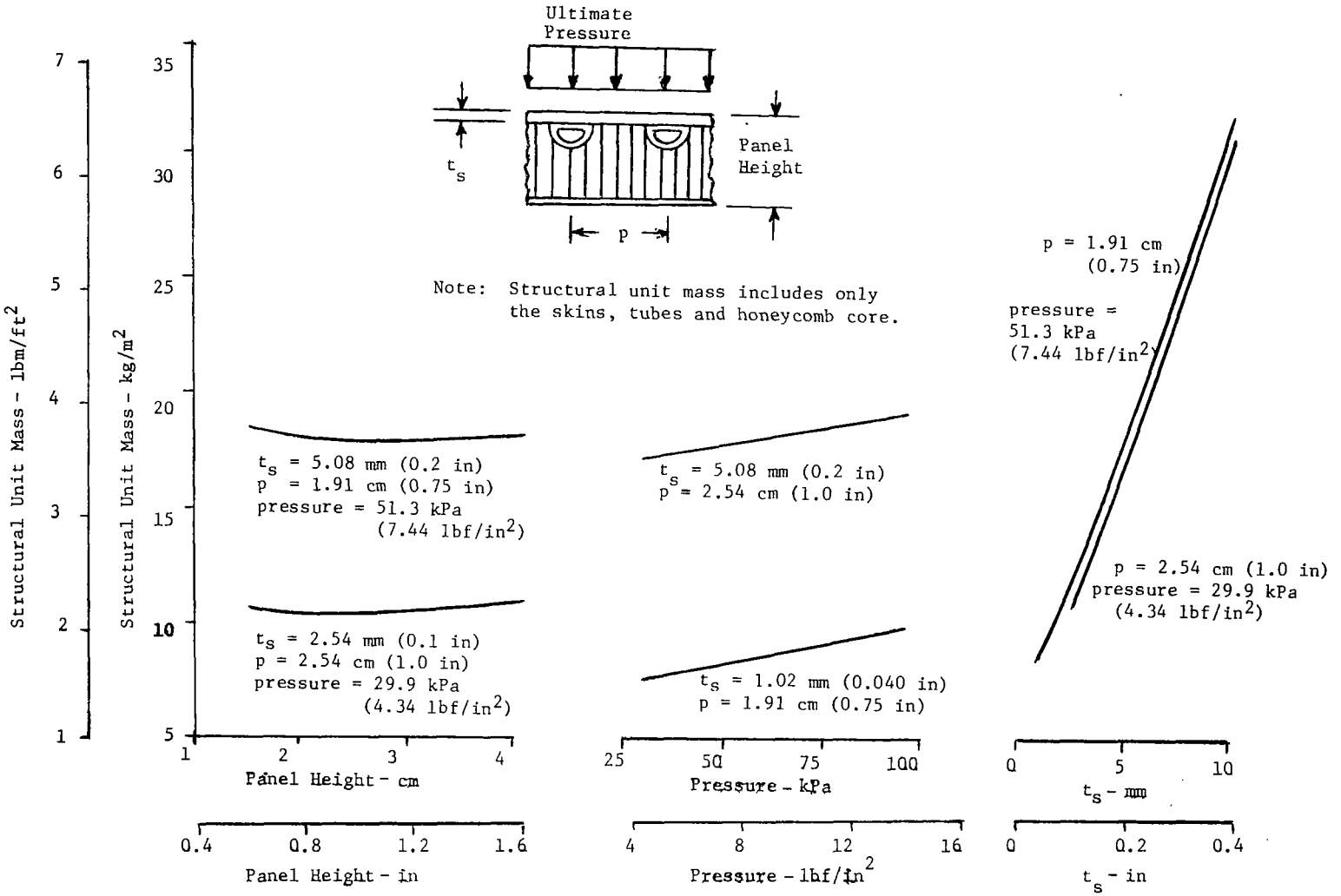

FIGURE 41
STRUCTURAL MASS TRENDS

Configuration	Panel Height		Interference Heating Area						Uniform Heating Area			
			Ultimate Pressure		Inner Skin Thickness		Structural Unit Mass		Inner Skin Thickness		Structural Unit Mass	
	cm	(in)	kPa	(lbf/in^2)	mm	(in)	kg/m^2	(lbm/ft^2)	mm	(in)	kg/m^2	(lbm/ft^2)
THICK. SKIN 1	2.64	(1.04)	29.9	(4.34)	0.48	(.019)	10.40	(2.13)	0.61	(.024)	6.64	(1.36)
THICK. SKIN 2	2.62	(1.03)	29.9	(4.34)	0.41	(.016)	17.09	(3.50)	0.64	(.025)	6.64	(1.36)
THICK. SKIN 3	2.69	(1.06)	29.9	(4.34)	0.41	(.016)	30.95	(6.34)	0.61	(.024)	6.64	(1.36)
THICK. SKIN 4	2.59	(1.02)	29.9	(4.34)	0.48	(.019)	10.64	(2.18)	0.56	(.022)	6.74	(1.38)
THICK. SKIN 5	2.46	(0.97)	29.9	(4.34)	0.41	(.016)	31.10	(6.37)	0.58	(.023)	6.74	(1.38)
THICK. SKIN 6	3.20	(1.26)	97.9	(14.2)	1.02	(.040)	19.04	(3.90)	0.56	(.022)	6.74	(1.38)
THICK. SKIN 7	3.05	(1.20)	97.9	(14.2)	1.27	(.050)	13.04	(2.67)	0.48	(.019)	6.79	(1.39)
THICK. SKIN 8	2.97	(1.17)	97.9	(14.2)	1.02	(.040)	33.00	(6.76)	0.48	(.019)	6.79	(1.39)
THICK. SKIN 9	2.62	(1.03)	51.3	(7.44)	0.66	(.026)	17.77	(3.64)	0.61	(.024)	6.64	(1.36)
THICK. SKIN 10	2.79	(1.10)	51.3	(7.44)	0.71	(.028)	11.38	(2.33)	0.51	(.020)	6.74	(1.38)
THICK. SKIN 11	2.92	(1.15)	51.3	(7.44)	0.58	(.023)	18.02	(3.69)	0.51	(.020)	6.74	(1.38)
THICK. SKIN 12	2.82	(1.11)	51.3	(7.44)	0.58	(.023)	31.78	(6.51)	0.51	(.020)	6.74	(1.38)

FIGURE 42
THICKENED SKIN CONCEPT GEOMETRIES AND UNIT MASSES

Configuration and Item	Ultimate Stresses and Margins of Safety					
	Outer Skin		Inner Skin		Tube	
	MPa	(lbf/in^2)	MPa	(lbf/in^2)	MPa	(lbf/in^2)
THICK. SKIN 7						
Thermal Stress	-15.0	(-2170)	3.1	(450)	43.8	(6350)
Mechanical Stress	$\pm$101.1	($\pm$14670)	$\pm$155.6	($\pm$22570)	$\pm$90.3	($\pm$13100)
Max. Compression Stress	-116.1	(-16840)	-155.6	(-22570)	-90.3	(-13100)
Max. Tension Stress	101.1	(14670)	158.7	(23020)	134.1	(19450)
Allowable Tension Stress	160.3	(23250)	160.3	(23250)	237.9	(34500)
Min. Margin of Safety			+0.01 Tension			
THICK. SKIN 9						
Thermal Stress	-16.1	(-2340)	8.6	(1250)	102.7	(14900)
Mechanical Stress	$\pm$57.5	($\pm$8340)	$\pm$149.8	($\pm$21720)	$\pm$42.8	($\pm$6210)
Max. Compression Stress	-73.6	(-10680)	-149.8	(-21720)	-42.8	(-6210)
Max. Tension Stress	57.5	(8340)	158.4	(22970)	145.5	(21110)
Allowable Tension Stress	160.3	(23250)	160.3	(23250)	237.9	(34500)
Min. Margin of Safety			+0.01 Tension			
THICK. SKIN 10						
Thermal Stress	-22.5	(-3260)	3.2	(470)	66.1	(9580)
Mechanical Stress	$\pm$94.7	($\pm$13740)	$\pm$156.7	($\pm$22730)	$\pm$84.0	($\pm$12180)
Max. Compression Stress	-117.2	(-17000)	-156.7	(-22730)	-84.0	(-12180)
Max. Tension Stress	94.7	(13740)	159.9	(23200)	150.1	(21760)
Allowable Tension Stress	160.3	(23250)	160.3	(23250)	237.9	(34500)
Min. Margin of Safety			0.0 Tension			

FIGURE 43
THICKENED SKIN CONCEPT STRESSES AND MARGINS OF SAFETY

Longitudinal thermal stresses in all cases were compression in the outer skin and tension in the tubes and inner skin. As with the Modified Baseline Panel Concept, the skins were not critical in compression. When the thermal tension stresses in the tubes and inner skin were superimposed on the mechanical tension stresses, negative margins of safety in some cases necessitated resizing the interference heating portions for positive margins of safety at the combined stresses. Transverse thermal stresses were calculated and found to not impact the panel mass. The uniformly heated portion of the panels were analyzed and the total panel heights that produced the minimum total structural masses were selected by the same type of trade-off analysis as for the Modified Baseline Panel Concept. The structural panel mass was calculated as follows. Because the thickened portion of the outer skin was 91.4 cm (36.0 in) in length and tapered back to 0.010 mm (.040 in) over two additional 30.5 cm (12.0 in) lengths, as shown in Figure 36, the effective length of the thickened portion for mass calculations was 121.9 cm (48.0 in). The inner skin thicknesses required for the interference heating conditions were assumed to extend 61.0 cm (24.0 in) each side of the nominal locus of peak heating for a total length of 121.9 cm (48.0 in), the same as the effective width of the thickened outer skin. Therefore, the area designed for interference heating was 1.86 m^2 (20 ft^2) and the area designed for uniform heating was 7.43 m^2 (80 ft^2). The total structural panel masses shown in Figure 37 were calculated by multiplying the unit masses of Figure 42 times the areas derived above and adding the mass of the manifolds and joint materials. The latter were the same as for the baseline panel, 33.7 kg (74 lbm).

4.3.3 Intermediate Manifold Concept - This concept is one of the three studied (along with the Branched Tubes and the Separate Panels Concepts) to evaluate increasing the number of tubes in the region exposed to interference heating. For each of these concepts, it was necessary to define a location for the transition in tube spacing.

Nominally, the locus of peak heating is 1.22 m (4 ft) from the coolant exit end of the panel and increased heating extends over a band 0.91 m (3 ft) wide. However, allowing for a shift in peak heating of 0.3 m (1 ft) in either direction, increased heating can occur as far as 1.98 m (78 in) from the exit end. It would be advantageous to locate the division line at a support. Since a structural support is located 2.03 m (80 in) from the end of the panel, this location was selected, as shown in Figure 44.

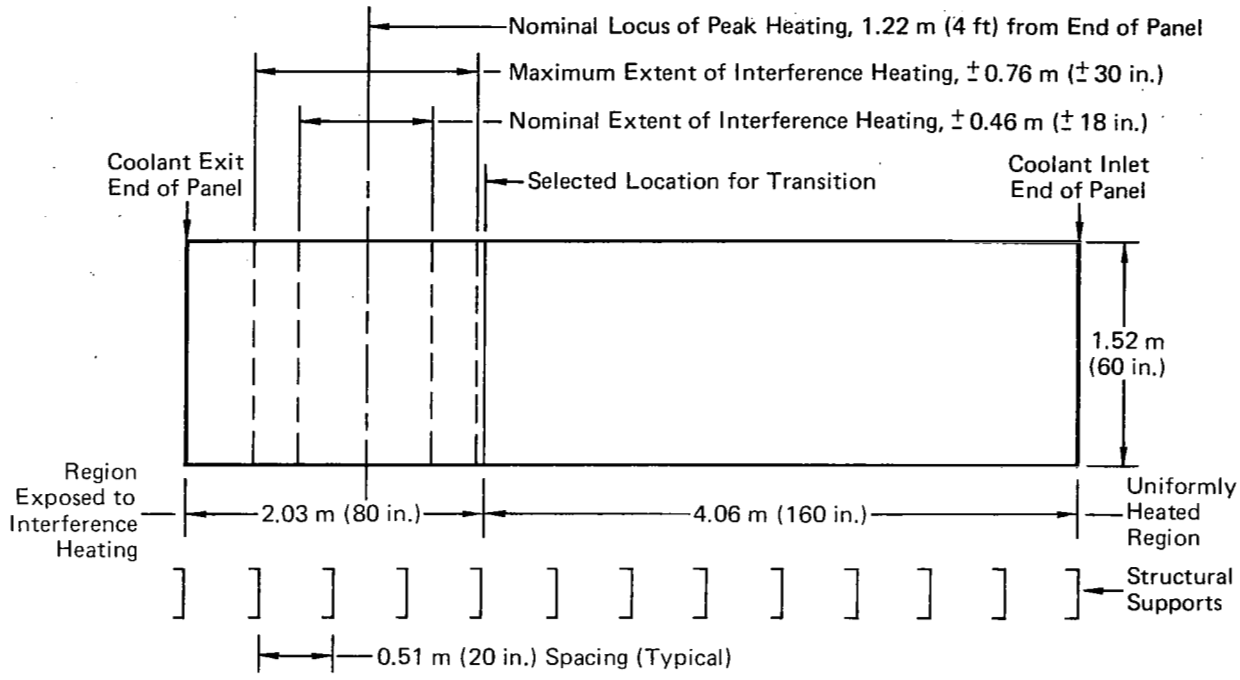

FIGURE 44
SELECTION OF TRANSITION LOCATION FOR INTERMEDIATE MANIFOLD, BRANCHED TUBES, AND SEPARATE PANELS CONCEPTS

Figure 45 defines the geometry and characteristics assumed for the Intermediate Manifold Concept. Coolant flow would be routed through the uniformly heated section and merged in a manifold 2.03 m (80 in) from the coolant exit end of the panel. The flow would then be redistributed to the more closely spaced tubes downstream. Tube spacing in the uniformly heated section was assumed fixed at 2.54 cm (1.0 in), based on the baseline panel analyses, and 1.91 cm (0.75 in) in the downstream region. Thus, the coolant mass flow in each downstream tube would be 75 percent that of each upstream tube.

Data generated during the baseline panel analyses were used to establish trends of coolant temperatures at the division line, as a function of tube diameter and flow rate. The coolant panel thermal model was modified to simulate only the final third of the panel and, using the coolant parametric data,

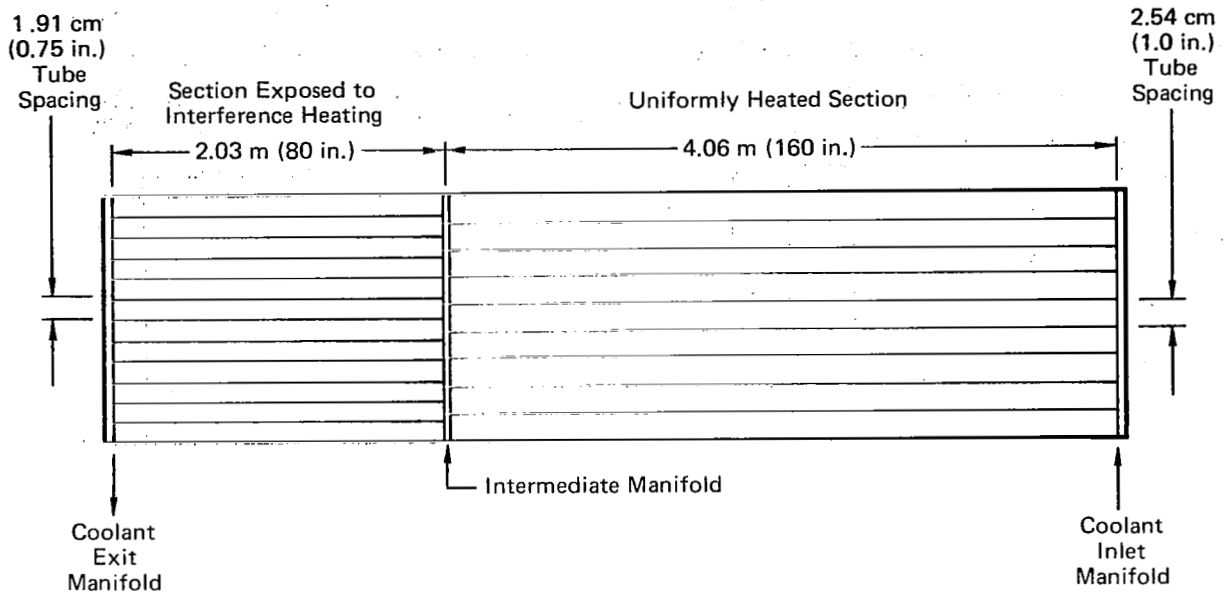

FIGURE 45
INTERMEDIATE MANIFOLD CONCEPT DEFINITION

the flowrates necessary to limit outer skin temperatures to 394 K (250°F) were determined. The converged configurations are summarized in Figure 46 and the associated ACS component masses presented in Figure 47.

For Design Condition 1, 0.48 and 0.64 cm (3/16 and 1/4 in) tubes were considered in both regions of the panel. If the larger tubes are used in both regions, flow requirements in the downstream region would be increased. This would result in larger overall panel pressure drops, even though pressure drops in the downstream section would be reduced. As shown in Figure 47 this would produce a significant ACS component mass increase (Configurations 3 and 4). In any case, since it is not probable that a 1.91 cm (0.75 in) tube spacing could be attained with 0.64 cm (1/4 in) tubes, only the smaller tubes were considered in subsequent analyses of the downstream section. With the smaller tubes, a flow of 12.0 g/s (95 lbm/hr) would maintain acceptable structural temperatures in the downstream region. However, with larger tubes in the upstream section (Configuration 2), coolant flow must increase to maintain acceptable temperatures in the uniformly heated region.

Configuration	Design Condition	Section Exposed to Interference Heating: Tube Diameter cm (in)	Coolant Flow/Tube g/s (lbm/hr)	Max. Struct. Temp. K (°F)	Uniformly Heated Section: Tube Diameter cm (in)	Coolant Flow/Tube g/s (lbm/hr)	Max. Struct. Temp. K (°F)
INT. MAN. 1	1	0.48 (3/16)	12.0 (95)	394 (250)	0.48 (3/16)	16.0 (127)	378 (220)
INT. MAN. 2	1	0.48 (3/16)	12.4 (98)	393 (248)	0.64 (1/4)	16.4 (130)	394 (250)
INT. MAN. 3	1	0.64 (1/4)	15.8 (125)	394 (250)	0.48 (3/16)	21.1 (167)	363 (194)
INT. MAN. 4	1	0.64 (1/4)	15.8 (125)	394 (250)	0.64 (1/4)	21.1 (167)	380 (225)
INT. MAN. 5	2	0.48 (3/16)	39.1 (310)	394 (250)	0.48 (3/16)	52.1 (413)	331 (137)
INT. MAN. 6	2	↓	↓	↓	0.64 (1/4)	↓	346 (163)
INT. MAN. 7	2	↓	↓	↓	0.95 (3/8)	↓	346 (164)
INT. MAN. 8	3	0.48 (3/16)	89.5 (710)	394 (250)	0.48 (3/16)	119.4 (947)	348 (167)
INT. MAN. 9	3	↓	↓	↓	0.64 (1/4)	↓	355 (180)
INT. MAN. 10	3	↓	↓	↓	0.95 (3/8)	↓	363 (194)

Note: All configurations have outer skin thickness = 1.02 mm (0.040 in)

Configuration	Total Panel ΔP kPa (lbf/in^2)	Panel Structural Mass kg (lbm)	ACS Components Mass kg (lbm)	Total Mass kg (lbm)
INT. MAN. 1	262 (38)	100 (221)	20 (44)	120 (265)
INT. MAN. 2	110 (16)	101 (223)	23 (50)	124 (273)
INT. MAN. 3	338 (49)	101 (223)	26 (57)	127 (280)
INT. MAN. 4	83 (12)	102 (224)	28 (61)	129 (285)
INT. MAN. 5	2915 (423)	109 (240)	70 (155)	179 (395)
INT. MAN. 6	772 (112)	109 (241)	52 (115)	161 (356)
INT. MAN. 7	531 (77)	114 (251)	58 (128)	172 (379)
INT. MAN. 8	10375 (1505)	103 (226)	290 (640)	393 (866)
INT. MAN. 9	3290 (477)	103 (228)	148 (326)	251 (554)
INT. MAN. 10	2225 (323)	107 (235)	135 (297)	241 (532)

FIGURE 46
INTERMEDIATE MANIFOLD CONCEPT CONFIGURATIONS

Configuration	Coolant in Panel		Coolant in Distribution Lines		Coolant Distribution Lines		Heat Exchanger		Pumps		Pumping Power Penalty		Reservoir		Total ACS Components Mass	
	kg	(lbm)	kg	(lbm)	kg	(lbm)	kg	(lbm)	kg	(lbm)	kg	(lbm)	kg	(lbm)	kg	(lbm)
INT. MAN. 1	3.5	(7.8)	8.7	(19.1)	2.5	(5.5)	2.4	(5.3)	0.5	(1.1)	1.7	(3.8)	0.8	(1.7)	20	(44)
INT. MAN. 2	6.1	(13.4)	8.8	(19.5)	2.3	(5.0	↓	↓	0.5	(1.0)	1.6	(3.5)	1.0	(2.1)	23	(50)
INT. MAN. 3	5.2	(11.5)	10.9	(24.0)	3.3	(7.2)	↓	↓	0.7	(1.6)	2.4	(5.3)	1.0	(2.3)	26	(57)
INT. MAN. 4	7.8	(17.1)	10.9	(24.0)	2.8	(6.1)	↓	↓	0.6	(1.3)	2.0	(4.3)	1.2	(2.6)	28	(61)
INT. MAN. 5	3.5	(7.8)	22.5	(49.5)	17.2	(38.0)	3.0	(6.7)	5.1	(11.2)	17.1	(37.7)	1.6	(3.6)	70	(155)
INT. MAN. 6	6.1	(13.4)	↓	↓	8.5	(18.7)	↓	↓	2.3	(5.1)	7.8	(17.2)	1.8	(3.9)	52	(115)
INT. MAN. 7	14.0	(30.8)	↓	↓	7.5	(16.5)	↓	↓	2.0	(4.4)	6.8	(14.9)	2.3	(5.0)	58	(128)
INT. MAN. 8	3.5	(7.8)	41.8	(92.2)	88.7	(195.5)	6.6	(14.5)	33.6	(74.1)	113.0	(249.1)	2.9	(6.3)	290	(640)
INT. MAN. 9	6.1	(13.4)	↓	↓	34.9	(77.0)	↓	↓	12.7	(28.1)	42.8	(94.4)	3.0	(6.7)	148	(326)
INT. MAN. 10	14.0	(30.8)	↓	↓	26.9	(59.2)	↓	↓	9.6	(21.2)	32.3	(71.2)	3.5	(7.7)	135	(297)

FIGURE 47
ACS COMPONENT MASSES - INTERMEDIATE MANIFOLD CONCEPT

For Design Conditions 2 and 3 only 0.48 cm (3/16 in) tubes were considered for the downstream section. However, with the high coolant flow requirements at these conditions, tube diameters as large as 0.95 cm (3/8 in) were considered in the upstream region to hold overall panel pressure drops to acceptable levels. As shown in Figure 47, the mass of the ACS components for Design Condition 2 would be minimized with 0.64 cm (1/4 in) tubes while, for Design Condition 3, a savings would be realized with 0.95 cm (3/8 in) tubes in the upstream section of the panel.

Tube size and pitch, skin thickness, panel height and structural loading had all been evaluated in the Modified Baseline Panel Concept and baseline panel analyses. Figure 48 shows the Intermediate Manifold Concept panel geometry and unit structural masses. Since the division line between the geometrically different regions was defined in Figure 44, areas of 3.10 m^2 (33.33 ft^2) and 6.20 m^2 (66.67 ft^2) were considered for the interference heating and uniform heating sections respectively. The only new consideration in panel structural mass involved the mass allowance for manifolds, fittings, bushings, splice plates, and attachments. Because an additional manifold is incorporated, this mass increased by 2.27 kg (5 lbm), to 35.8 kg (79 lbm).

The thermodynamic advantages of the Intermediate Manifold Concept are evident in the region of increased heating where the convective heat transfer coefficients within the tubes are considerably higher than obtainable without the manifold.

The calculated magnitude of the heat transfer coefficient is influenced by the expression used to determine laminar flow coefficients. As mentioned in Section 3.2, the expression used is as follows:

$$h = C_L \frac{k}{D} \left[(R_e)(P_r) \frac{D}{L} \right]^{1/3} \left(\frac{\mu}{\mu_w} \right)^{0.14}$$

where $C_L = 10.55$ (1.86)

If the coolant were dispersed into the tubes just upstream of the region of increased heating from the intermediate manifold, the characteristic flow length (L) would be greatly reduced. Examination of the heat transfer coefficient expression shows that, for the same Reynolds Number with a large reduction in flow length (L), the laminar flow Nusselt Number would be significantly increased.

Configuration	Panel Height		Interference Heating Area						Uniform Heating Area			
			Ultimate Pressure		Inner Skin Thickness		Structural Unit Mass		Inner Skin Thickness		Structural Unit Mass	
	cm	(in)	kPa	(lbf/in^2)	mm	(in)	kg/m^2	(lbm/ft^2)	mm	(in)	kg/m^2	(lbm/ft^2)
INT. MAN. 1	2.59	(1.02)	29.9	(4.34)	0.86	(.034)	7.57	(1.55)	0.64	(.025)	6.64	(1.36)
INT. MAN. 2	2.59	(1.02)	29.9	(4.34)	0.86	(.034)	7.57	(1.55)	0.53	(.021)	6.79	(1.39)
INT. MAN. 3	2.69	(1.06)	29.9	(4.34)	0.76	(.030)	7.81	(1.60)	0.61	(.024)	6.64	(1.36)
INT. MAN. 4	2.69	(1.06)	29.9	(4.34)	0.76	(.030)	7.81	(1.60)	0.51	(.020)	6.74	(1.38)
INT. MAN. 5	3.58	(1.41)	97.9	(14.2)	1.52	(.060)	9.86	(2.02)	0.53	(.021)	6.88	(1.41)
INT. MAN. 6	3.58	(1.41)	97.9	(14.2)	1.52	(.060)	9.86	(2.02)	0.46	(.018)	6.93	(1.42)
INT. MAN. 7	3.58	(1.41)	97.9	(14.2)	1.52	(.060)	9.86	(2.02)	0.41	(.016)	7.71	(1.58)
INT. MAN. 8	2.97	(1.16)	51.3	(7.44)	1.07	(.042)	8.30	(1.70)	0.58	(.023)	6.64	(1.36)
INT. MAN. 9	2.97	(1.16)	51.3	(7.44)	1.07	(.042)	8.30	(1.70)	0.48	(.019)	6.79	(1.39)
INT. MAN. 10	2.97	(1.16)	51.3	(7.44)	1.07	(.042)	8.30	(1.70)	0.41	(.016)	7.27	(1.49)

FIGURE 48
INTERMEDIATE MANIFOLD CONCEPT GEOMETRIES AND UNIT MASSES

Figure 42 was prepared to illustrate this effect for typical design condition. Laminar flow heat transfer is shown to be quite sensitive to the local flow characteristic length, while turbulent flow heat transfer is not. For most of the cases analyzed during this study, the flow in the downstream region of the panel would be transitional but nearer to laminar than turbulent flow.

As indicated in Figure 49, heat transfer in the transitional region was predicted by logarithmic interpolation between the last laminar and first turbulent values. It can be seen that, in the region of interest, heat transfer, at a specified Reynolds Number, is quite sensitive to the characteristic length of laminar flow. Therefore, techniques that effectively reduce this characteristic flow length would be expected to result in improved heat transfer.

4.3.4 Branched Tubes Concept - As shown in Figure 50, this concept is based on directing the flow from each tube in the upstream section into two tubes in the downstream section. Previous analysis had shown that 1.91 cm (0.75 in) tube spacing is required in the region exposed to interference heating for adequate heat transfer. This dictated 3.81 cm (1.5 in) tube spacing in the upstream region of the panel. Various tube diameters were investigated.

The analytical techniques used to evaluate the Branched Tubes configurations were similar to those described for the Intermediate Manifold configurations except for one major difference. The laminar flow characteristic lengths for the downstream section were measured from the coolant inlet end of the panel. This was considered to be realistic since it is improbable that the flow which has ceased to be laminar would revert back to laminar as a result of branching.

The significance of this assumption is shown in Figure 49. For the same Reynolds Number condition in the downstream section of the panel, the Branched Tubes Concepts heat transfer characteristics were not as good as those for the Intermediate Manifold Concept.

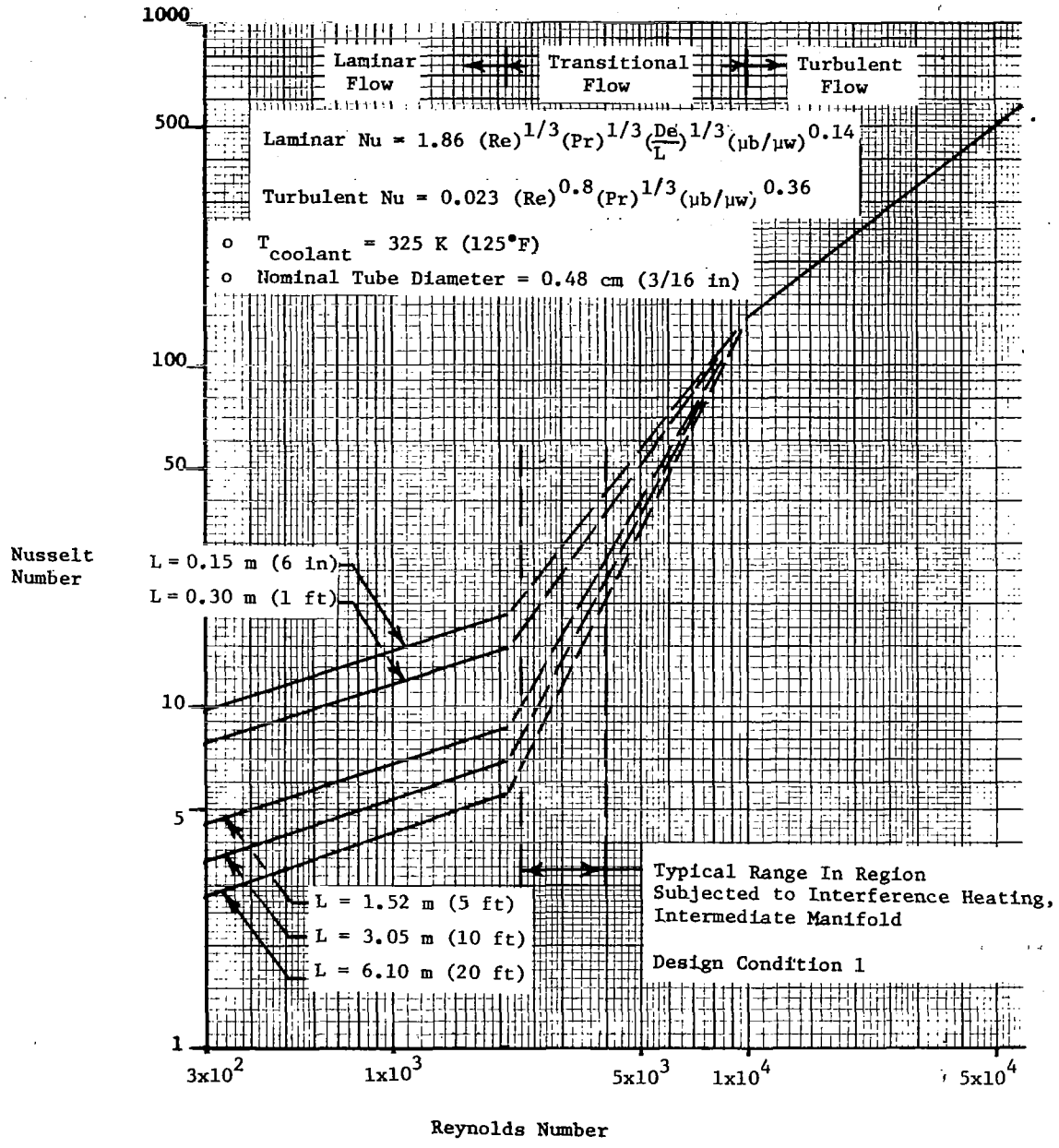

FIGURE 49
LAMINAR FLOW CHARACTERISTIC FLOW LENGTH INFLUENCES HEAT TRANSFER

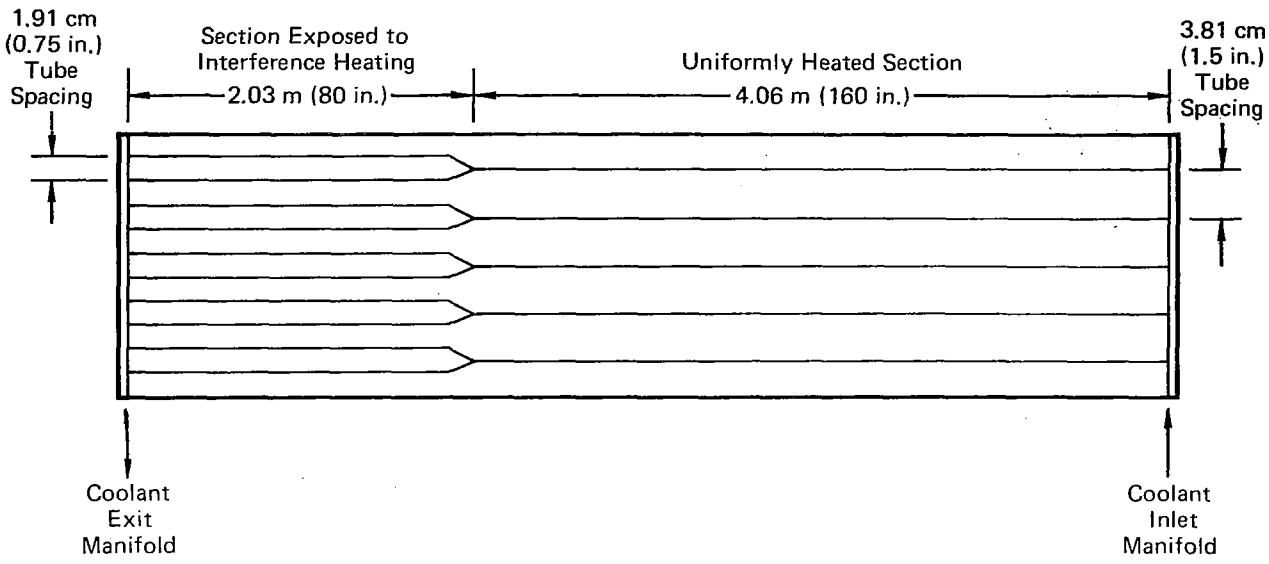

FIGURE 50
BRANCHED TUBES CONCEPT DEFINITION

Converged design solutions for the allowable structural temperature are summarized by Figure 51. ACS component masses are presented in Figure 52. At Design Condition 1, the Branched Tubes Concept total panel mass is not sensitive to the tube diameter in the upstream region. However, at Design Conditions 2 and 3, the upstream tube size definitely impacts panel mass. At both conditions, mass is reduced as upstream tube diameter is enlarged. This trend is attributable to the large pressure drops encountered in the upstream tubes as a result of the coolant flow requirements at the wide tube spacing assumed. Tubes even larger than 0.95 cm (3/8 in) could be employed in the upstream region to further reduce the total mass. However, a cursory examination revealed that improvements realized with still larger tubes rapidly become negligible.

The Branched Tubes Concept, like the Intermediate Manifold Concept, did not introduce any structural combinations of tube size and pitch, skin thicknesses, panel heights and loading not previously analyzed. The Branched Tubes Concept panel geometry and unit structural masses are shown in Figure 53. The areas considered for the interference heating and uniform heating sections were

Configuration	Design Condition	Section Exposed to Interference Heating						Uniformly Heated Section					
		Tube Diameter		Coolant Flow/Tube		Max. Struct. Temp.		Tube Diameter		Coolant Flow/Tube		Max. Struct. Temp.	
		cm	(in)	g/s	(lbm/hr)	K	(°F)	cm	(in)	g/s	(lbm/hr)	K	(°F)
BR. TUBES 1	1	0.48	(3/16)	17.0	(135)	394	(250)	0.48	(3/16)	34.0	(270)	369	(204)
BR. TUBES 2	1							0.64	(1/4)			385	(234)
BR. TUBES 3	2	0.48	(3/16)	51.0	(405)	394	(250)	0.48	(3/16)	102.1	(810)	335	(144)
BR. TUBES 4	2							0.64	(1/4)			336	(145)
BR. TUBES 5	2							0.95	(3/8)			341	(155)
BR. TUBES 6	3	0.48	(3/16)	93.3	(740)	394	(250)	0.48	(3/16)	186.6	(1480)	387	(237)
BR. TUBES 7	3							0.64	(1/4)			385	(234)
BR. TUBES 8	3							0.95	(3/8)			388	(239)

Note: All configurations have outer skin thickness = 1.02mm (0.040 in)

Configuration	Total Panel ΔP		Panel Structural Mass		ACS Components Mass		Total Mass	
	kPa	(lbf/in^2)	kg	(lbm)	kg	(lbm)	kg	(lbm)
BR. TUBES 1	848	(123)	98	(215)	26	(58)	124	(273)
BR. TUBES 2	214	(31)	98	(216)	25	(56)	123	(272)
BR. TUBES 3	6200	(899)	106	(234)	125	(276)	231	(510)
BR. TUBES 4	2440	(354)	107	(236)	81	(178)	188	(414)
BR. TUBES 5	1235	(179)	108	(238)	72	(158)	180	(396)
BR. TUBES 6	18800	(2727)	100	(220)	474	(1044)	573	(1264)
BR. TUBES 7	4805	(697)	101	(222)	181	(399)	282	(621)
BR. TUBES 8	2505	(363)	102	(224)	138	(305)	240	(529)

FIGURE 51
BRANCHED TUBES CONCEPT CONFIGURATIONS

Configuration	Coolant in Panel kg (lbm)	Coolant in Distribution Lines kg (lbm)	Coolant Distribution Lines kg (lbm)	Heat Exchanger kg (lbm)	Pumps kg (lbm)	Pumping Power Penalty kg (lbm)	Reservoir kg (lbm)	Total ACS Components Mass kg (lbm)
BR. TUBES 1	2.9 (6.3)	11.2 (24.6)	4.4 (9.6)	2.4 (5.3)	1.1 (2.4)	3.6 (7.9)	0.9 (2.0)	26 (58)
BR. TUBES 2	4.5 (10.0)	↓	3.1 (6.8)	↓	0.7 (1.6)	2.4 (5.3)	1.0 (2.2)	25 (56)
BR. TUBES 3	2.9 (6.3)	27.3 (60.2)	37.2 (82.0)	3.0 (6.7)	12.1 (26.7)	40.7 (89.8)	1.9 (4.2)	125 (276)
BR. TUBES 4	4.5 (10.0)	↓	18.6 (41.0)	↓	5.8 (12.8)	19.5 (43.1)	2.0 (4.5)	81 (178)
BR. TUBES 5	9.8 (21.6)	↓	12.6 (27.8)	↓	3.8 (8.4)	12.8 (28.2)	2.4 (5.2)	72 (158)
BR. TUBES 6	2.9 (6.3)	42.1 (92.9)	153.8(339.0)	6.6 (14.5)	60.8(134.1)	204.6 (451.1)	2.9 (6.3)	474 (1044)
BR. TUBES 7	4.5 (10.0)	↓	46.8(103.1)	↓	17.9 (39.5)	60.2 (132.8)	2.9 (6.5)	181 (399)
BR. TUBES 8	9.8 (21.6)	↓	29.2 (64.3)	↓	10.8 (23.9)	36.5 (80.4)	3.3 (7.2)	138 (305)

FIGURE 52
ACS COMPONENT MASSES - BRANCHED TUBES CONCEPT

Configuration	Panel Height		Interference Heating Area						Uniform Heating Area			
			Ultimate Pressure		Inner Skin Thickness		Structural Unit Mass		Inner Skin Thickness		Structural Unit Mass	
	cm	(in)	kPa	(lbf/in^2)	mm	(in)	kg/m^2	(lbf/ft^2)	mm	(in)	kg/m^2	(lbf/ft^2)
BR. TUBES 1	2.59	(1.02)	29.9	(4.34)	0.86	(.034)	7.57	(1.55)	0.71	(.028)	6.54	(1.34)
BR. TUBES 2	2.59	(1.02)	29.9	(4.34)	0.86	(.034)	7.57	(1.55)	0.66	(.026)	6.59	(1.35)
BR. TUBES 3	3.58	(1.41)	97.9	(14.2)	1.52	(.060)	9.86	(2.02)	0.61	(.024)	6.79	(1.39)
BR. TUBES 4	3.58	(1.41)	97.9	(14.2)	1.52	(.060)	9.86	(2.02)	0.53	(.021)	6.88	(1.41)
BR. TUBES 5	3.58	(1.41)	97.9	(14.2)	1.52	(.060)	9.86	(2.02)	0.43	(.017)	7.03	(1.44)
BR. TUBES 6	2.97	(1.17)	51.3	(7.44)	1.07	(.042)	8.30	(1.70)	0.66	(.026)	6.54	(1.34)
BR. TUBES 7	2.97	(1.17)	51.3	(7.44)	1.07	(.042)	8.30	(1.70)	0.58	(.023)	6.64	(1.36)
BR. TUBES 8	2.97	(1.17)	51.3	(7.44)	1.07	(.042)	8.30	(1.70)	0.48	(.019)	6.79	(1.39)

FIGURE 53
BRANCHED TUBES CONCEPT GEOMETRIES AND UNIT MASSES

3.10 m^2 (33.33 ft^2) and 6.20 m^2 (66.67 ft^2) respectively. Design considerations providing for tube branching, as indicated in Figure 50, were examined to determine their effect on panel mass. The design selected was a formed and welded "Y" at each branch with the same "D" cross section as the tubes. The mass calculated for these Y's was less than 0.45 kg (1.0 lbm) greater than the lengths of tubes they replaced and was, therefore, neglected. The mass of the manifolds and joint materials was the same as for the Modified Baseline Panel Concept, 33.7 kg (74.0 lbm).

4.3.5 Separate Panels Concept - Figure 54 illustrates that this concept is the same as the Intermediate Manifold Concept in regard to tube spacing in the two sections, but there is a distinct structural division between the sections. In both the basic and alternate configurations, separate coolant inlet and exit manifolds are provided for each panel.

Each panel would be supplied with 283 K (50°F) coolant. The flow requirements were determined individually to limit each panel to 394 K (250°F).

The basic Separate Panels configuration retains the same tube orientation employed in all previously considered concepts. Two manifolds are, therefore, located at the division line.

The alternate configuration incorporates a different tube orientation downstream, and requires a different manifold arrangement. This configuration was studied in order to determine if any benefits were derived by arranging the tubes parallel to the heating pattern and effectively shortening the coolant flow length.

Converged basic Separate Panel configurations are summarized by Figure 55. The associated ACS component masses are presented in Figure 56. These results differ significantly from those derived for the Intermediate Manifold and Branched Tubes Concepts. For example, the Separate Panel configurations sized for Design Condition 1 require less coolant flow and display lower pressure drops, but the ACS components mass is not significantly reduced. At Design Conditions 2 and 3, the coolant flow requirements for the downstream panel are high even though the flow characteristic length is small and the average temperature of the coolant is lower than for the other designs.

The reason for these apparent discrepancies can be traced to the effects of the low coolant temperatures on coolant density and viscosity, particularly the latter. Since the temperature rise of the coolant is much lower than that

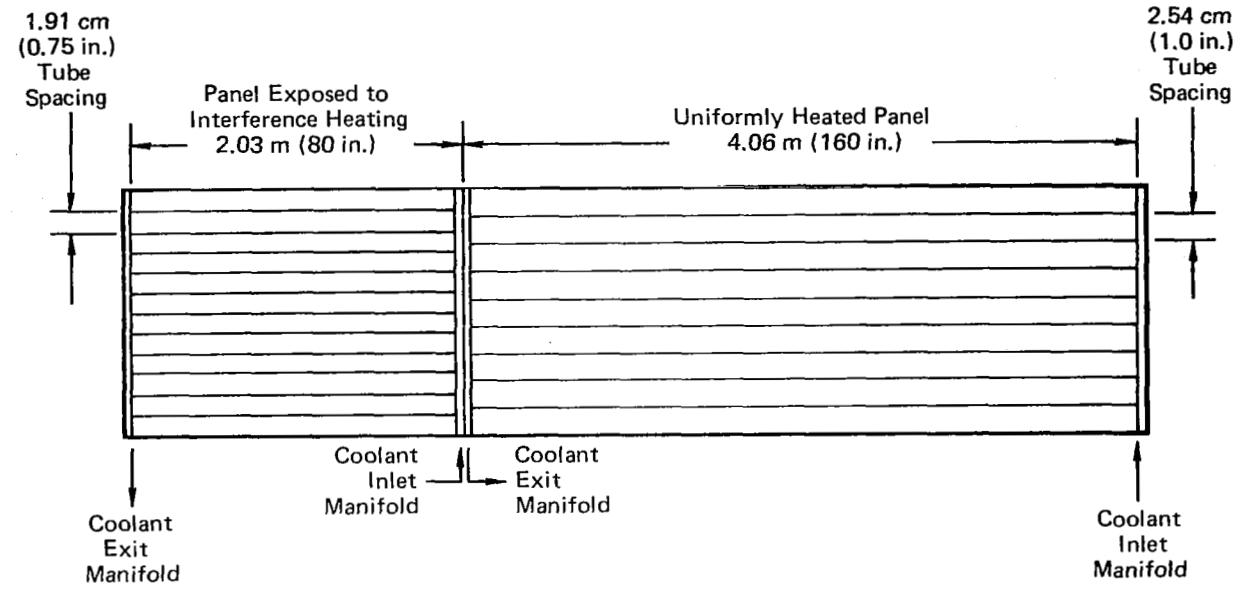

Basic Configuration

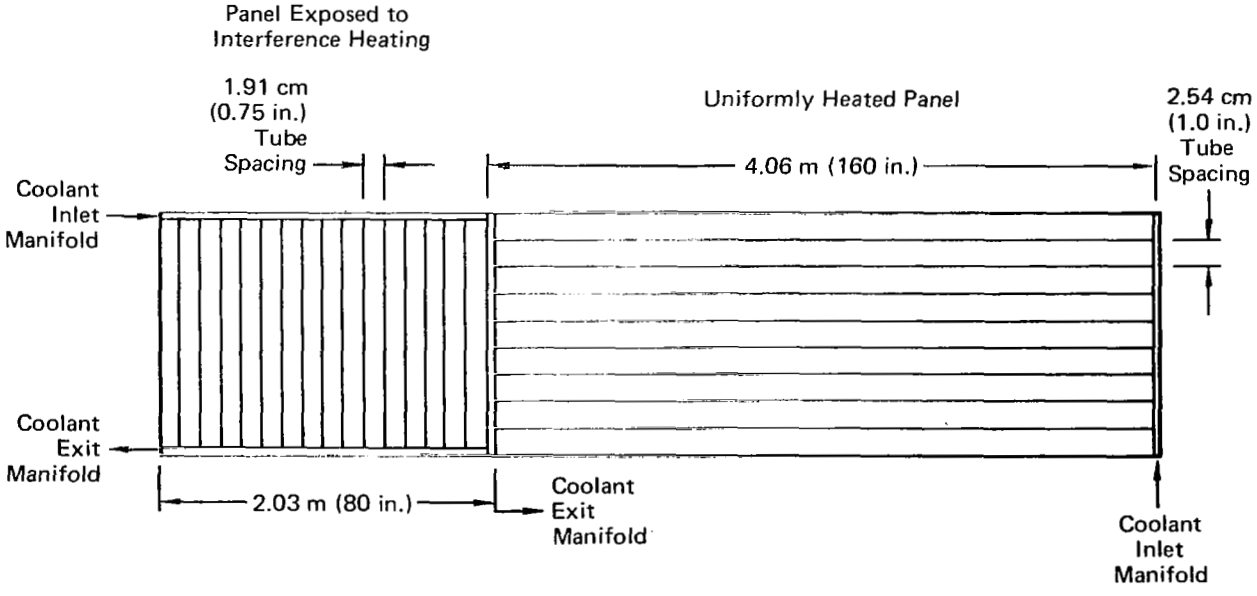

Alternate Configuration

FIGURE 54
SEPARATE PANELS CONCEPT DEFINITION

Configuration	Design Condition	Panel Exposed to Interference Heating: Tube Diameter cm (in)	Coolant Flow/Tube g/s (lbm/hr)	Panel ΔP kPa (lbf/in^2)	Uniformly Heated Panel: Tube Diameter cm (in)	Coolant Flow/Tube g/s (lbm/hr)	Panel ΔP kPa (lbf/in^2)
SEP. PANELS 1	1	0.48 (3/16)	6.1 (48)	28 (4)	0.48 (3/16)	12.6 (100)	138 (20)
SEP. PANELS 2	1	↓	↓	↓	0.64 (1/4)	16.4 (130)	41 (6)
SEP. PANELS 3	2	0.48 (3/16)	44.8 (355)	696 (101)	0.48 (3/16)	12.6 (100)	138 (20)
SEP. PANELS 4	2	↓	↓	↓	0.64 (1/4)	16.4 (130)	41 (6)
SEP. PANELS 5	2	↓	↓	↓	0.95 (3/8)	16.4 (130)	7 (1)
SEP. PANELS 6	3	0.48 (3/16)	85.1 (675)	2145 (311)	0.48 (3/16)	32.2 (255)	655 (95)
SEP. PANELS 7	3	↓	↓	↓	0.64 (1/4)	39.7 (315)	145 (21)
SEP. PANELS 8	3	↓	↓	↓	0.95 (3/8)	67.5 (535)	34 (5)

Note: All configurations have outer skin thickness = 1.02 mm (0.040 in)

Configuration	Panel Structural Mass kg	(lbm)	ACS Components Mass kg	(lbm)	Total Mass kg	(lbm)
SEP. PANELS 1	104	(229)	25	(56)	129	(285)
SEP. PANELS 2	105	(231)	30	(67)	135	(298)
SEP. PANELS 3	112	(248)	66	(145)	178	(393)
SEP. PANELS 4	113	(249)	71	(156)	184	(405)
SEP. PANELS 5	118	(260)	79	(174)	197	(434)
SEP. PANELS 6	106	(234)	146	(321)	252	(555)
SEP. PANELS 7	107	(236)	150	(330)	257	(566)
SEP. PANELS 8	110	(243)	173	(381)	283	(624)

FIGURE 55
BASIC SEPARATE PANELS CONCEPT CONFIGURATIONS

Configuration	Coolant in Panels		Coolant in Distribution Lines		Coolant Distribution Lines		Heat Exchanger		Pumps		Pumping Power Penalty		Reservoir		Total ACS Components Mass	
	kg	(lbm)	kg	(lbm)	kg	(lbm)	kg	(lbm)	kg	(lbm)	kg	(lbm)	kg	(lbm)	kg	(lbm)
SEP. PANELS 1	3.5	(7.8)	12.7	(28.0)	3.2	(7.1)	2.4	(5.3)	0.6	(1.3)	2.0	(4.3)	1.0	(2.3)	25	(56)
SEP. PANELS 2	6.0	(13.3)	14.5	(31.9)	3.5	(7.8)	2.4	(5.3)	0.7	(1.5)	2.2	(4.8)	1.3	(2.8)	30	(67)
SEP. PANELS 3	3.5	(7.8)	32.8	(72.4)	11.2	(24.7)	3.0	(6.7)	2.9	(6.4)	9.8	(21.5)	2.3	(5.0)	66	(145)
SEP. PANELS 4	6.0	(13.3)	34.6	(76.3)	11.5	(25.4)	3.0	(6.7)	3.0	(6.6)	10.0	(22.0)	2.5	(5.5)	71	(156)
SEP. PANELS 5	14.0	(30.8)	34.6	(76.3)	11.5	(25.3)	3.0	(6.7)	2.9	(6.5)	9.9	(21.9)	3.0	(6.6)	79	(174)
SEP. PANELS 6	3.5	(7.8)	56.2	(123.8)	31.2	(68.7)	6.6	(14.5)	10.2	(22.5)	34.3	(75.7)	3.7	(8.2)	146	(321)
SEP. PANELS 7	6.0	(13.3)	59.0	(130.0)	30.5	(67.3)	6.6	(14.5)	10.0	(22.1)	33.7	(74.3)	4.0	(8.9)	150	(330)
SEP. PANELS 8	14.0	(30.8)	68.4	(150.8)	32.5	(71.6)	6.6	(14.5)	10.6	(23.4)	35.8	(78.9)	5.1	(11.2)	173	(381)

FIGURE 56
ACS COMPONENT MASSES - BASIC SEPARATE PANELS CONCEPT

associated with continuous flow from one end of the panel to the other, the average viscosity is much higher. This results in reducing the Reynolds Number, and hence, the coolant heat transfer coefficients. Previous studies, such as Reference 2, have indicated advantages by operating the coolant to as high a temperature as practical. This analysis confirms the advantages of maintaining high coolant temperatures.

The basic Separate Panels geometry and unit structural masses are shown in Figure 57. Areas of 3.10 m^2 (33.33 ft^2) and 6.20 m^2 (66.67 ft^2) were considered for the panels exposed to interference and uniform heating respectively. The basic Separate Panel Concept did not introduce any new combinations of tube size and pitch, skin thicknesses, panel heights and loading. Therefore, the only structural mass change for this concept was due to the added splice and manifolds. This mass change is based on the masses of the manifolds and joint materials presented in Figure 15 as shown in Figure 58. The resulting total mass of the manifolds and joint materials was 39.8 kg (87.0 lbm).

Comparison of the basic Separate Panels Concept with other concepts revealed that this approach was too heavy to be competitive. As a result, analysis of the alternate Separate Panels design was simply used to verify that no significant advantages existed over the basic configuration that might affect this observation.

Since previous analyses consistently indicated that minimum tube spacing results in minimum panel mass, the tubes were spaced at 1.91 cm (0.75 in) intervals in the smaller panel. Thermodynamically, the advantage derived from the alternate tube orientation is that the tubes in the downstream region are 1.52 m (60 in) rather than 1.93 m (80 in) long, and pressure drops are reduced Structurally, however, there are two distinct disadvantages: (1) the coolant manifolds are significantly longer, and (2) the tubes are not efficiently oriented with respect to the applied loads and thus, additional mass is required in the panel skins.

Figure 59 summarizes the analysis of the alternate Separate Panels design. At all three design conditions, the structural mass was found to be larger, as expected. The ACS components mass for Design Conditions 2 and 3 was determined to be less than that for the basic Separate Panels design, due to reduced pressure drops. However, total mass would be lower only at Design Condition 3. In any case, at all design conditions, the alternate Separate Panels design would still be much heavier than other concepts.

Configuration	Panel Height cm	(in)	Interference Heating Area: Ultimate Pressure kPa	(lbf/in^2)	Inner Skin Thickness mm	(in)	Structural Unit Mass kg/m^2	(lbf/ft^2)	Uniform Heating Area: Inner Skin Thickness mm	(in)	Structural Unit Mass kg/m^2	(lbf/ft^2)
SEP. PANELS 1	2.59	(1.02)	29.9	(4.34)	0.86	(.034)	7.57	(1.55)	0.64	(.025)	6.64	(1.36)
SEP. PANELS 2	2.59	(1.02)	29.9	(4.34)	0.86	(.034)	7.57	(1.55)	0.53	(.021)	6.79	(1.39)
SEP. PANELS 3	3.58	(1.41)	97.9	(14.2)	1.52	(.060)	9.86	(2.02)	0.53	(.021)	6.88	(1.41)
SEP. PANELS 4	3.58	(1.41)	97.9	(14.2)	1.52	(.060)	9.86	(2.02)	0.46	(.018)	6.93	(1.42)
SEP. PANELS 5	3.58	(1.41)	97.9	(14.2)	1.52	(.060)	9.86	(2.02)	0.41	(.016)	7.71	(1.58)
SEP. PANELS 6	2.97	(1.17)	51.3	(7.44)	1.07	(.042)	8.30	(1.70)	0.58	(.023)	6.64	(1.36)
SEP. PANELS 7	2.97	(1.17)	51.3	(7.44)	1.07	(.042)	8.30	(1.70)	0.48	(.019)	6.79	(1.39)
SEP. PANELS 8	2.97	(1.17)	51.3	(7.44)	1.07	(.042)	8.30	(1.70)	0.41	(.016)	7.27	(1.49)

FIGURE 57
BASIC SEPARATE PANELS CONCEPT GEOMETRIES AND UNIT MASSES

Component	Mass Difference	
	kg	(lbm)
Closure Angles	0.0	(0.0)
Two Manifolds and Bellmouth	+5.4	(+11.8)
Splice Plates	+0.6	(+ 1.3)
Adhesives	0.0	(0.0)
Connectors	+0.1	(+ 0.1)
Bushings/Fasteners	+0.2	(+ 0.3)
Total Added	+6.3	(+13.5)
Core Removed	-0.2	(- 0.5)
Total Difference	+6.1	(+13.0)

FIGURE 58
MASS OF ADDITIONAL MANIFOLDS AND JOINT MATERIALS REQUIRED FOR BASIC SEPARATE PANELS CONCEPT

Configuration	Panel Structural Mass		Difference from Basic Panel Structural Mass		ACS Components Mass		Difference from Basic ACS Components Mass		Total Mass		Difference from Basic Total Mass	
	kg	(lbm)	kg	(lbm)	kg	(lbm)	kg	(lbm)	kg	(lbm)	kg	(lbm)
ALT. SEP. PANELS 1	108	(238)	+4	(+9)	25	(56)	0	(0)	133	(294)	+4	(+9)
ALT. SEP. PANELS 2	108	(239)	+4	(+8)	30	(67)	0	(0)	139	(306)	+4	(+8)
ALT. SEP. PANELS 3	121	(266)	+8	(+18)	64	(140)	-2	(-5)	184	(406)	+6	(+13)
ALT. SEP. PANELS 4	121	(267)	+8	(+18)	69	(152)	-2	(-4)	190	(419)	+6	(+14)
ALT. SEP. PANELS 5	126	(278)	+8	(+18)	77	(170)	-2	(-4)	203	(448)	+6	(+14)
ALT. SEP. PANELS 6	112	(246)	+5	(+12)	135	(298)	-10	(-23)	247	(544)	-5	(-11)
ALT. SEP. PANELS 7	113	(248)	+5	(+12)	139	(307)	-10	(-23)	252	(555)	-5	(-11)
ALT. SEP. PANELS 8	116	(255)	+5	(+12)	162	(358)	-10	(-23)	278	(613)	-5	(-11)

FIGURE 59
ALTERNATE SEPARATE PANELS CONCEPT CONFIGURATIONS

In the alternate Separate Panels design the tubes run across the panel. Thus, the longitudinal (parallel to the tubes) thermal stresses would act perpendicular to the mechanical stresses and the transverse (perpendicular to the tubes) thermal stress would act in the same direction as the mechanical stresses and would, therefore, add directly to them. These transverse thermal stresses were compression in all cases. When combined with the mechanical stresses, they were less critical than the mechanical tension stresses, as for all previously considered concepts. Because the tubes were ineffective for mechanical loads the skins had to be thickened to maintain strength, making the structural unit mass of this design greater than that of the basic Separate Panels Design Concept. The alternate Separate Panels geometry and unit structural masses are shown in Figure 60. The areas considered for this configuration were the same as those defined for the basic Separate Panels configuration. Because the alternate Separate Panel design has a 1.02 m (40 in) greater length of manifolds than the basic Separate Panel design, the mass of the manifolds and splice materials was greater by 1.4 kg (3.0 lbm) for a total of 41.2 kg (90.0 lbm). Panel structural mass is included in Figure 59.

4.3.6 High Heat Transfer Tubes Concept - A literature search was conducted to identify ways to augment heat transfer in tubular flow. References 13 and 14 provide overviews and detailed bibliographies on this subject. A review of these references led to the conclusion that available techniques can be classified as those that: involve roughened tube wall surfaces, include tube inserts, use internally finned tube surfaces, or use dimpled tubes.

Many sources imply that augmentation of heat transfer via roughened tube walls is ineffective because the measured increase in heat transfer is countered by a pressure drop which makes the increase in overall efficiency negligible. However, it is noted in Reference 15 that, with high Prandtl number fluids, heat transfer improvements can be achieved through roughness without corresponding increases in pressure drop. Reference 16 acknowledges this point and also notes that very few data have been published for fluids with Prandtl numbers greater than 8. Therefore, Reference 16 presents data collected with flow of a fluid with a very high Prandtl number (349) in roughened tubes (see Figure 61).

Configuration	Panel Height		Interference Heating Area						Uniform Heating Area			
			Ultimate Pressure		Inner Skin Thickness		Structural Unit Mass		Inner Skin Thickness		Structural Unit Mass	
	cm	(in)	kPa	(lbf/in^2)	mm	(in)	kg/m^2	(lbm/ft^2)	mm	(in)	kg/m^2	(lbm/ft^2)
ALT. SEP. PANELS 1	2.92	(1.15)	29.9	(4.34)	1.07	(.042)	8.30	(1.70)	0.58	(.023)	6.64	(1.36)
ALT. SEP. PANELS 2	3.05	(1.20)	29.9	(4.34)	1.04	(.041)	8.25	(1.69)	0.48	(.019)	6.79	(1.39)
ALT. SEP. PANELS 3	4.39	(1.73)	97.9	(14.2)	2.03	(.080)	11.62	(2.38)	0.51	(.020)	7.13	(1.46)
ALT. SEP. PANELS 4	4.88	(1.92)	97.9	(14.2)	1.78	(.070)	11.18	(2.29)	0.41	(.016)	7.37	(1.51)
ALT. SEP. PANELS 5	4.39	(1.73)	97.9	(14.2)	2.03	(.080)	11.62	(2.38)	0.41	(.016)	7.96	(1.63)
ALT. SEP. PANELS 6	3.33	(1.31)	51.3	(7.44)	1.40	(.055)	9.37	(1.92)	0.56	(.022)	6.74	(1.38)
ALT. SEP. PANELS 7	3.02	(1.19)	51.3	(7.44)	1.52	(.060)	9.57	(1.96)	0.48	(.019)	6.79	(1.39)
ALT. SEP. PANELS 8	3.02	(1.19)	51.3	(7.44)	1.52	(.060)	9.57	(1.96)	0.41	(.016)	7.27	(1.49)

FIGURE 60
ALTERNATE SEPARATE PANELS CONCEPT GEOMETRIES AND UNIT MASSES

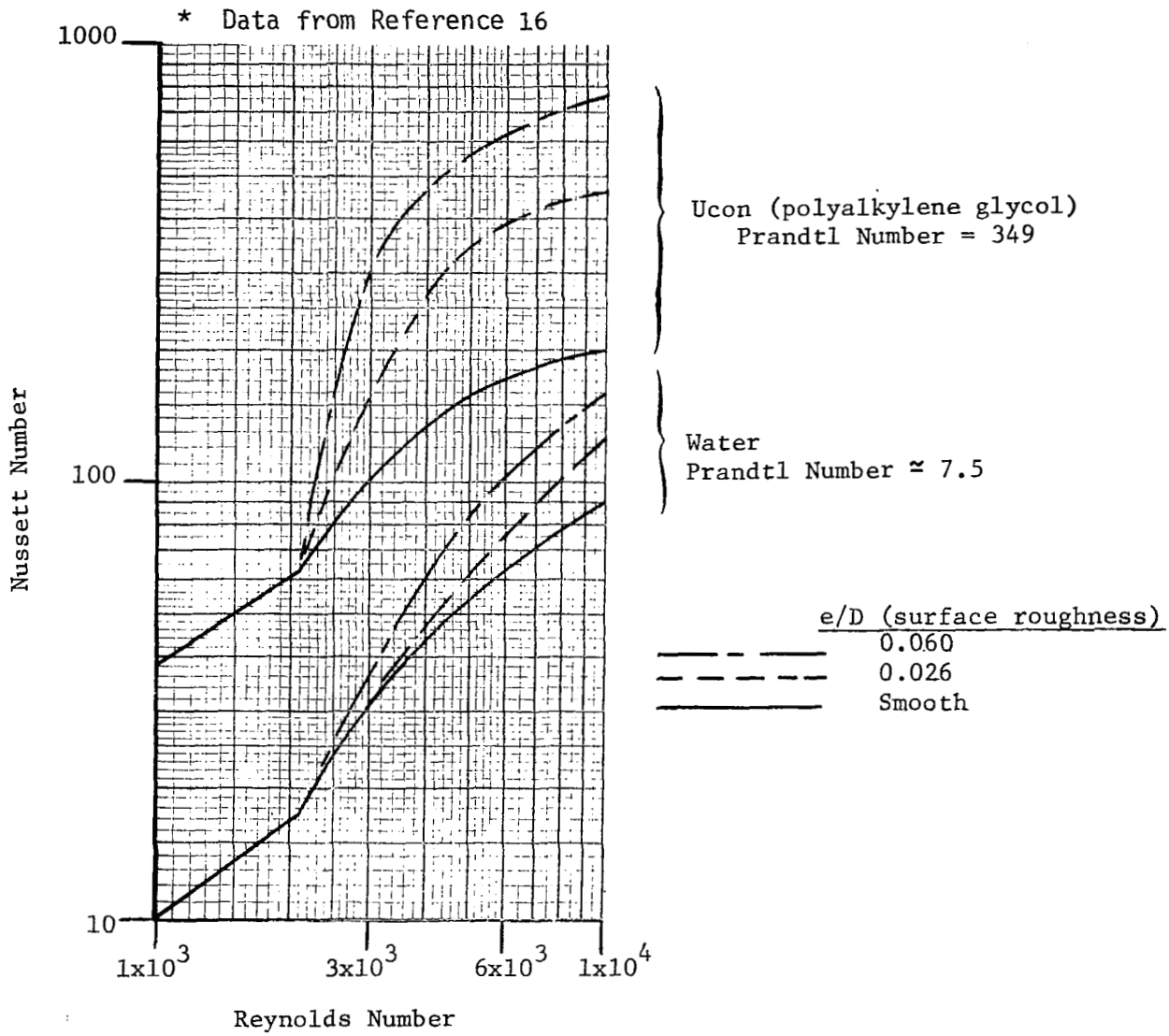

FIGURE 61
SURFACE ROUGHNESS EFFECTS ON HEAT TRANSFER

The laminar flow, smooth tube data in Figure 61 can be approximated using conventional expressions with the quoted Prandtl numbers. However, it is obvious that the higher Prandtl number fluid is more sensitive to surface roughness, both in the maximum level attained (at Re = 1 x 10^4) and throughout the Reynolds number range beyond laminar flow.

To apply these data to ethylene glycol/water, Figures 62 and 63 were prepared by logarithmically interpolating the available data. To calculate the Nusselt number at Re $\geq$ 1 x 10^4 the following expression was used:

$$N_u = \frac{\phi_{rough}}{\phi_{smooth}} \times 0.023 \ (R_e)^{.8} (P_r)^{.33} \ (\mu_b/\mu_w)^{.36}$$

The value of the factor $\frac{\phi_{rough}}{\phi_{smooth}}$ was obtained from Figure 62.

The use of Figure 62 requires a knowledge of the fluid's Prandtl number and a realistic estimate of the wall roughness. The Prandtl number for the assumed coolant varies from 57 at 283 K (50°F) to 14 at 339 K (150°F). An average value of 30, which corresponds to 305 K (90°F), was used for the conditions studied.

Surface roughness is the parameter that must be controlled if this technique is to be practical. The available information indicated that a roughness expressed in terms of e/D = 0.06 is attainable and representative of the roughened tube configurations fabricated for testing. Based on these values, the constant used in the turbulent heat transfer expression was modified by a factor of 2.5.

The correction curve presented in Figure 63 was used in simulating the transitional region (2100 < Re < 1 x 10^4). In the smooth tube analysis the technique used for estimating transitional heating was to logarithmically interpolate, with Reynolds number, the Nusselt number from the last laminar value to the initial turbulent value. However, without correction this interpolation would not predict the increase in heat transfer afforded by roughened surfaces at the near laminar, transitional Reynolds number conditions. As indicated in Figure 63, the correction involved is significant in

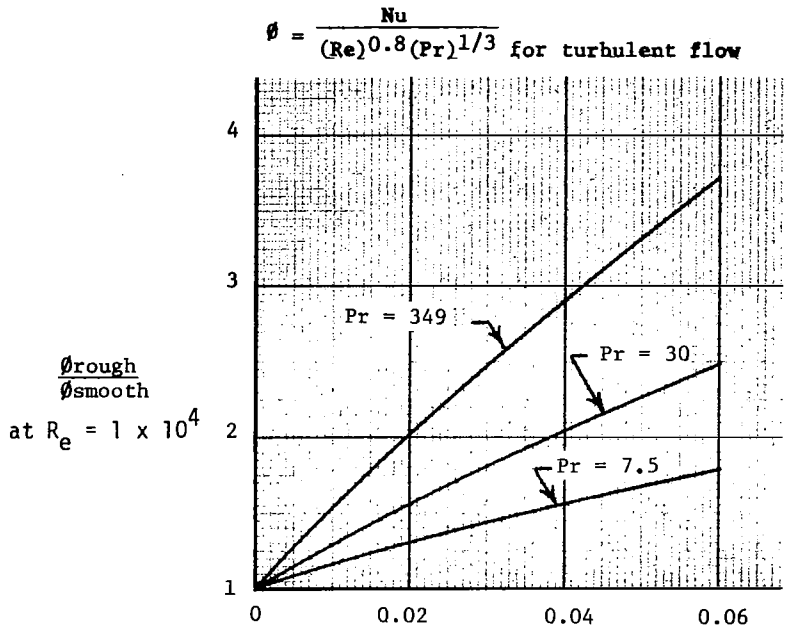

FIGURE 62
TURBULENT FLOW NUSSELT NUMBER CORRECTION FACTOR FOR ROUGHNESS EFFECTS

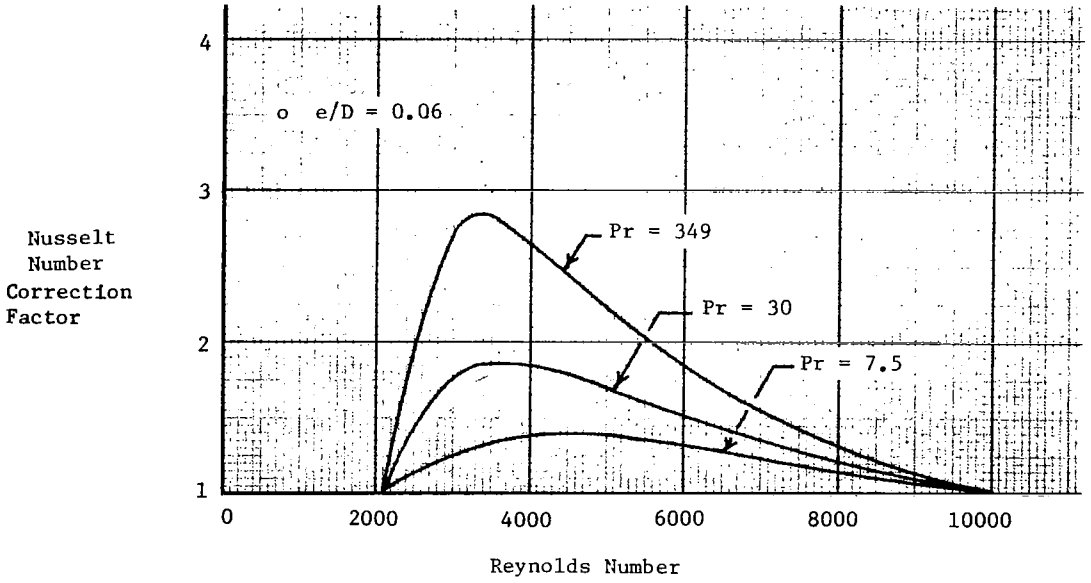

FIGURE 63
TRANSITIONAL FLOW NUSSELT NUMBER CORRECTION FOR ROUGHNESS EFFECTS

the Reynolds number range of interest in this study. Figure 64 illustrates the technique used to predict roughened tube heat transfer. It is based on a typical set of design conditions.

The information in standard texts on roughened tube friction factors is adequate for high Prandtl number fluids. The friction factor data used for the roughened tube analysis were obtained from Reference 4 for an e/D = 0.06 and are presented in Figure 65.

Figure 66 summarizes the results of the roughened tube analysis. In all cases, the tubes were assumed to have an internal surface roughness (e/D) of 0.06 over the full length and the panel outer skin thickness was assumed to be 1.02 mm (0.040 in). As shown, the configurations with 0.48 cm (3/16 in) diameter tubes would be lighter than those with larger tubes for Design Conditions 2 and 3. A significant observation can be made by comparing results for these configurations with those for the Modified Baseline Panel Concept, Figure 32. The coolant flow requirements for the Roughened Tube Concepts would be so much lower (due to the improved heat transfer characteristics) that the resultant coolant pressure drop would also be lower even though, for a given flow, the Roughened Tube Concept pressure drops would be considerably higher. As a result, ACS component mass requirements would be reduced by the use of the roughened tube technique.

Techniques that involve placing inserts in coolant tubes to augment heat transfer have been shown to dramatically accomplish that task but usually at great expense in terms of pressure drop. This trend is particularly evident with mesh and brush insert results reported in Reference 17. Promoting swirl flow with twisted tape inserts is apparently more efficient. This technique has been analyzed and reported a number of times, References 18 through 24. However, there appears to be some inconsistencies in the reported results.

Swirl flow heat transfer augmentation was analyzed using information from Reference 24 to develop laminar flow characteristics, and from Reference 19 for turbulent flow characteristics. The resulting expressions for heat transfer and friction factor are compared to smooth tube relationships in Figures 67 and 68. Only one value of tape twist ratio (inside diameters per 180° of tape twist), y = 2.5, was analyzed. This value represents a fairly

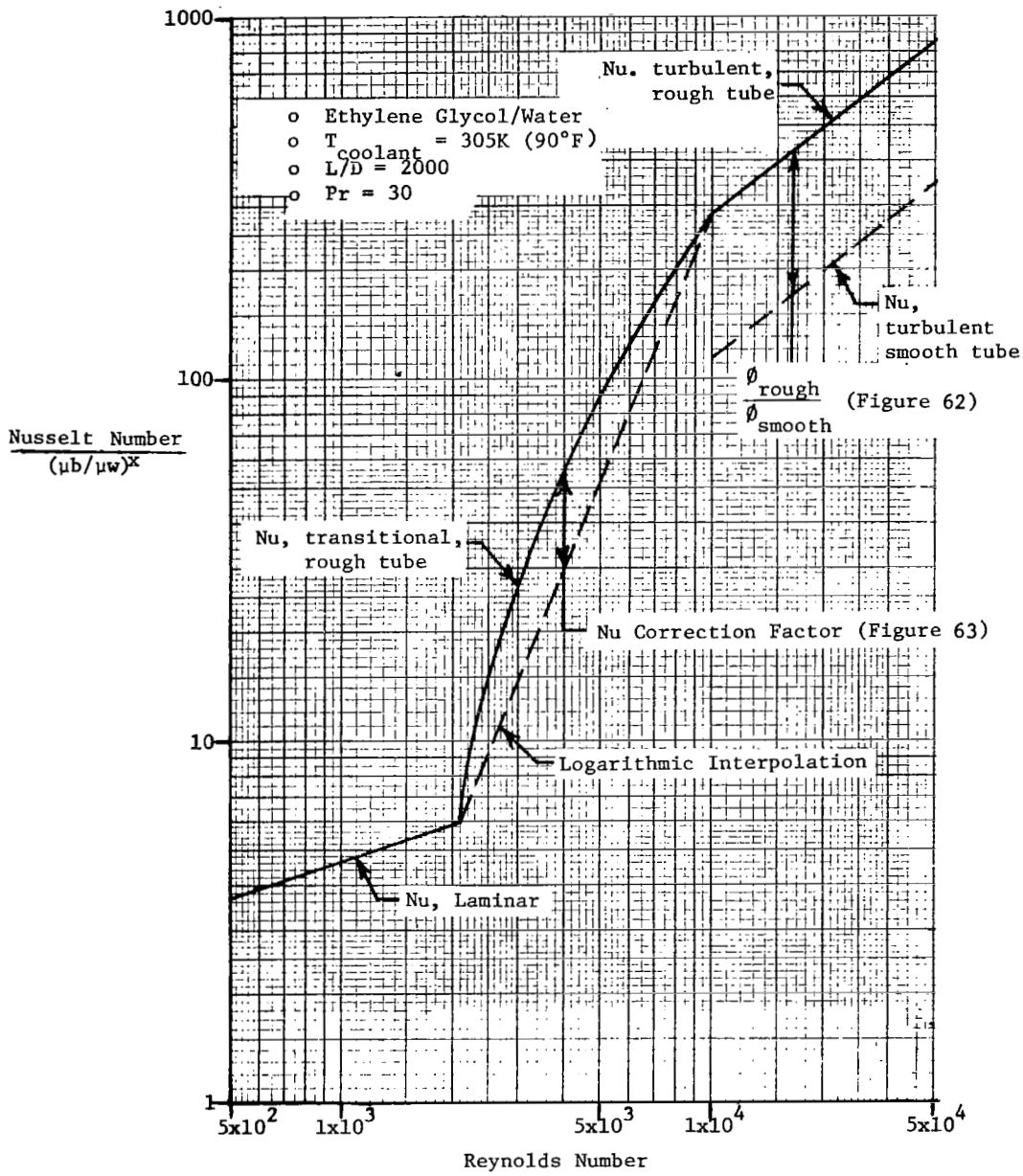

FIGURE 64
ROUGHENED TUBE CONCEPT HEAT TRANSFER PREDICTION TECHNIQUE

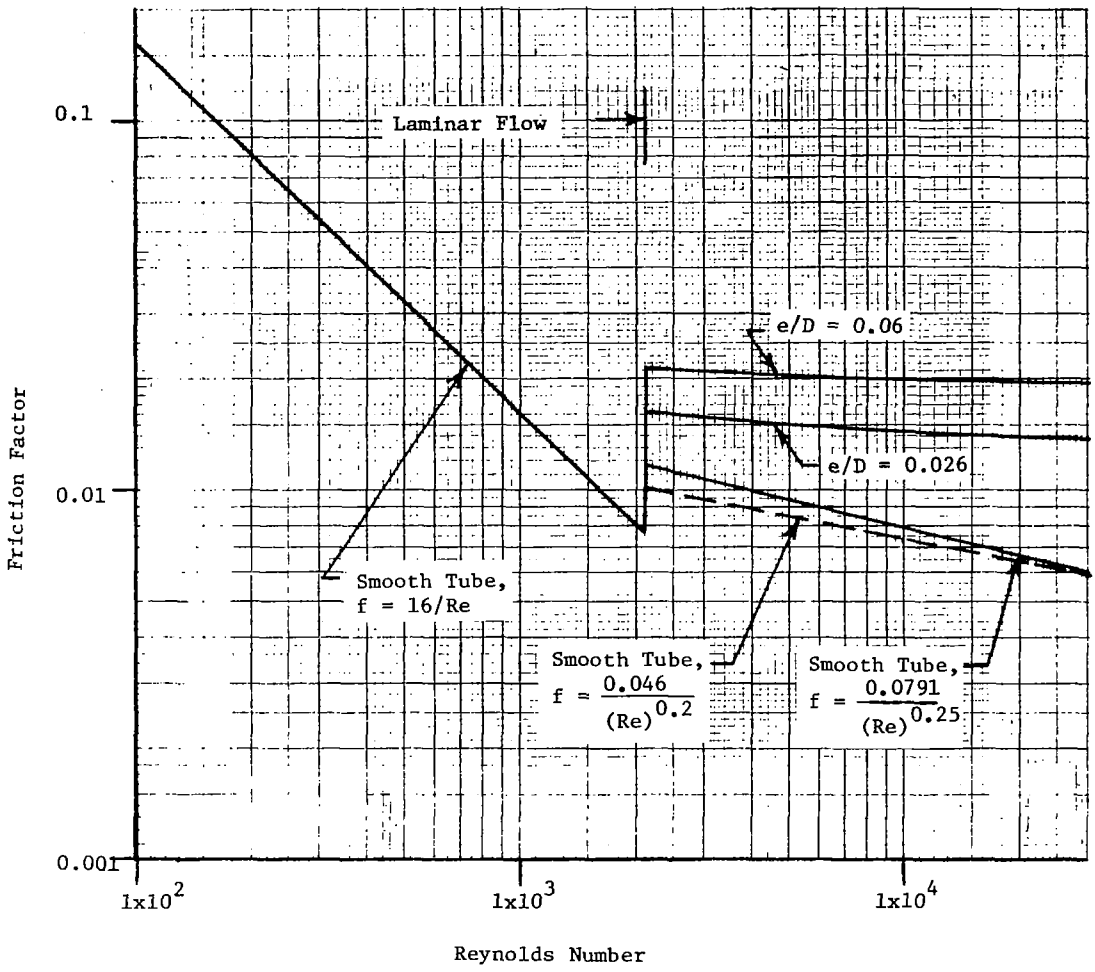

FIGURE 65
ROUGHENED TUBE FRICTION FACTOR

Configuration	Design Condition	Tube Pitch cm	Tube Pitch (in)	Tube Diameter cm	Tube Diameter (in)	Coolant Flow/Tube g/s	Coolant Flow/Tube (lbm/hr)	Panel Δp kPa	Panel Δp (lbf/in²)	Panel Structural Mass kg	Panel Structural Mass (lbm)	ACS Components Mass kg	ACS Components Mass (lbm)	Total Mass kg	Total Mass (lbm)
ROUGH. TUBE 1	1	2.54	(1.00)	0.48	(3/16)	14.8	(117)	352	(51)	98	(216)	19	(42)	117	(258)
ROUGH. TUBE 2	1	1.91	(0.75)	0.48	(3/16)	10.7	(85)	200	(29)	99	(218)	20	(43)	118	(261)
ROUGH. TUBE 3	2	1.91	(0.75)	0.48	(3/16)	26.5	(210)	1015	(147)	107	(236)	40	(88)	147	(324)
ROUGH. TUBE 4	2	2.54	(1.00)	0.64	(1/4)	78.2	(620)	1725	(250)	106	(234)	83	(184)	190	(418)
ROUGH. TUBE 5	2	2.54	(1.00)	0.95	(3/8)	112.2	(890)	296	(43)	110	(243)	94	(208)	205	(451)
ROUGH. TUBE 6	3	1.91	(0.75)	0.48	(3/16)	60.5	(480)	7060	(1024)	101	(223)	161	(354)	262	(577)
ROUGH. TUBE 7	3	2.54	(1.00)	0.95	(3/8)	201.8	(1600)	931	(135)	106	(233)	162	(357)	268	(590)

Note: All configurations have outer skin thickness = 1.02 mm (0.040 in)

Configuration	Coolant in Panel kg	Coolant in Panel (lbm)	Coolant in Distribution Lines kg	Coolant in Distribution Lines (lbm)	Coolant Distribution Lines kg	Coolant Distribution Lines (lbm)	Heat Exchanger kg	Heat Exchanger (lbm)	Pumps kg	Pumps (lbm)	Pumping Power Penalty kg	Pumping Power Penalty (lbm)	Reservoir kg	Reservoir (lbm)	Total ACS Components Mass kg	Total ACS Components Mass (lbm)
ROUGH. TUBE 1	3.2	(7.1)	8.1	(17.9)	2.4	(5.4)	2.4	(5.3)	0.5	(1.1)	1.7	(3.8)	0.7	(1.6)	19	(42)
ROUGH. TUBE 2	4.3	(9.4)	7.9	(17.4)	2.2	(4.8)	↓	↓	0.5	(1.0)	1.5	(3.3)	0.8	(1.7)	20	(43)
ROUGH. TUBE 3	4.3	(9.4)	16.4	(36.2)	6.9	(15.3)	3.0	(6.7)	1.8	(3.9)	6.0	(13.3)	1.3	(2.9)	40	(88)
ROUGH. TUBE 4	6.9	(15.3)	30.8	(68.0)	17.0	(37.5)	↓	↓	5.3	(11.7)	17.8	(39.3)	2.4	(5.2)	83	(184)
ROUGH. TUBE 5	18.8	(41.5)	40.8	(89.9)	11.9	(26.2)	↓	↓	3.7	(8.1)	12.3	(27.2)	3.6	(8.0)	94	(208)
ROUGH. TUBE 6	4.3	(9.4)	30.6	(67.4)	46.4	(102.4)	6.6	(14.5)	16.1	(35.6)	54.3	(119.8)	2.3	(5.0)	161	(354)
ROUGH. TUBE 7	18.8	(41.5)	63.1	(139.1)	25.7	(56.6)	↓	↓	9.8	(21.5)	32.7	(72.2)	5.1	(11.2)	162	(357)

FIGURE 66
SUMMARY OF ROUGHENED TUBE CONCEPT CONFIGURATIONS

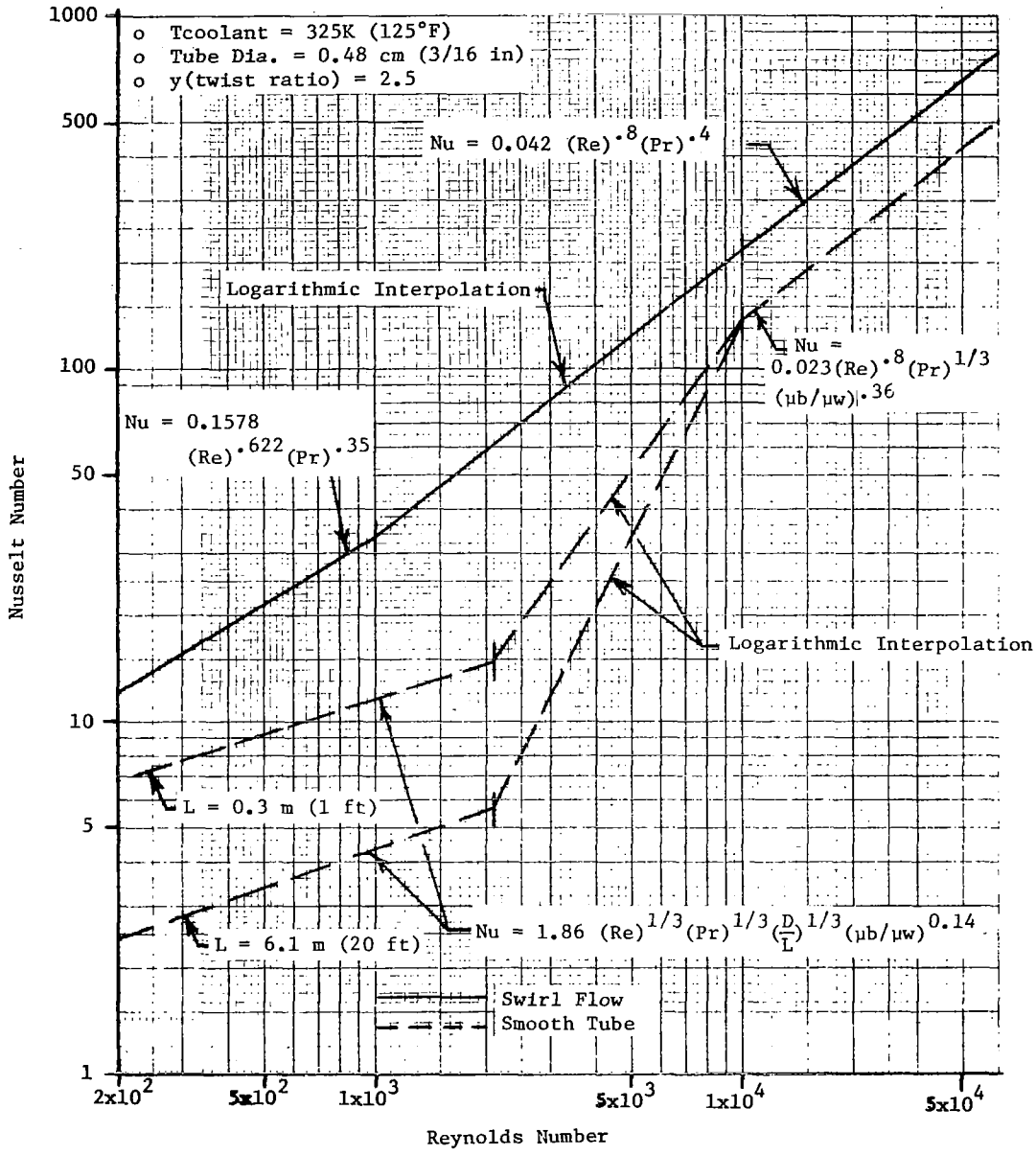

FIGURE 67

SWIRL FLOW CONCEPT HEAT TRANSFER EXPRESSIONS

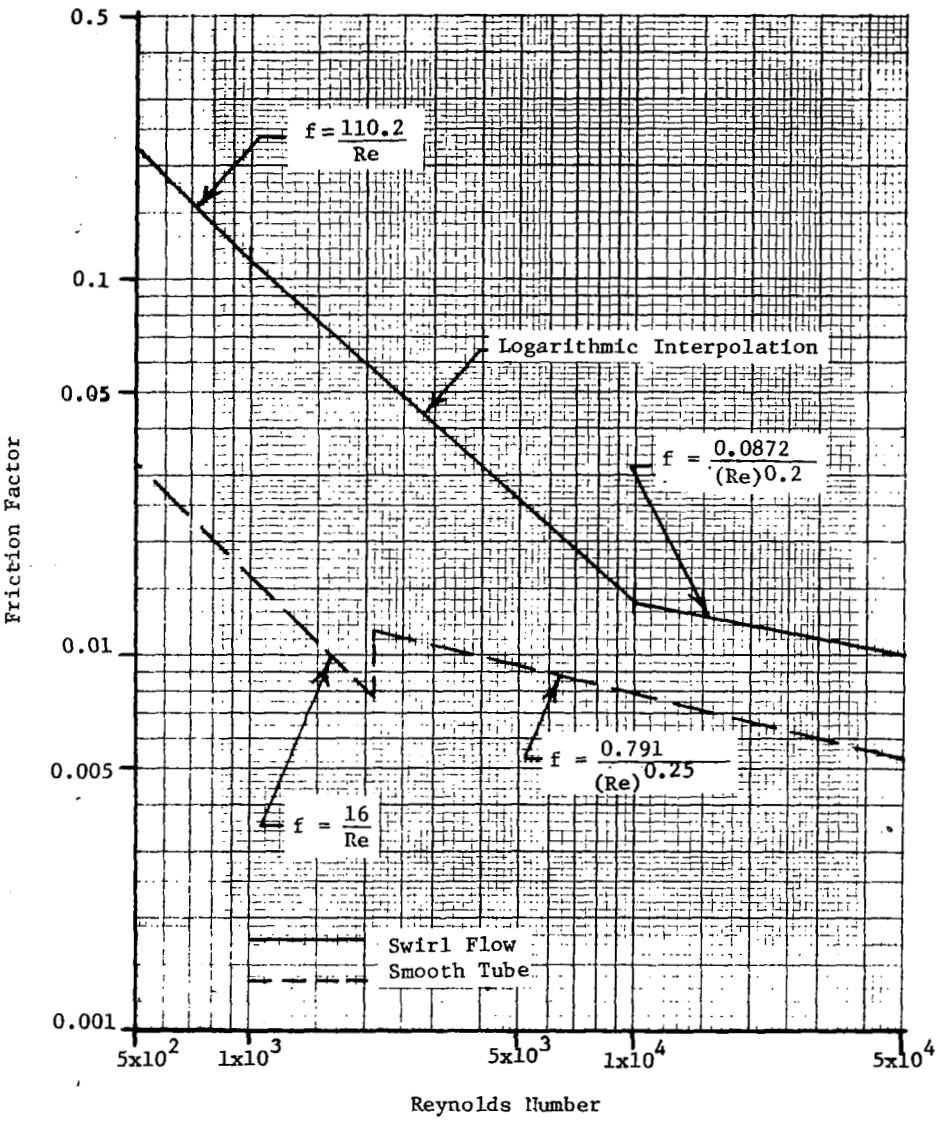

FIGURE 68
SWIRL FLOW CONCEPT FRICTION FACTOR

tight twist (trend data indicate that tight twists are more efficient). Data in Reference 24 are presented only up to a Re = 1000 while data in Reference 19 are applicable for Re $\geq$ 1 x 10^4. These values were accepted as the critical Reynolds numbers for laminar and turbulent flow, respectively. Logarithmic interpolation was again used to estimate trends in the intermediate range of Reynolds numbers.

Figures 67 and 68 reveal that large increases in heat transfer and friction factor result at low Reynolds numbers with swirl flow. At high Reynolds numbers the differences between swirl flow and smooth tube turbulent flow are smaller.

A summary of the swirl flow analysis results is presented as Figure 69. The panel structural masses reflect an allowance for the mass of the tape insert based on stainless steel, 0.1 mm (0.004 in) thick foil. This allowance was 1.36 kg (3 lbm) for the 0.48 cm (3/16 in) and 0.64 cm (1/4 in) diameter tubes. It was 2.27 kg (5 lbm) for the 0.95 cm (3/8 in) diameter tubes. The total panel masses for Design Condition 1 are essentially the same as those determined for roughened tubes as presented in Figure 66. However, at Design Conditions 2 and 3, the Swirl Flow Concept masses are less than those for the Roughened Tube Concepts. The heat transfer characteristics created by swirling the flow are enhanced to the point that larger tubes become attractive, particularly for the large flow requirements associated with Design Condition 3.

References 25 and 26 provided the information used to predict the internal heat transfer performance of finned tubes in the laminar and turbulent flow regimes respectively. Figure 70 summarizes the laminar heat transfer characteristics from Reference 25. As shown, the tubes discussed in this reference were characterized by fin geometry either straight or spiraled. Since the intent of this analysis was to evaluate the effects of a typical rather than specific finned tube geometry, the data pertaining to straight fin tubes was used. This data, for the most part, falls between the high and low spiral fin data and maintains a slope consistent with that of a smooth tube. Finned tube flow ceases to display laminar characteristics at a lower Reynolds number than smooth tube flow. The extent of laminar flow is indicated in Figure 70 for each characteristic fin type, where straight fin tubes have a critical Reynolds number of 1300.

Configuration	Design Condition	Tube Pitch cm	(in)	Tube Diameter cm	(in)	Coolant Flow/Tube g/s	(lbm/hr)	Panel ΔP kPa	(lbf/in^2)	Panel Structural Mass kg	(lbm)	ACS Components Mass kg	(lbm)	Total Mass kg	(lbm)
SWIRL FLOW 1	1	2.54	(1.00)	0.48	(3/16)	12.6	(100)	993	(144)	99	(219)	19	(42)	118	(261)
SWIRL FLOW 2	1	1.91	(0.75)	0.48	(3/16)	8.6	(68)	614	(89)	100	(221)	18	(40)	118	(261)
SWIRL FLOW 3	2	1.91	(0.75)	0.48	(3/16)	15.8	(125)	1655	(240)	108	(239)	31	(68)	139	(307)
SWIRL FLOW 4	2	2.54	(1.00)	0.64	(1/4)	37.8	(300)	1130	(164)	108	(237)	51	(113)	159	(350)
SWIRL FLOW 5	2	2.54	(1.00)	0.95	(3/8)	31.5	(250)	110	(16)	112	(248)	47	(103)	159	(351)
SWIRL FLOW 6	3	1.91	(0.75)	0.48	(3/16)	53.6	(425)	8095	(1174)	103	(226)	158	(348)	260	(574)
SWIRL FLOW 7	3	2.54	(1.00)	0.95	(3/8)	132.4	(1050)	669	(97)	108	(238)	116	(255)	224	(493)

Note: All configurations have outer skin thickness = 1.02 mm (0.040 in)

Configuration	Coolant in Panel kg	(lbm)	Coolant in Distribution Lines kg	(lbm)	Coolant Distribution Lines kg	(lbm)	Heat Exchanger kg	(lbm)	Pumps kg	(lbm)	Pumping Power Penalty kg	(lbm)	Reservoir kg	(lbm)	Total ACS Components Mass kg	(lbm)
SWIRL FLOW 1	3.2	(7.1)	7.1	(15.7)	3.0	(6.6)	2.4	(5.3)	0.6	(1.4)	2.2	(4.8)	0.7	(1.5)	19	(42)
SWIRL FLOW 2	4.3	(9.4)	6.5	(14.4)	2.3	(5.0)	↓	↓	0.5	(1.0)	1.6	(3.5)	0.7	(1.6)	18	(40)
SWIRL FLOW 3	4.3	(9.4)	10.7	(23.6)	5.8	(12.7)	3.0	(6.7)	1.4	(3.1)	4.8	(10.5)	1.0	(2.1)	31	(68)
SWIRL FLOW 4	6.9	(15.3)	19.9	(43.9)	8.8	(19.5)	↓	↓	2.4	(5.4)	8.2	(18.0)	1.7	(3.7)	51	(113)
SWIRL FLOW 5	18.8	(41.5)	15.0	(33.1)	3.9	(8.5)	↓	↓	0.9	(2.0)	3.0	(6.6)	2.1	(4.6)	47	(103)
SWIRL FLOW 6	4.3	(9.4)	27.7	(61.0)	47.2	(104.1)	6.6	(14.5)	16.1	(35.6)	54.3	(119.7)	2.1	(4.6)	158	(348)
SWIRL FLOW 7	18.8	(41.5)	45.5	(100.3)	16.3	(36.0)	↓	↓	5.5	(12.2)	18.7	(41.2)	4.0	(8.9)	116	(255)

FIGURE 69
SUMMARY OF SWIRL FLOW CONCEPT CONFIGURATIONS

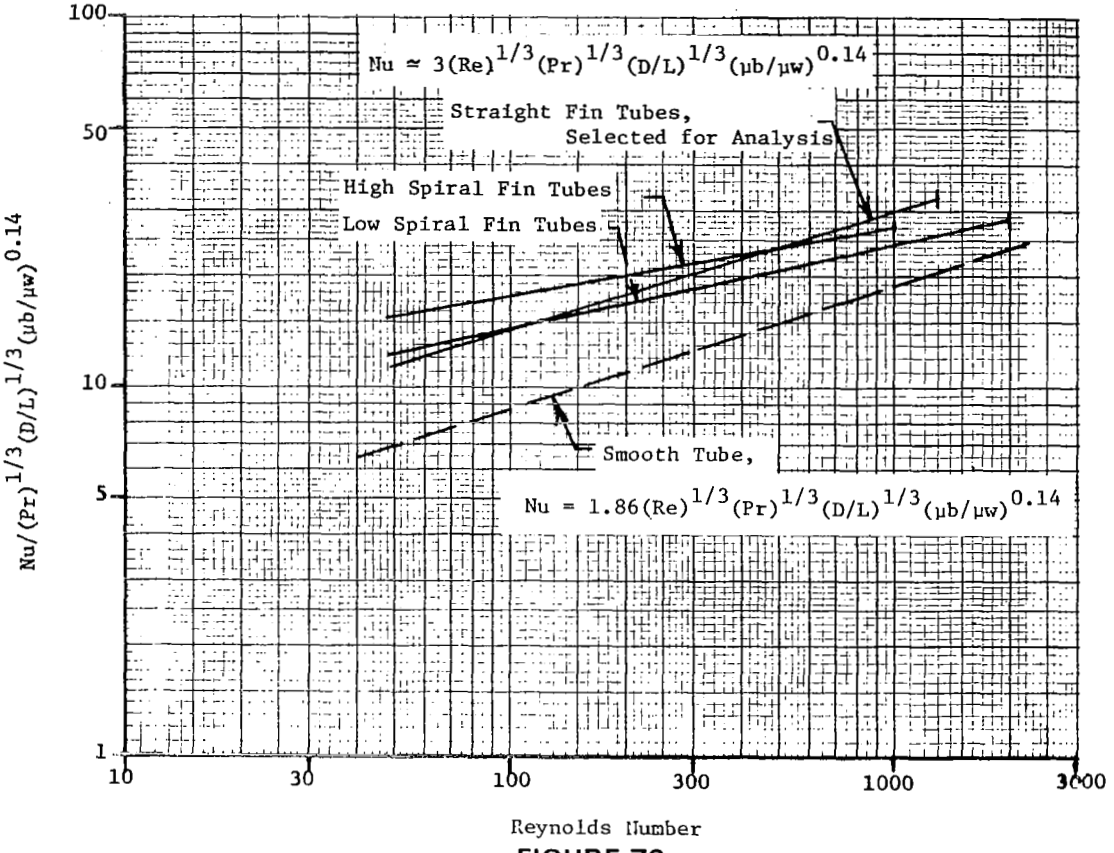

FIGURE 70
LAMINAR FLOW HEAT TRANSFER - FINNED TUBES CONCEPT

Figure 71 presents turbulent flow heat transfer data from Reference 26. These data indicate a critical Reynolds number of 3000 for turbulent flow. A correlating expression in the form similar to that used for smooth tube, turbulent flow, heat transfer was selected. As shown in Figure 71, the selected expression, which modifies only the constant of the smooth tube expression, passes through the center of the data band without exceeding data extremes. As in previous analyses, heat transfer in the transition region, in this case between Reynolds Numbers of 1300 and 3000, was determined by logarithmic interpolation.

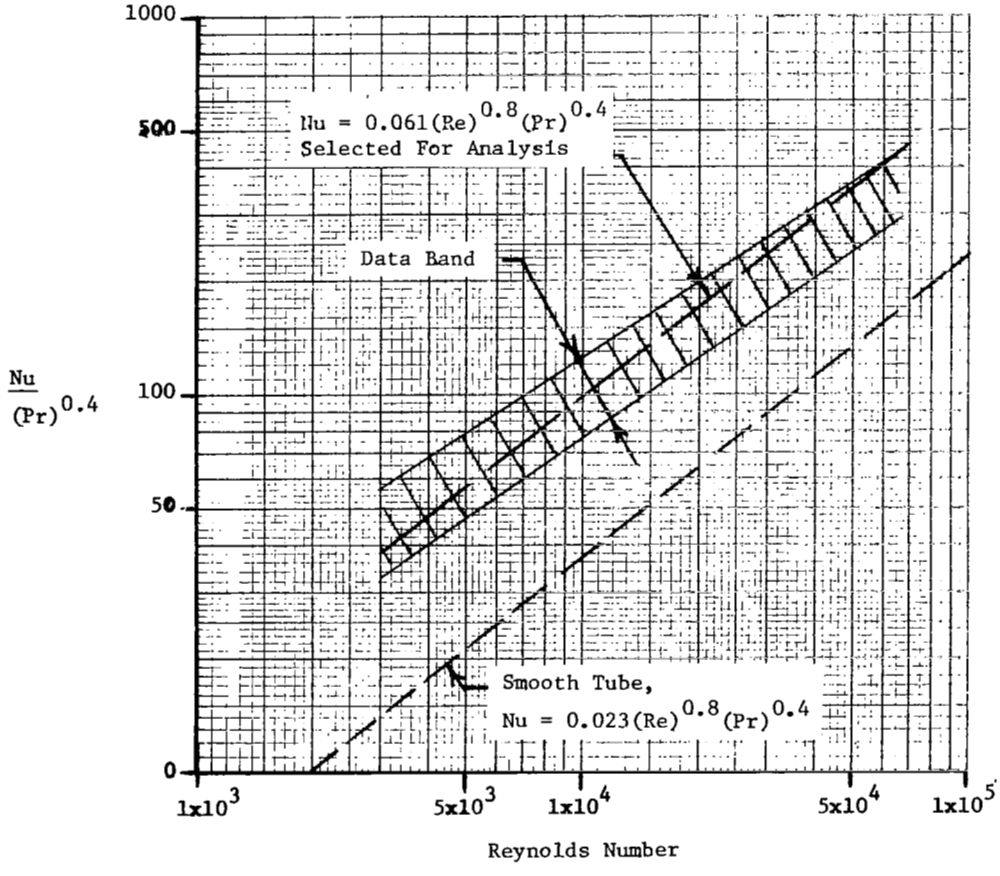

FIGURE 71
TURBULENT FLOW HEAT TRANSFER - FINNED TUBES CONCEPT

Friction factors (Figure 72) used in the finned tube analysis were also derived from References 25 and 26. In the laminar range, an average value line was drawn through the band of available data. Reference 26 provided the expression used in the turbulent flow range which was assumed to be applicable above the maximum laminar flow Reynolds number.

Figure 73 summarizes the results from the Finned Tube Concept analysis. The panel structural masses include an allowance for heavier tubes to account for the additional fin mass. These allowances were determined to coincide with the Swirl Flow Concept allowances which had accounted for the tape inserts.

In Figure 73, it can be noted that minimum panel mass is associated with minimum tube diameter. The minimum total panel mass at Design Condition 1 is slightly less than the masses obtained with previously discussed design approaches. Similarly, the Finned Tube Concept masses for Design Conditions 2 and 3 are substantially below those associated with the other High Heat Transfer Tube Concepts.

The final heat transfer augmentation technique investigated was that involving geometric discontinuities designed into the tubes themselves. Figure 74 presents data from Reference 27 comparing heat transfer and friction factor characteristics for a dimpled flattened tube and a smooth tube. Although the apparent gain in heat transfer with this configuration is impressive, the friction factor data do not appear to be correct. While the shape of the friction factor data is believable there is no logic that can explain how the friction in a dimpled tube can be below that of the smooth tube. Due to the doubts concerning the validity of this available data and to the producibility complications that would arise when using such tubes in a cooled panel design, this technique was not studied in any further detail.

In summary, the Roughened Tubes, Swirl Flow, and Finned Tube Concepts all afford an overall mass savings because the heat transfer improvements outweigh the pressure drop penalties. These savings are of sufficient magnitude that heat transfer augmentation should be considered in any subsequent study of actively cooled panels. For the purposes of this study, it appears

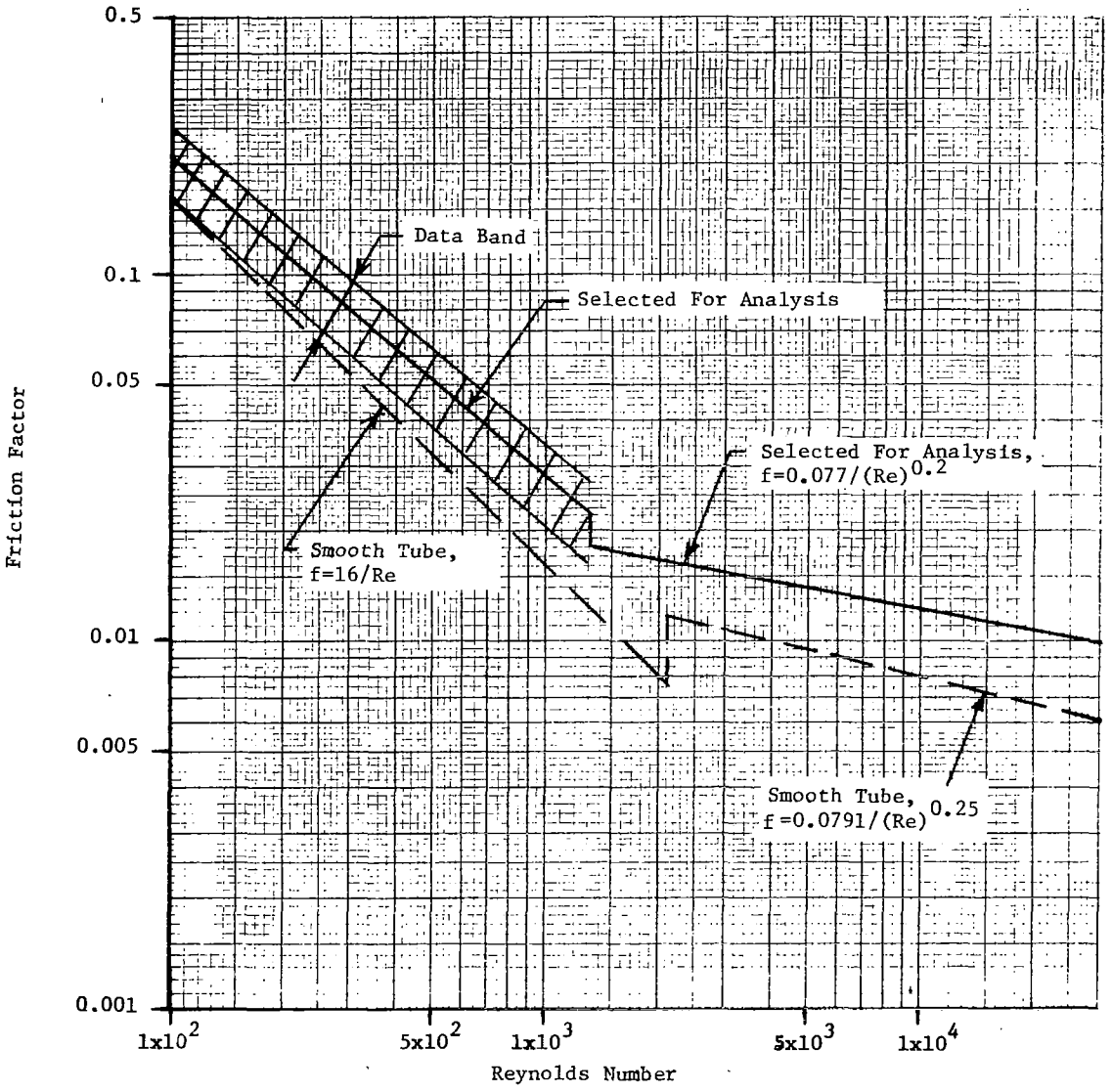

FIGURE 72
FINNED TUBES CONCEPT FRICTION FACTOR

Configuration	Design Condition	Tube Pitch cm	Tube Pitch (in)	Tube Diameter cm	Tube Diameter (in)	Coolant Flow/Tube g/s	Coolant Flow/Tube (lbm/hr)	Panel ΔP kPa	Panel ΔP (lbf/in^2)	Panel Structural Mass kg	Panel Structural Mass (lbm)	ACS Components Mass kg	ACS Components Mass (lbm)	Total Mass kg	Total Mass (lbm)
FIN. TUBE 1	1	1.91	(0.75)	0.48	(3/16)	8.8	(70)	97	(14)	100	(221)	17	(37)	117	(258)
FIN. TUBE 2	1	2.54	(1.00)	0.64	(1/4)	12.4	(98)	28	(4)	101	(222)	20	(43)	120	(265)
FIN. TUBE 3	1	2.54	(1.00)	0.95	(3/8)	18.0	(143)	7	(1)	105	(232)	35	(77)	140	(309)
FIN. TUBE 4	2	1.91	(0.75)	0.48	(3/16)	16.8	(133)	276	(40)	108	(239)	25	(56)	134	(295)
FIN. TUBE 5	2	2.54	(1.00)	0.64	(1/4)	38.5	(305)	186	(27)	108	(237)	38	(84)	146	(321)
FIN. TUBE 6	2	2.54	(1.00)	0.95	(3/8)	53.2	(422)	34	(5)	112	(248)	57	(126)	170	(374)
FIN. TUBE 7	3	1.91	(0.75)	0.48	(3/16)	52.3	(415)	1860	(270)	103	(226)	77	(170)	180	(396)
FIN. TUBE 8	3	2.54	(1.00)	0.95	(3/8)	145.6	(1155)	193	(28)	108	(238)	109	(241)	217	(479)

Note: All configurations have outer skin thickness = 1.02 mm (0.040 in)

Configuration	Coolant in Panel kg	Coolant in Panel (lbm)	Coolant in Distribution Lines kg	Coolant in Distribution Lines (lbm)	Coolant Distribution Lines kg	Coolant Distribution Lines (lbm)	Heat Exchanger kg	Heat Exchanger (lbm)	Pumps kg	Pumps (lbm)	Pumping Power Penalty kg	Pumping Power Penalty (lbm)	Reservoir kg	Reservoir (lbm)	Total ACS Components Mass kg	Total ACS Components Mass (lbm)
FIN. TUBE 1	3.9	(8.5)	6.7	(14.8)	1.7	(3.8)	2.4	(5.3)	0.3	(0.7)	1.1	(2.5)	0.7	(1.5)	17	(37)
FIN. TUBE 2	6.3	(13.8)	7.0	(15.4)	1.7	(3.7)	↓	↓	0.3	(0.7)	1.1	(2.4)	0.9	(1.9)	20	(43)
FIN. TUBE 3	16.9	(37.3)	9.6	(21.1)	2.3	(5.0)	↓	↓	0.5	(1.0)	1.6	(3.5)	1.6	(3.6)	35	(77)
FIN. TUBE 4	3.9	(8.5)	11.2	(24.8)	3.2	(7.1)	3.0	(6.7)	0.7	(1.6)	2.4	(5.4)	1.0	(2.2)	25	(56)
FIN. TUBE 5	6.3	(13.8)	17.6	(38.8)	4.8	(10.5)	↓	↓	1.2	(2.6)	3.9	(8.6)	1.5	(3.3)	38	(84)
FIN. TUBE 6	16.9	(37.3)	22.8	(50.3)	5.6	(12.3)	↓	↓	1.4	(3.1)	4.7	(10.4)	2.4	(5.4)	57	(126)
FIN. TUBE 7	3.9	(8.5)	27.1	(59.8)	15.6	(34.4)	6.6	(14.5)	5.0	(11.0)	16.9	(37.2)	2.0	(4.4)	77	(170)
FIN. TUBE 8	16.9	(37.3)	49.0	(108.1)	13.4	(29.5)	↓	↓	4.4	(9.7)	14.8	(32.6)	4.1	(9.1)	109	(241)

FIGURE 73
SUMMARY OF FINNED TUBES CONCEPT CONFIGURATIONS

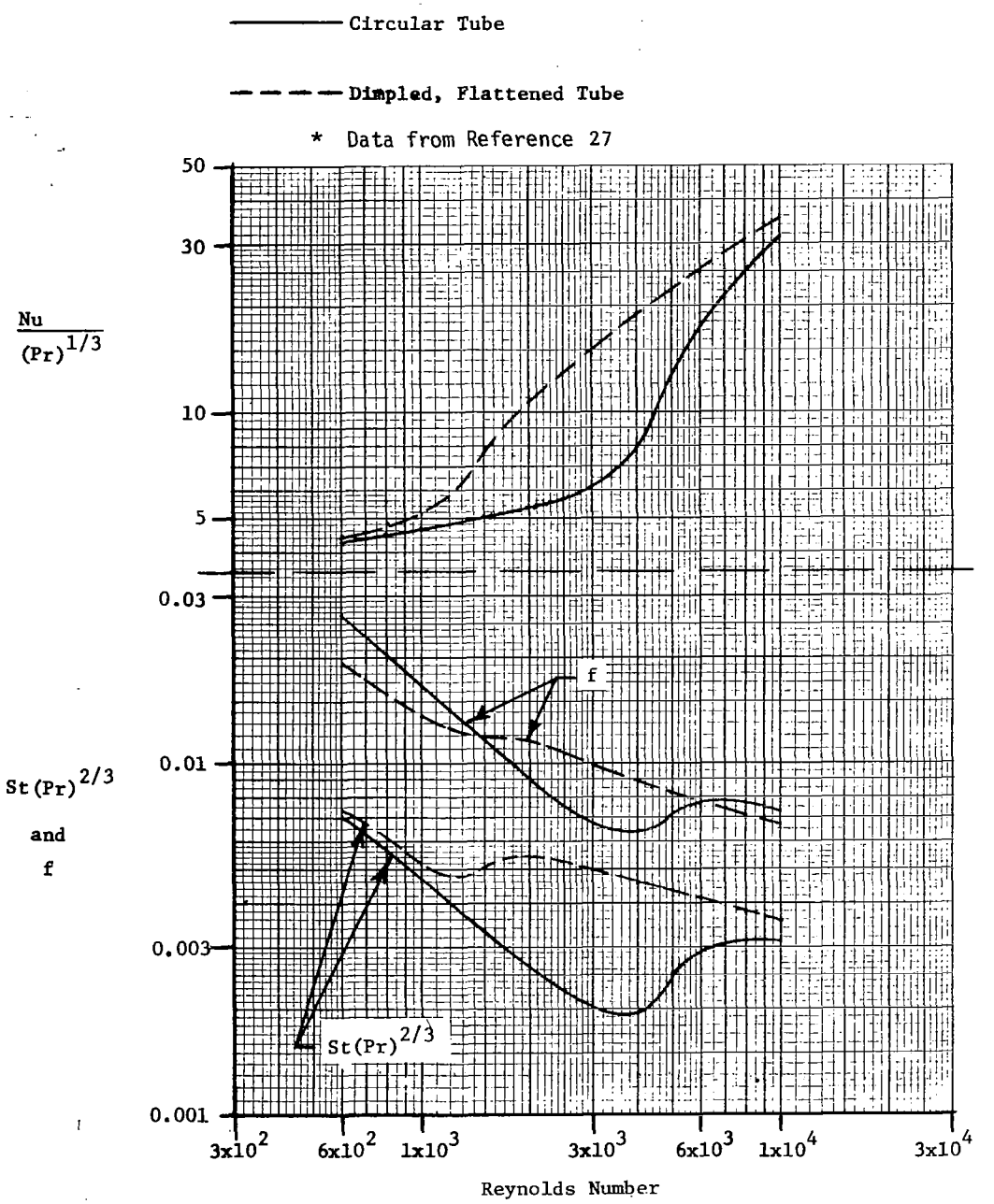

FIGURE 74
FLOW CHARACTERISTICS - DIMPLED, FLATTENED TUBES

that the Finned Tube Concept is the most attractive augmentation technique examined. This can be explained by examining Figures 75 and 76. These figures merge the heat transfer and friction factor characteristic data of all of the promising techniques discussed in this section. In the Reynolds number range of 2×10^3 to 1×10^4, where the majority of design configurations analyzed can be characterized, the finned tubes provide both the most desirable heat transfer and friction factor characteristics.

4.3.7 Insulated Panel - The results of MCAIR's Radiative Actively Cooled Panel program (NAS1-13939) provided the basis for analysis of an Insulated Panel design. As shown in Figure 28, the concept assumed for analysis employs an external thermal protection system (TPS) attached to the cooled panel. The TPS consists of a Rene shingle and a layer of insulation. The shingle reaches sufficiently high temperatures that large quantities of incoming aerodynamic heat are radiated away. The layer of insulation protects the cooled panel from direct contact with the hot shingle. A minimum thickness layer of insulation has been shown, in the concurrent study to be sufficient for heat loads of the magnitude considered in this study. Therefore, a 0.32 cm (1/8 in) layer of insulation was assumed without resorting to detailed TPS optimization studies.

While the addition of these external TPS provisions adds 66.2 kg (146 lbm) to the structural mass, the ACS component masses are drastically reduced since the heat that must be absorbed by the coolant is small. Figure 77 compares the heat that must be absorbed by the Insulated Panel with the bare cooled panel's external surface heat load. To derive these relationships, the design heat loads were converted to convective heating parameters of an adiabatic wall temperature and external surface heat transfer coefficients. For Mach 6 cruise at an altitude of 30.5 km (100,000 ft), an adiabatic wall temperature of 1672 K (2550°F) is representative. Based on the TPS configuration described above, the following equivalences were obtained:

$\dot{q}$ to Bare Cooled Panel at 394 K (250°F)		Heat Transfer Coefficient, Mach 6 Insulated Panel Surface	
kW/m^2 ($Btu/sec\ ft^2$)		$W/m^2 \cdot K$ ($Btu/hr\ ft^2\ °F$)	
22.7	(2)	17.8	(3.12)
45.4	(4)	35.5	(6.26)
56.7	(5)	44.4	(7.83)
113.5	(10)	88.8	(15.65)
170.2	(15)	133.2	(23.48)

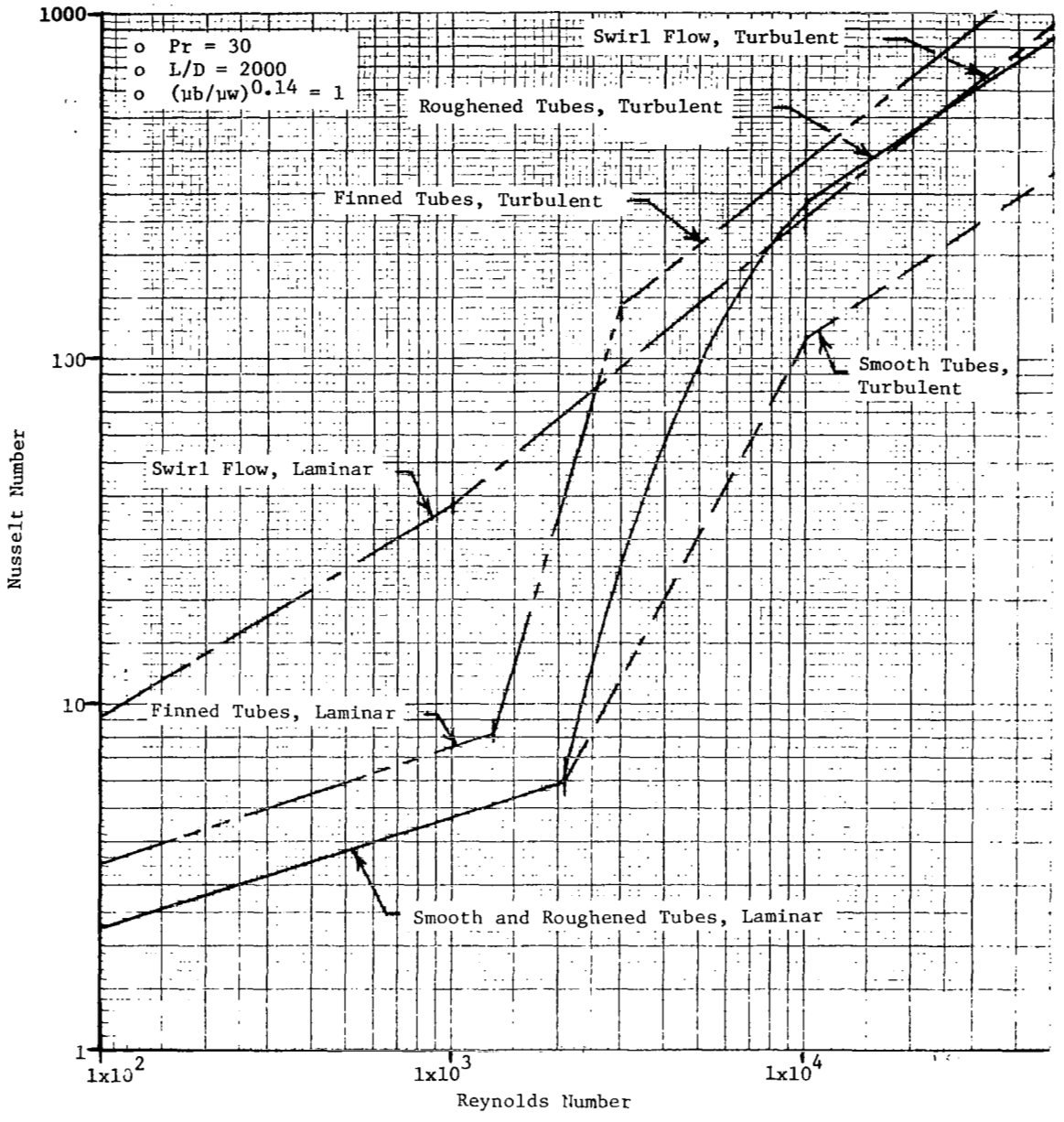

FIGURE 75
COMPARISON OF HEAT TRANSFER AUGMENTATION TECHNIQUES

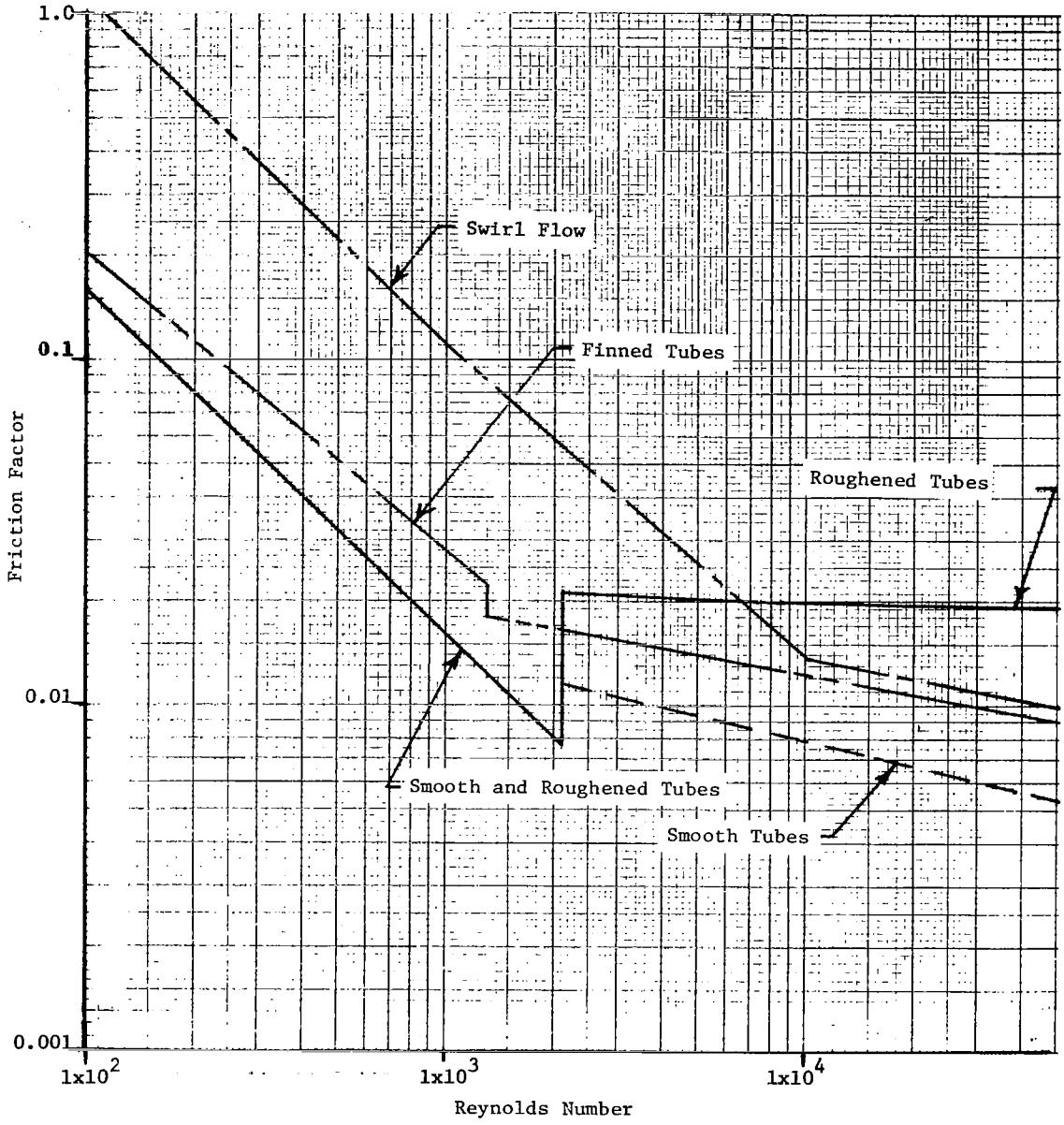

FIGURE 76
COMPARISON OF FRICTION FACTORS ASSOCIATED WITH AUGMENTATION TECHNIQUES

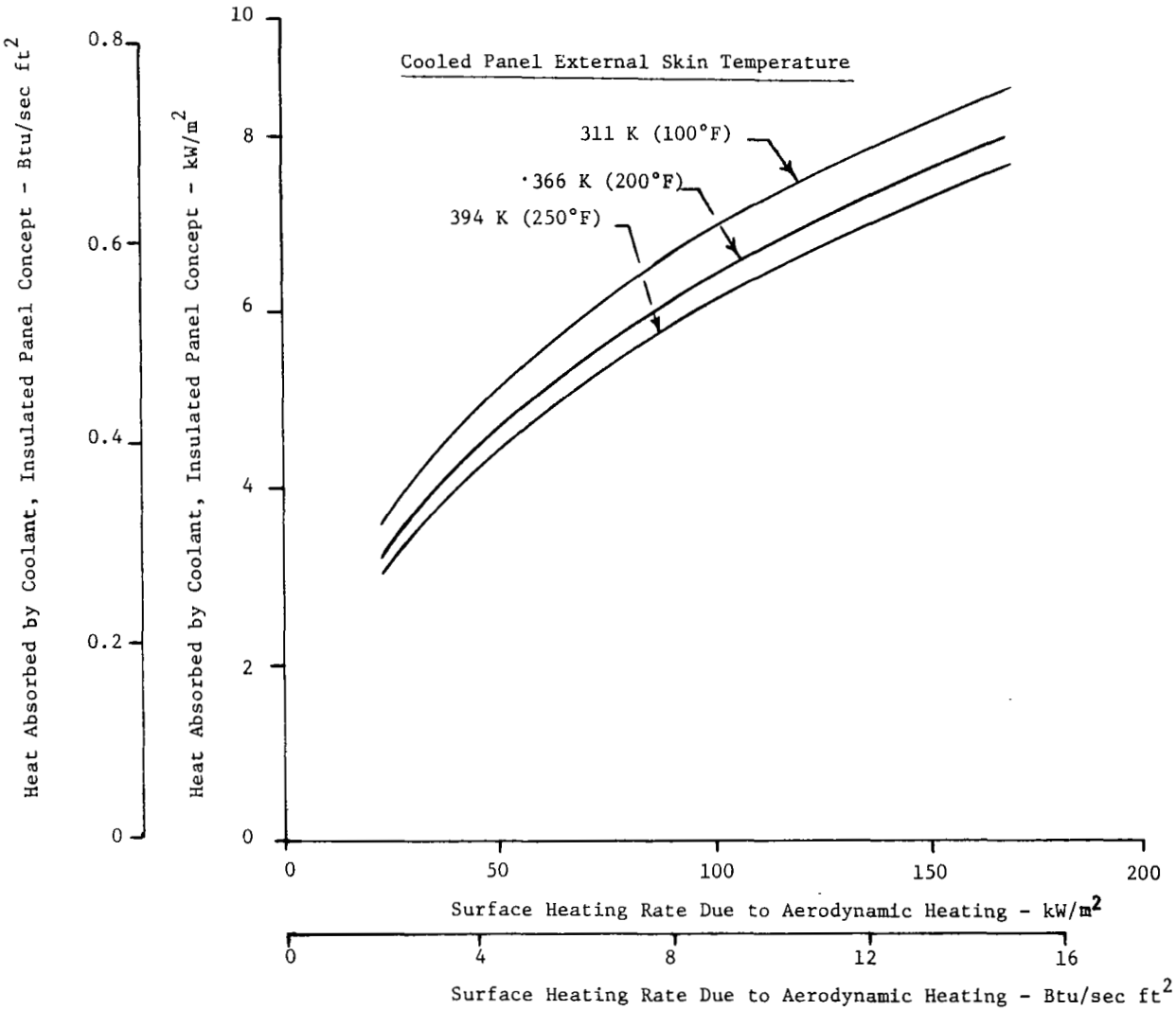

FIGURE 77
ACTIVE COOLING SYSTEM HEAT ABSORPTION REQUIREMENTS ARE REDUCED WITH INSULATED PANEL CONCEPT

The insulation thermal conductivity used reflected the beneficial effects of the reduced pressures at 30.5 km (100,000 ft) altitude. Heat inputs to the cooled panel thermal model also reflected the effects of the local cooled panel skin temperature as indicated in Figure 77. As a result, the total heat absorbed by the Insulated Panel cooling system compared to that absorbed by the cooling systems sized for the other concepts was reduced as follows:

Design Condition	$\left(\frac{\text{Insulated Panel Heat Load}}{\text{Heat Load, Other Concepts}}\right)$
1	0.141
2	0.119
3	0.081

These large reductions in absorbed heat are reflected in the ACS component masses summarized in Figure 78. This figure also provides total Insulated Panel masses for each of the design conditions. As expected, the mass variation for this concept was small. While its total panel mass makes this concept uncompetitive with other candidate concepts at low heating conditions, the Insulated Panel becomes increasingly competitive with more severe heating conditions.

The reduced coolant flows required by the Insulated Panel resulted in smaller structural temperature gradients and, therefore, lower thermal stress levels than those identified for other concepts. Since this design concept introduced no new structural combinations, additional structural analysis was not necessary. The panel unit masses shown for the Insulated Panel in Figure 78, are the same as the Modified Baseline Panel Concept.

Configuration	Design Condition	Coolant Flow/Tube g/s	Coolant Flow/Tube (lbm/hr)	Panel ΔP kPa	Panel ΔP (lbf/in²)	Thermal Protection System: Shingle Mass kg	Shingle Mass (lbm)	Insulation and Attachment Mass kg	Insulation and Attachment Mass (lbm)	Panel Structural Mass kg	Panel Structural Mass (lbm)	ACS Components Mass kg	ACS Components Mass (lbm)	Total Mass kg	Total Mass (lbm)
INS. PANEL 1	1	1.8	(14)	21	(3)	40	(89)	26	(57)	98	(216)	6	(14)	171	(376)
INS. PANEL 2	2	2.1	(17)	28	(4)	40	(89)	26	(57)	106	(234)	6	(14)	179	(394)
INS. PANEL 3	3	3.2	(25)	41	(6)	40	(89)	26	(57)	100	(221)	8	(17)	174	(384)

Note: All configurations have outer skin thickness = 1.02 mm (0.040 in), tube pitch = 2.54 cm (1.00 in), and tube diameter = 0.48 cm (3/16 in).

Configuration	Coolant in Panel kg	Coolant in Panel (lbm)	Coolant in Distribution Lines kg	Coolant in Distribution Lines (lbm)	Coolant Distribution Lines kg	Coolant Distribution Lines (lbm)	Heat Exchanger kg	Heat Exchanger (lbm)	Pumps kg	Pumps (lbm)	Pumping Power Penalty kg	Pumping Power Penalty (lbm)	Reservoir kg	Reservoir (lbm)	Total ACS Components Mass kg	Total ACS Components Mass (lbm)
INS. PANEL 1	3.2	(7.1)	1.6	(3.6)	0.4	(0.9)	0.4	(0.8)	0.1	(0.1)	0.1	(0.3)	0.3	(0.7)	6	(14)
INS. PANEL 2	3.2	(7.1)	1.9	(4.1)	0.5	(1.0)	0.4	(0.8)	0.1	(0.1)	0.2	(0.4)	0.3	(0.7)	6	(14)
INS. PANEL 3	3.2	(7.1)	2.5	(5.6)	0.6	(1.4)	0.5	(1.2)	0.1	(0.2)	0.3	(0.6)	0.4	(0.8)	8	(17)

FIGURE 78
SUMMARY OF INSULATED PANEL CONCEPT CONFIGURATIONS

4.3.8 Heat Pipe Concept - In theory, heat pipes can absorb large quantities of heat and transport the heat to another region, and will function with only a small temperature difference. As indicated in Figure 29, two arrangements were considered. In the first arrangement, heat pipes were located between the coolant tubes to absorb the heat in the region exposed to interference heating and to redistribute it to other regions of the panel. However, this approach would not reduce the total heat load so that ACS component masses would not be significantly different from those determined for the Modified Baseline Panel Concepts. Thus, while temperature gradients in the highly heated structure would be reduced, this would not produce significant mass savings (previous analyses show the designs to be relatively insensitive to thermal gradients). In addition, insertion of heat pipes would require wider coolant tube spacing which would reduce the system's structural efficiency.

The second arrangement shown in Figure 29 was then examined. It was assumed that, if heat pipes could be used to absorb the excess heat load in the region of increased heating and transfer this heat to the coolant in the panel exit manifold, a reduction in ACS component mass might be obtained since the total heat absorbed would be reduced. However a cursory examination revealed that the combination of heat pipe length, on the order of 1.83 m (6 ft), and the necessity to operate against the gravitational effects of flight, resulted in heat pipe diameters that were incompatible with the basic cooled panel geometry. It was readily apparent that the heat pipe masses involved could be quite large.

Discussions with various MCAIR personnel currently involved in heat pipe studies revealed that other problems would exist for this application. For example, due to the lack of long life data on heat pipes it would be necessary to provide for frequent inspections which would impose restrictions on panel assembly. Also, to maintain compatibility with aluminum structure the choice of working fluids becomes limited and most of the highly efficient fluids cease to be candidates. Thus, Heat Pipe Concepts do not appear to be attractive.

4.4 Concept Comparisons

The concept evaluation, Section 4.3, emphasized design requirements in terms of total mass chargeable to each 9.29 m^2 (100 ft^2) panel. A rough comparison of the concepts can be made by examining those masses. The minimum total panel masses associated with each concept are summarized in Figures 79, 80 and 81 for Design Conditions 1, 2 and 3 respectively. These masses are compared to the uniformly heated baseline panel designs discussed in Section 3.4.

Design Condition 1 is the least severe of the heating conditions considered. As shown in Figure 79, the mass increase (over the baseline panel design) required to satisfy this condition is nominal in most instances, a number of concepts can be considered competitive solely on a mass basis.

At the more severe Design Condition 2, the mass differences between concepts become more pronounced, Figure 80. The Intermediate Manifold Concept and the High Heat Transfer Tube Concepts offer distinct mass reductions compared to the other concepts. Of the three design conditions, Design Condition 2 requires the highest panel structural masses for all concepts. This is attributable to the high design limit loads imposed on the regions designed for interference heating. As explained in Section 3.3, the peak external normal pressures in these regions are a function of the ratio $(\dot{q}_{peak}/\dot{q}_{uniform})$ which is higher for Design Condition 2 than either of the other conditions. This shows that, in addition to the increased heating associated with disturbed flow regions, local pressure effects are important as a cooled panel design parameter.

Since Design Condition 3 imposes the largest heat load on the panels, the panel masses are significantly higher with wider spreads between concepts, Figure 81. Although the Insulated Panel Concept was non-competitive at the lower design conditions, it is clearly the minimum mass concept to satisfy Design Condition 3. However, the Thickened Skin Concept and the Finned Tubes Concept are still competitive due to considerations other than mass. A basic study objective was "to evaluate the designs on the basis of weight, reliability, and ease of manufacture." Therefore, it was necessary to derive a ranking system that included these considerations.

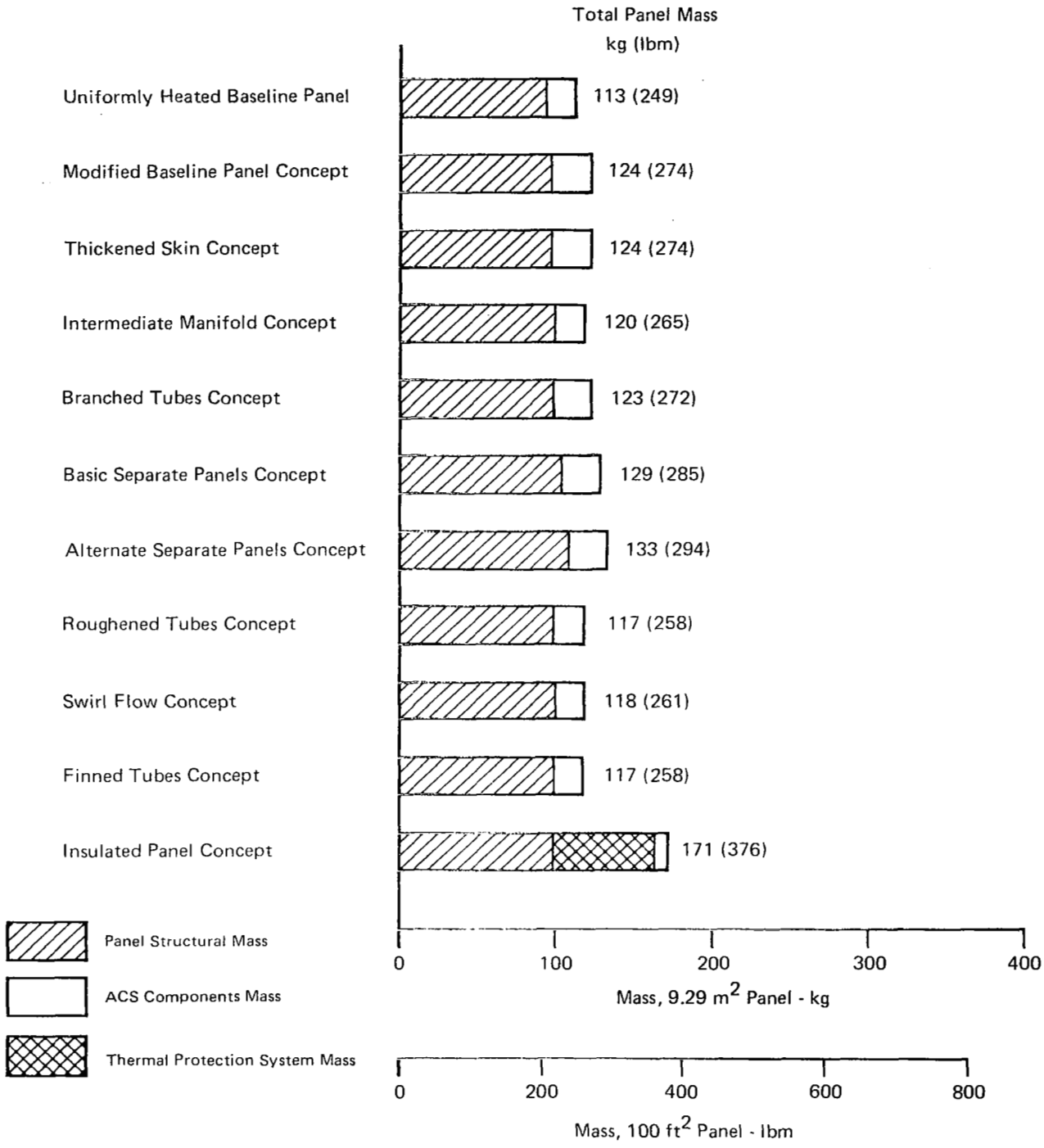

FIGURE 79
CONCEPT MASS SUMMARY - DESIGN CONDITION 1

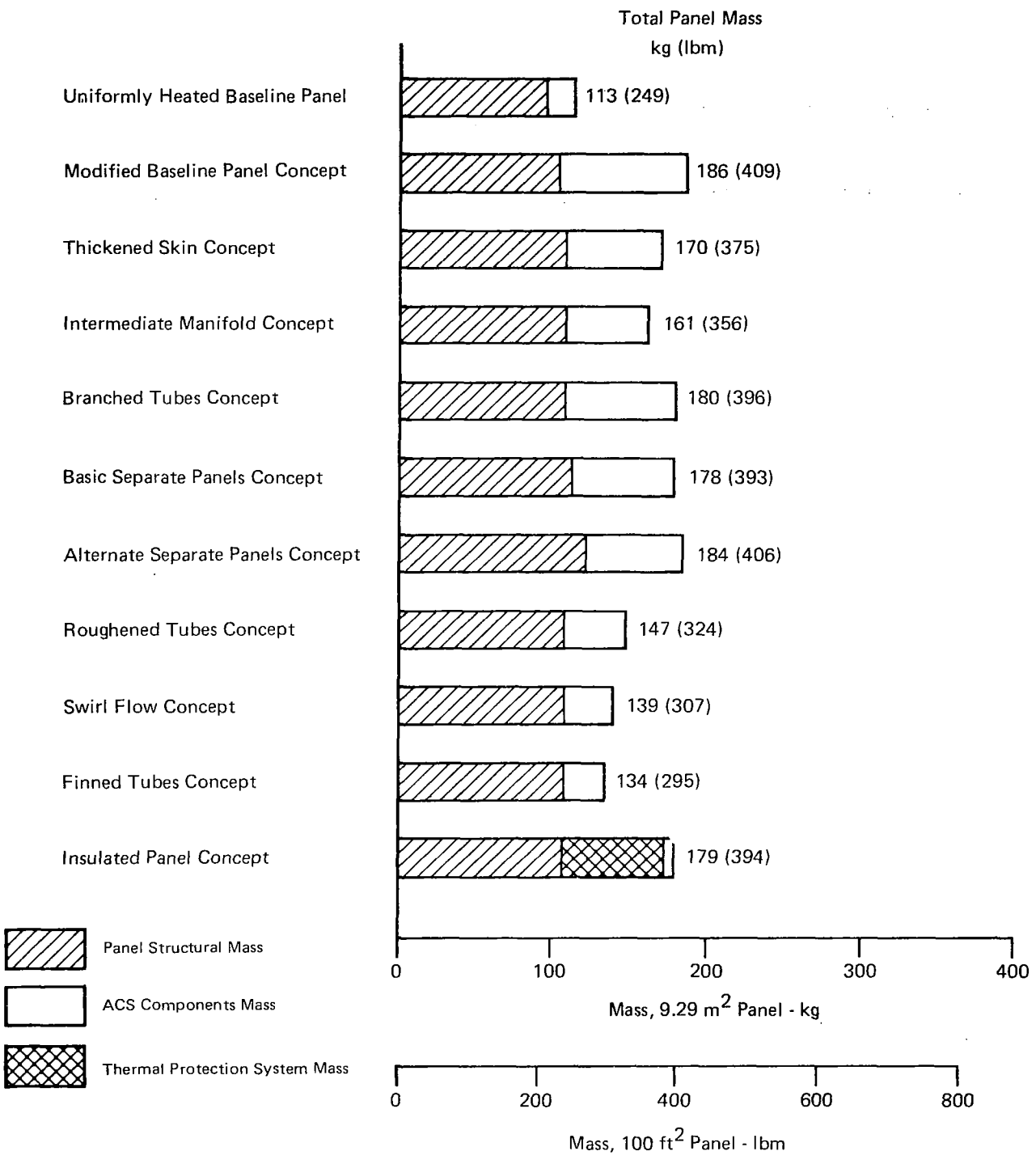

FIGURE 80
CONCEPT MASS SUMMARY - DESIGN CONDITION 2

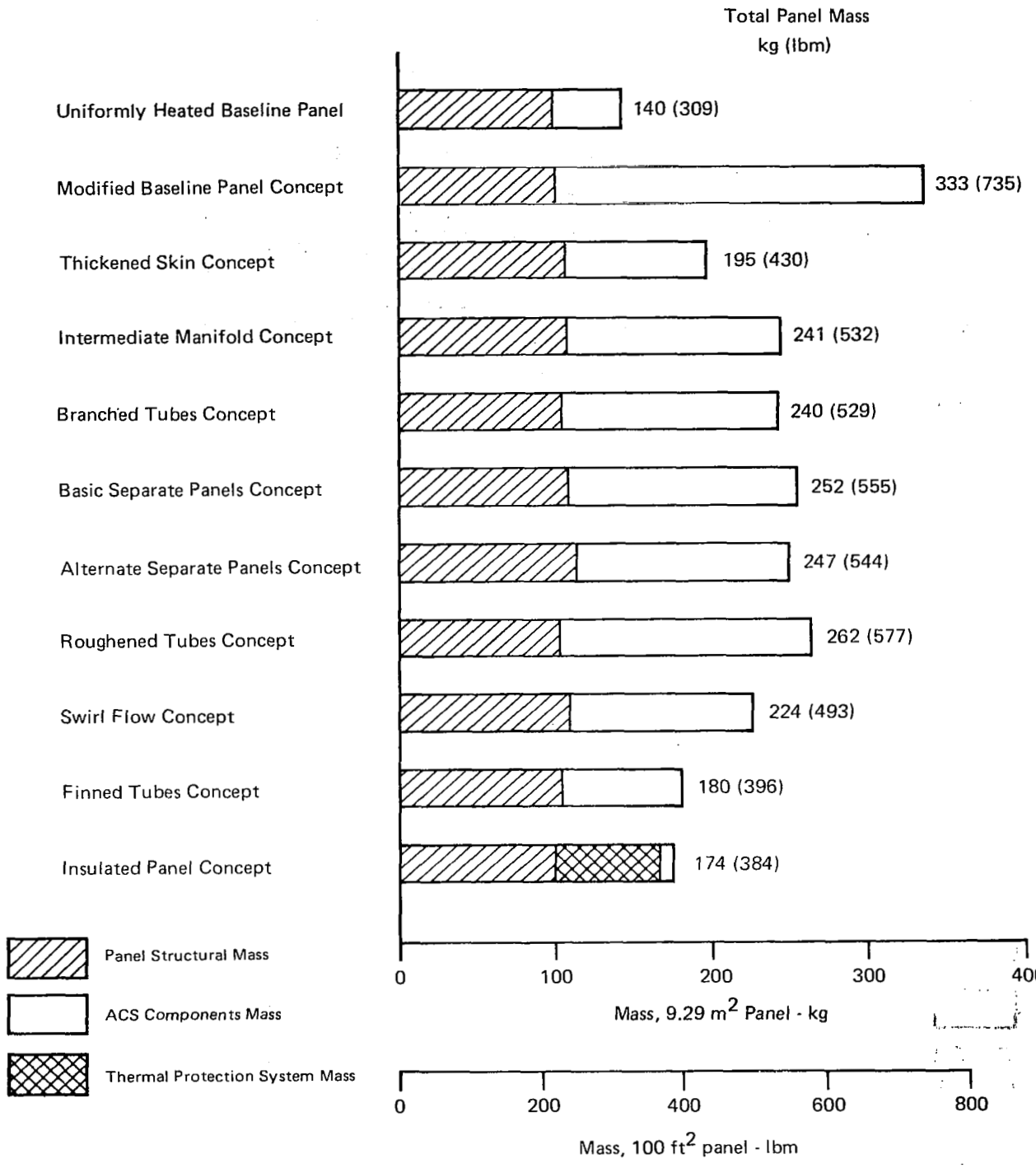

FIGURE 81
CONCEPT MASS SUMMARY - DESIGN CONDITION 3

4.4.1 Ranking System - Ranking systems developed for other studies including the Reference 2 program were reviewed. Most were found to be rather detailed and to involve unique considerations pertinent to those studies. It was therefore decided to formulate a ranking system specifically for this study that would merge and simplify those systems. This ranking system is summarized in Figure 82.

Four figures of merit (mass, producibility, reliability, and inspectability/maintainability) were identified. A weighing factor was assigned to each figure of merit. The emphasis was placed on mass. Although cost was not identified as a specific figure of merit, cost considerations were included. For example, mass affects both the initial and operating cost of a flight vehicle. Producibility rankings to a large extent involve the considerations leading to the initial item cost. Reliability and inspectability/maintainability considerations are also factors contributing to operational cost.

As shown in Figure 82, the ranking scale was set up so that a grade of 1.0 indicates that a concept is equivalent to the baseline panel concept. Grades below 1.0 reflect qualities inferior to the baseline panel concept while those above 1.0 reflect superior qualities. Mass grading was accomplished by ratioing the concept mass to the applicable baseline panel mass. Producibility grading was based on quantitative evaluations of the relative initial costs of the concepts. The remaining figures of merit were rated qualitatively based on the consensus of engineering judgements obtained from various MCAIR individuals involved in related design studies.

4.4.2 Concept Grading and Selection - Figure 83 presents the results of the ranking. Grades reflecting the effect of minimum total panel mass were determined for each concept at each of the three design conditions. Grades for the three remaining figures of merit (producibility, reliability, and inspectability/maintainability) were assigned for each concept. These were considered to be independent of the design condition. These grades were used in conjunction with the applicable mass grade to obtain an integrated score for each concept at all three design conditions using the following expression:

$$\text{Integrated score} = F_W G_W + F_P G_P + F_R G_R + F_{I/M} G_{I/M}$$

Where F_W = Total panel mass weighing factor = 0.5

G_W = Total panel mass grade

RATING SCALE - FACTORS RELATIVE TO BASELINE PANEL CONCEPTS

FIGURE OF MERIT	WEIGHING FACTOR	GRADE → 0	0.25	0.5	0.75	1.0	1.25
1. TOTAL PANEL (STRUCTURAL + ACS) MASS	50%	≥ 200% INCREASE	150% INCREASE	100% INCREASE	50% INCREASE	NO CHANGE	50% DECREASE
2. PRODUCIBILITY, EASE OF MANUFACTURE	20%	(3+) x BASE	2.5 x BASE	2 x BASE	1.5 x BASE	NO CHANGE	BASE / 1.5
3. RELIABILITY	20%	BASE / 3+	BASE / 2.5	BASE / 2	BASE / 1.5	NO CHANGE	1.5 x BASE
4. INSPECTABILITY/ MAINTAINABILITY	10%	(3+) x BASE	2.5 x BASE	2 x BASE	1.5 x BASE	NO CHANGE	BASE / 1.5

FIGURE 82
CONCEPT RANKING SYSTEM

	GRADE						INTEGRATED SCORE		
	Total Panel Mass Design Condition			Producibility Ease of Manufacture	Reliability	Inspectibility Maintainability	Design Condition		
	1	2	3				1	2	3
Uniformly Heated Baseline Panel	1.0	1.0	1.0	1.0	1.0	1.0	-	-	-
Modified Baseline Panel Concept	0.95	0.68	0.31	0.99	0.95	1.0	[0.96]	0.83	0.64
Thickened Skin Concept	0.95	0.75	0.80	0.95	0.80	0.95	0.92	0.82	0.85
Intermediate Manifold Concept	0.97	0.79	0.64	0.97	0.80	0.95	0.93	0.84	0.77
Branched Tubes Concept	0.95	0.70	0.64	0.96	0.75	0.9	0.91	0.78	0.75
Basic Separate Panels Concept	0.93	0.71	0.60	0.97	0.75	1.05	0.91	0.80	0.75
Alternate Separate Panels Concept	0.91	0.68	0.62	0.95	0.75	1.05	0.90	0.79	0.76
Roughened Tubes Concept	0.98	0.85	0.57	0.96	0.75	1.0	0.93	0.87	0.73
Swirl Flow Concept	0.98	0.88	0.70	0.96	0.95	1.0	0.97	0.92	0.83
Finned Tubes Concept	0.98	0.91	0.86	0.96	0.85	1.0	0.95	[0.92]	0.89
Insulated Panel Concept	0.74	0.71	0.88	0.77	1.25	0.8	0.85	0.84	[0.92]

[ ] - Selected Concepts

FIGURE 83
CONCEPT COMPARISONS - TWO DIMENSIONAL INTERFERENCE HEATING

F_P = Producibility, ease of manufacture, weighing factor = 0.2

G_P = Producibility grade

F_R = Reliability weighing factor = 0.2

G_R = Reliability grade

$F_{I/M}$ = Inspectability/Maintainability weighing factor = 0.1

$G_{I/M}$ = Inspectability/Maintainability grade

Total Panel Mass - This reflects the ratio of the concept mass to the applicable baseline panel mass. The masses used were those presented in Figures 79, 80 and 81 for the three design conditions. Grades were calculated with the following relationship:

Grade = 1 - (% change in mass) x (grade sensitivity)

$$= 1 - \left(\frac{M}{Mb} - 1\right) \times (.5) = 1 - \left(\frac{M - Mb}{2 \times Mb}\right)$$

Where M = Mass of subject concept

Mb = Mass of applicable baseline panel

For example, at Design Condition 3, the Thickened Skin Concept total panel mass = 195 kg (430 lbm) while the uniformly heated baseline panel mass = 140 kg (309 lbm).

Therefore: $\text{Grade} = 1 - \left(\frac{195 - 140}{2 \times 140}\right) = 0.8$

Producibility - These grades reflect the ratio of the cost associated with the subject concept with that of the baseline panel. The costs determined were representative of a panel ready for aircraft installation. Pertinent assumptions made for this evaluation were; only flat panels are involved, 1985 - 1990 technology bases, and more than 200 units will be produced. Once the costs were determined, the grades were calculated with a relationship similar to that used to derive mass grades.

Producibility grades, except for that of the Insulated Panel Concept, fall between 0.95 and 1.0; i.e. only one concept will cost more than 10 percent above the baseline panel cost. The significant increase in cost associated with the Insulated Panel Concept is attributable to the additional thermal protection system (TPS) components - the Rene shingle, insulation, insulation retainer, etc.

The producibility insensitivity was related to several major factors. First of all, the basic cost of fabricating the baseline panel is quite high due, in large part, to the complexities encountered in working with honeycomb structure. As a result, modifications required by the proposed panel designs such as additional manifolding and/or variable skin thicknesses can be accommodated at relatively small expense. Secondly, while some concepts, such as those incorporating high heat transfer tubes, would require a development program, the costs of such a program would be insignificant once amortized into the basic panel fabrication program.

Reliability - The grades assigned to reliability and inspectability/maintainability were derived from a consensus of engineering judgements. Significant differences in the considerations contributing to reliability (durability, damage and failure tolerances, and overall design complexity) were identified. As a result, reliability grades vary widely. Factors that influenced the reliability grading, expressed as conceptual differences from the baseline panel design, were as follows:

a. Modified Baseline Panel - increased leakage potential due to more tubes and higher pressures.

b. Thickened Skin - questionable peel strength capability in tube/skin interface due to shaping and contouring required.

c. Intermediate Manifold - increased leakage potential due to additional manifold.

d. Branched Tubes - potential bending failures in fittings, questionable peel strength capability and reduced fatigue life characteristics.

e. Separate Panels - increased leakage potential due to additional manifolds and cooling system interfaces.

f. High Heat Transfer Tubes - all concepts display increased potential for flow clogging, roughened tubes downgraded due to possibility of structural degradation during roughening process, finned tubes downgraded due to possibility of stress concentrations in fin roots.

g. Insulated Panel - high failure tolerance, particularly in the event of loss of coolant; also TPS offers positive protection to panel outer surface.

Inspectability/Maintainability - Grades reflecting the degree of difficulty required to inspect and maintain the panel concepts do not indicate any great deviation from the baseline panel requirements. This is due pri-

marily to the fact that inspection of the baseline panel is expected to be difficult and, once an acceptable technique is established, further complications imposed by the unique characteristics of another concept could be readily accommodated. The Thickened Skin, Intermediate Manifold, and Branched Tubes Concepts were judged to be slightly more difficult to inspect than the baseline due to the more complex structural arrangements involved.

The Modified Baseline Panel and High Heat Transfer Tube Concepts were judged to be not much more difficult to inspect. While the Separate Panels Concept would be somewhat more difficult to inspect, it does offer a unique advantage in terms of maintainability that was judged to more than outweigh the increased inspection complexity. In the event of a required panel replacement, the effort and cost involved to replace a smaller panel provides a distinct advantage. Finally, the Insulated Panel Concept was judged lowest in this category since the TPS must be removed for inspection/maintenance of the cooled panel.

Based on the integrated scores presented in Figure 83, concept recommendations and selections were made for each of the three design conditions. For Design Condition 1, the Swirl Flow Concept has a high integrated score as do the Modified Baseline Panel and Finned Tubes Concepts. However, the Swirl Flow Concept was not selected for the following reasons: It was desirable to consider a single option as representative of the High Heat Transfer Tubes Concepts to ensure diversity in subsequent analyses. Of the three heat transfer augmentation techniques considered, the Roughened Tube Concept was inferior at all three design conditions. Based on the integrated scores in Figure 83, the differences between the Swirl Flow and Finned Tubes Concepts are small. However, the slight advantage of swirl flow at Design Condition 1 is attributable to its superior reliability grade which must be recognized as subjective. One factor that should be considered in comparing these heat transfer augmentation techniques is the level of confidence in the data correlations. In this respect, confidence in the finned tube data correlation was greater than that in the swirl flow data correlation because data trends typifying swirl flow characteristics contain some inconsistencies. Thus, the Finned Tubes Concept was selected as representative of the High Heat Transfer Tube Concepts.

With the Design Condition 1 selection now limited to the Finned Tubes and Modified Baseline Panel Concepts, a final criterion was considered.

Since any heat transfer augmentation technique involves some design complexities and uncertainties, it was felt that these concepts should show a definite advantage over alternate competitive concepts before being selected. Therefore, the Modified Baseline Panel Concept was selected as the most attractive concept for Design Condition 1.

For Design Condition 2, the selection is obvious from Figure 83. The Finned Tubes Concept was the most attractive option, and only the other High Heat Transfer Tubes Concepts scored competitively.

The Finned Tubes Concept also scored high at Design Condition 3. However, the Insulated Panel Concept scored even higher and was selected for this most severe design heating condition.

Thus, a different concept was selected as the most attractive for each of the three specified heating conditions. Figure 84 summarizes the results for two dimensional heating patterns in terms of selected concepts, which concepts were considered sufficiently competitive to be examined for three dimensional heating patterns, and which concepts were eliminated from further consideration.

DESIGN CONDITION	RECOMMENDED CONCEPT 2-D HEATING PATTERN	ADDITIONAL CONCEPTS CHOSEN FOR 3-D HEATING PATTERN ANALYSIS AND PARAMETRIC EVALUATION
1	o MODIFIED BASELINE	o FINNED TUBES o INTERMEDIATE MANIFOLD
2	o FINNED TUBES	o INTERMEDIATE MANIFOLD o INSULATED PANEL
3	o INSULATED PANEL	o FINNED TUBES o THICKENED SKIN

CONCEPTS ELIMINATED FROM FURTHER CONSIDERATION

- o BRANCHED TUBES
- o SEPARATE PANELS (BOTH TUBE ORIENTATIONS)
- o ROUGHENED TUBES
- o SWIRL FLOW TUBES

FIGURE 84
STUDY CONCLUSIONS - TWO DIMENSIONAL INTERFERENCE HEATING

5. THREE DIMENSIONAL INTERFERENCE HEATING PATTERNS

The effects of three dimensional interference heating patterns on actively cooled panel design were also evaluated. Heating rate distributions for each of the three specified design conditions involving two dimensional heating patterns are presented in Figure 23. These distributions were modified to reflect three dimensional effects as shown in Figure 85. The heating rate distribution along the panel as a function of distance from the locus of peak heating is the same for the two and three dimensional heating patterns. That is, the local heating rate in the region between the peak and uniform heating regions varies sinusoidally for 45.7 cm (18 in) on either side of the locus of peak heating.

Figure 86, an isometric view of a representative two dimensional heating pattern, indicates that the pattern is constant across the panel width. The three dimensional heating patterns consider peak heating across only 1/3 of the panel width as shown in Figure 85. The middle third of the panel width experiences local heating rates between the peak and uniform levels. The other third of the panel width experiences no increase in heating above the uniform level. The isometric view of a representative 3D heating pattern presented in Figure 87 shows this panel-width dependence.

Two approaches to the evaluation of three dimensional heating effects were examined: The basic approach used was to determine increase in structural mass that would enable a panel designed for two dimensional heating to handle a three dimensional pattern. Analytical predictions of the shape and extent of interference heating patterns are not very accurate. Therefore, panels of the size analyzed would probably be designed to accommodate the increased heating across the entire panel width. A panel located at the termination of an interference heating pattern could experience a three dimensional pattern rather than the two dimensional pattern for which it was designed. This situation could increase the thermal stresses to the point where additional structural mass would be necessary.

The second approach considered the possibility that the interference heating could be accurately defined to the extent that the panel design need consider only the specific patterns presented in Figure 85. This would permit a reduction in ACS component mass since the total heat which the panel must be

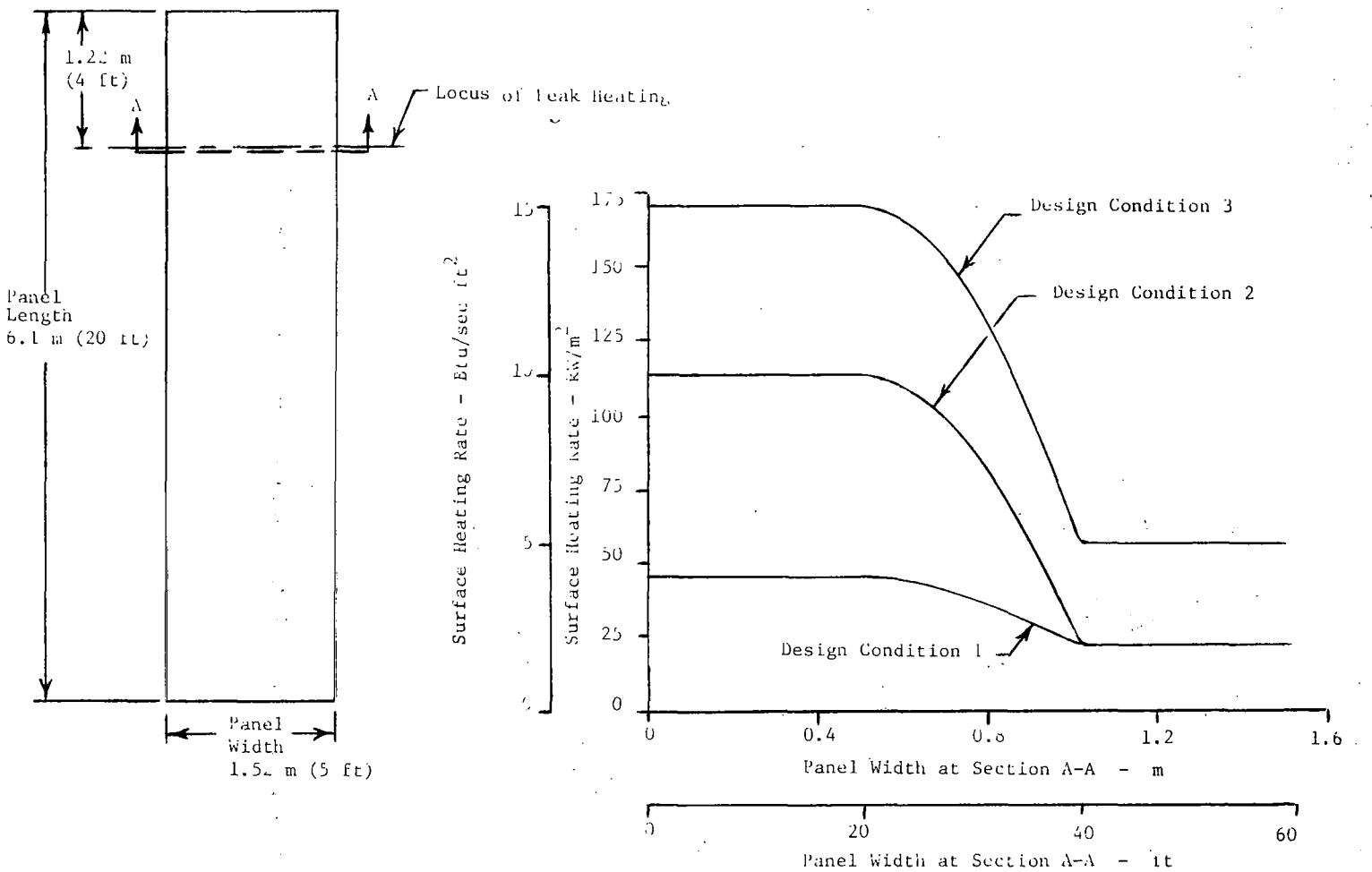

FIGURE 85
THREE DIMENSIONAL INTERFERENCE HEATING DESIGN CONDITIONS

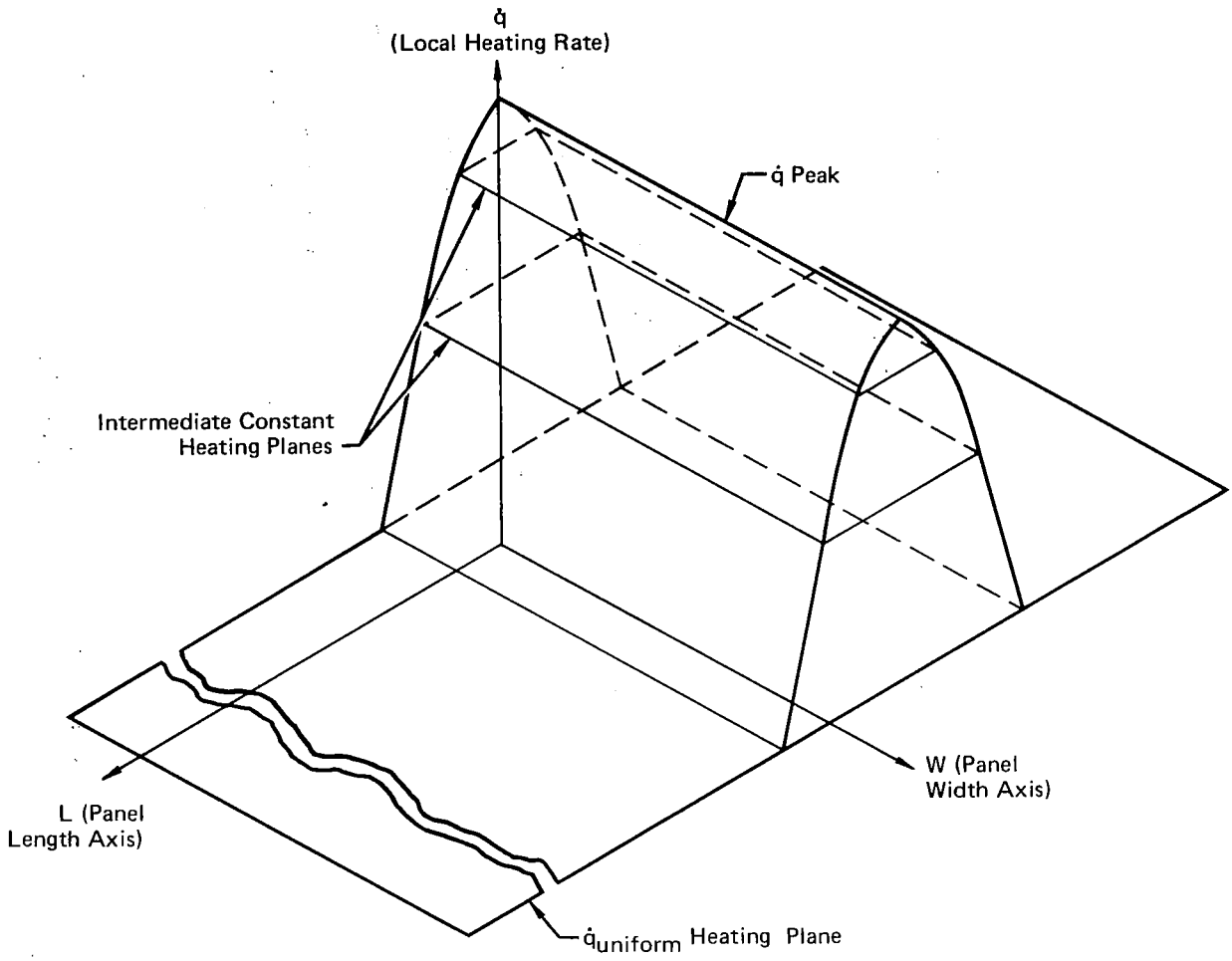

FIGURE 86
ISOMETRIC VIEW - TWO DIMENSIONAL HEATING PATTERN

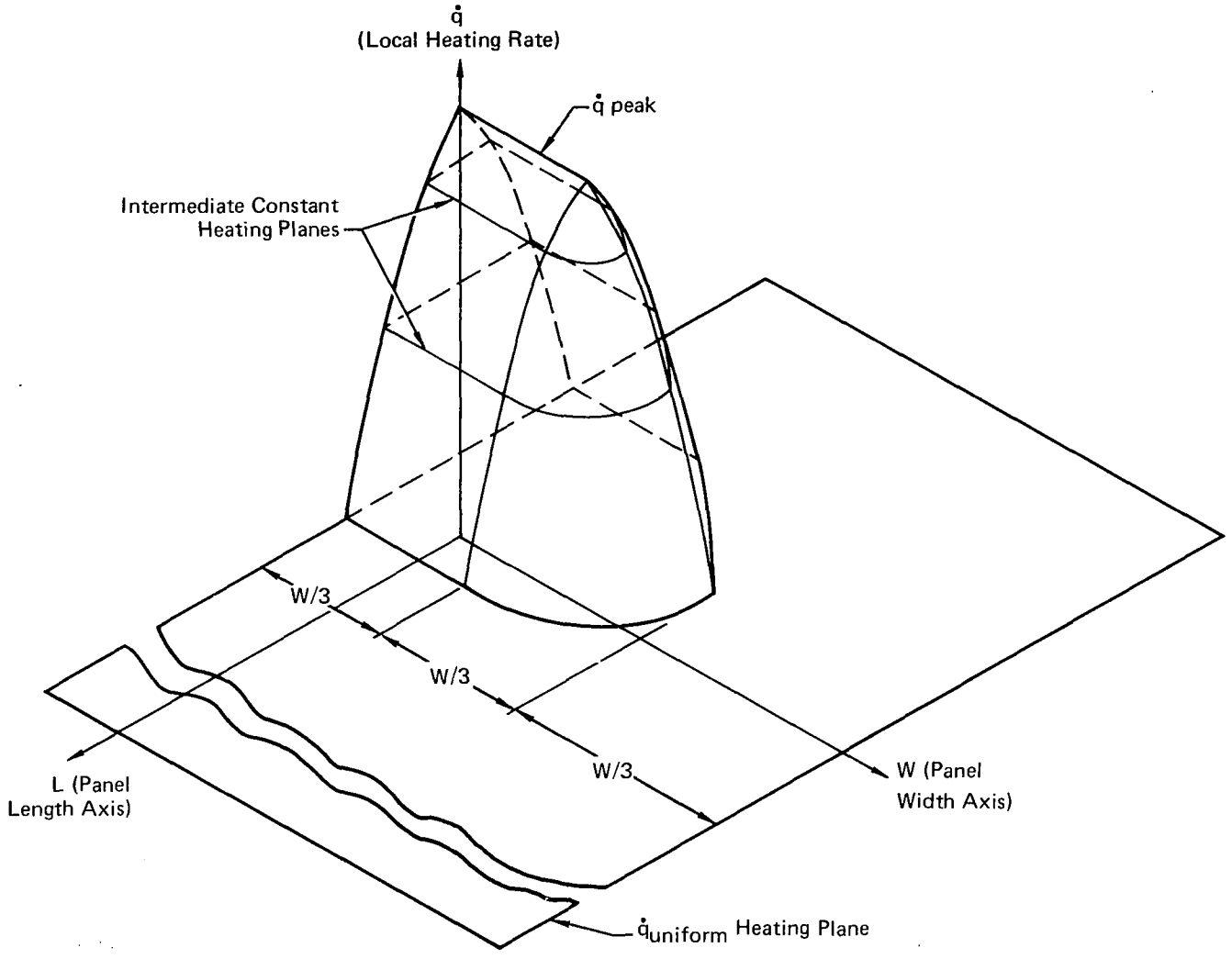

FIGURE 87
ISOMETRIC VIEW - THREE DIMENSIONAL HEATING PATTERN

designed to absorb would be reduced. However, this design approach would be risky based on current analytical techniques. It is extremely doubtful if the required degree of accuracy, in determining the location of the heating pattern, could be achieved for an operational aircraft.

5.1 Panels Designed for Two Dimensional Heating

Ten combinations of panel concept and design condition were examined to determine the effects of three dimensional heating on configurations designed for two dimensional heating. These cases included at least three competitive designs for each design condition:

Design Condition	Design Concept
1	Modified Baseline Panel, Finned Tubes, and Intermediate Manifold
2	Finned Tubes, Intermediate Manifold, Insulated Panel, and Modified Baseline Panel
3	Insulated Panel, Finned Tubes, and Thickened Skin

The structural analyses of panels designed for two dimensional heating assumed that panels adjoining the uniformly heated portion of the panel had the same uniform heating rates. The region of increased heating was also assumed to extend across the adjacent panels. The subject panels were, therefore, able to expand along with the rest of the structure, as temperatures increased, with no external reactions.

For the three dimensional heating patterns, the edge effects could not be neglected because the adjacent panels have different heating patterns. In addition, the heating patterns on the subject panel are unsymmetrical as shown in Figure 87. These differences cause thermal stresses and external reactions at the edges in addition to the thermal stresses caused by local thermal gradients, such as exist in the outer skin from tube to tube. These additional loads and reactions were determined by use of the Computer Aided Structural Design (CASD) finite element computer program. The structural model is shown in Figure 88. The model represents the outer skin and coolant tubes over the entire width of the panel between the locus of peak heating and a station 1.22 m (4.0 ft) from the locus of peak heating. Because the heating patterns were symmetrical about the locus of peak heating, the model represented a 2.44 m (8.0 ft) length of the panel. Except for the area of peak heating, the adjacent panels would experience heating similar to that of the

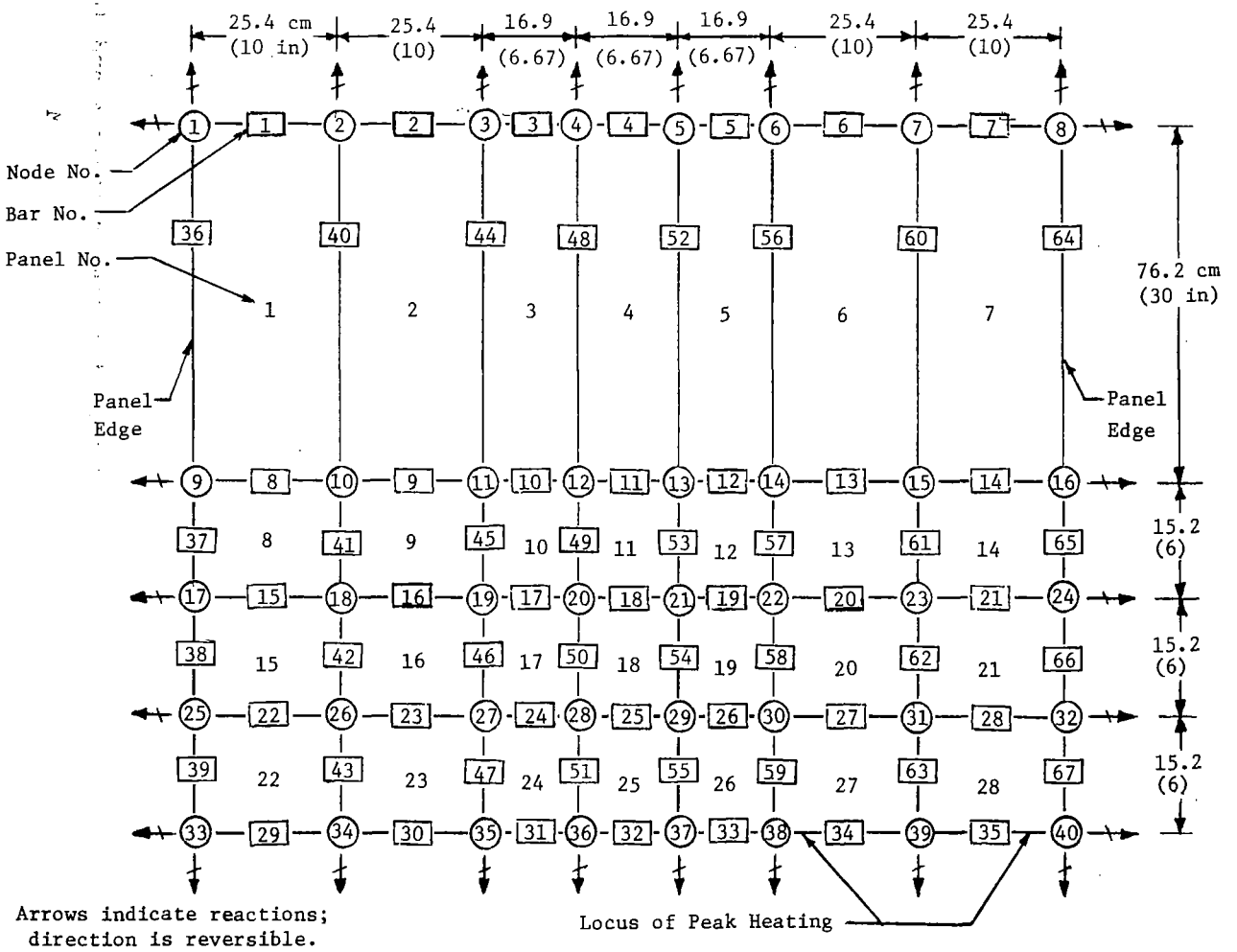

FIGURE 88
STRUCTURAL FINITE ELEMENT COMPUTER MODEL

uniformly heated portion of the subject panel. A slightly conservative assumption was made that all adjacent panels were subjected to only the uniform heating rate. Therefore, temperatures in the subject panel up to the magnitude of those in the uniformly heated area would cause the panel to grow with no external reactions in the plane of the panel. The amount by which temperatures in the peak heating region exceeded those in the uniform heating area caused the external reactions and the additional internal thermal stresses. At each node the weighted average temperatures were calculated by multiplying the area of each element of the thermal model cross section (shown in Figure 8, View A-A) by its temperature and dividing by the total area. The differences between these average temperatures in the interference heating area and the uniformly heated area were determined and used as inputs to the CASD program.

All of the nodes, except those nodes around the periphery were free to deflect in the plane of the skin. The nodes at the panel periphery were supported against deflection normal to the panel edges, producing external reactions at those nodes. To keep the program to a reasonable size, the model was simplified by modeling only the outer skin and tubes and by combining an appropriate width of panel into each bar. The omission of the inner skin was justified by a comparison of inner skin and average outer skin temperatures. This comparison showed that the inner skin temperatures were no more than 8.3K (15°F) less than the average outer skin temperature at each location. Therefore, inner skin thermal stresses and reactions would be nearly the same as for the outer skin. The bar areas used in the program were the product of the outer skin thickness and half the distance to the adjacent bars plus, for bars parallel to the coolant tubes, the area of the included tubes. The shear panel thicknesses used were the actual outer skin thicknesses.

Figures 89 and 90 show typical CASD input (joint temperature differences and bar areas) and output (bar thermal stresses) for the transverse and longitudinal directions respectively. The values shown represent the Modified Baseline Panel Concept at Design Condition 2. This case produced the maximum tension stresses and near maximum compression stresses resulting from the unsymmetric heating pattern. These stresses were then added to the stresses due to temperature gradients as determined with the KBEB program to establish the total thermal stresses. Figure 91 presents a summary of the maximum longitudinal thermal stresses for all the configurations analyzed. These

BAR	AREA cm^2	AREA (in^2)	NODE	TEMPERATURE DIFFERENCE K	TEMPERATURE DIFFERENCE (°F)	TRANSVERSE STRESS MPa	TRANSVERSE STRESS (lbf/in^2)
			1	0	(0)	- 2.2	(-312)
1	3.87	(0.60)	2	0	(0)	- 1.9	(-280)
2	3.87	(0.60)	3	0	(0)	- 1.2	(-175)
3	3.87	(0.60)	4	0	(0)	- 0.4	(- 56)
4	3.87	(0.60)	5	0	(0)	0.5	(75)
5	3.87	(0.60)	6	0	(0)	1.2	(175)
6	3.87	(0.60)	7	0	(0)	1.8	(266)
7	3.87	(0.60)	8	0	(0)	2.2	(315)
			9	0.6	(1)	- 5.7	(-824)
8	4.65	(0.72)	10	0.6	(1)	- 5.3	(-771)
9	4.65	(0.72)	11	0.6	(1)	- 3.8	(-554)
10	4.65	(0.72)	12	0.6	(1)	- 1.1	(-165)
11	4.65	(0.72)	13	0.6	(1)	2.4	(343)
12	4.65	(0.72)	14	0.6	(1)	4.2	(607)
13	4.65	(0.72)	15	0.6	(1)	3.5	(513)
14	4.65	(0.72)	16	0.6	(1)	1.4	(199)
			17	1.1	(2)	- 8.9	(-1297)
15	1.55	(0.24)	18	1.1	(2)	- 9.0	(-1306)
16	1.55	(0.24)	19	1.1	(2)	- 9.3	(-1345)
17	1.55	(0.24)	20	6.7	(12)	- 9.1	(-1315)
18	1.55	(0.24)	21	27.8	(50)	-15.3	(-2225)
19	1.55	(0.24)	22	33.3	(60)	-18.1	(-2627)
20	1.55	(0.24)	23	33.3	(60)	-17.9	(-2589)
21	1.55	(0.24)	24	33.3	(60)	-15.7	(-2281)
			25	1.1	(2)	-11.3	(-1640)
22	1.55	(0.24)	26	1.1	(2)	-12.2	(-1774)
23	1.55	(0.24)	27	1.1	(2)	-15.3	(-2226)
24	1.55	(0.24)	28	27.8	(50)	-23.0	(-3331)
25	1.55	(0.24)	29	45.6	(82)	-27.3	(-3961)
26	1.55	(0.24)	30	52.8	(95)	-30.3	(-4392)
27	1.55	(0.24)	31	52.8	(95)	-29.9	(-4320)
28	1.55	(0.24)	32	52.8	(95)	-27.5	(-3982)
			33	1.7	(3)	-13.2	(-1919)
29	0.77	(0.12)	34	1.7	(3)	-14.6	(-2112)
30	0.77	(0.12)	35	1.7	(3)	-20.4	(-2958)
31	0.77	(0.12)	36	33.3	(60)	-25.7	(-3733)
32	0.77	(0.12)	37	52.8	(95)	-30.0	(-4354)
33	0.77	(0.12)	38	58.9	(106)	-32.9	(-4775)
34	0.77	(0.12)	39	58.9	(106)	-33.4	(-4846)
35	0.77	(0.12)	40	58.9	(106)	-31.3	(-4543)

FIGURE 89
TYPICAL TRANSVERSE THERMAL STRESSES - THREE DIMENSIONAL HEATING

BAR	AREA cm^2	AREA (in^2)	NODE	TEMPERATURE DIFFERENCE K	TEMPERATURE DIFFERENCE (°F)	LONGITUDINAL STRESS MPa	LONGITUDINAL STRESS (lbf/in^2)
			1	0	(0)	- 1.7	(-240)
36	1.89	(0.293)					
			9	0.6	(1)	- 0.3	(- 42)
37	1.89	(0.293)					
			17	1.1	(2)	0.5	(76)
38	1.89	(0.293)					
			25	1.1	(2)	1.3	(189)
39	1.89	(0.293)					
			33	1.7	(3)	1.6	(236)
			2	0	(0)	- 1.9	(-282)
40	3.79	(0.587)					
			10	0.6	(1)	- 0.4	(- 59)
41	3.79	(0.587)					
			18	1.1	(2)	0.7	(106)
42	3.79	(0.587)					
			26	1.1	(2)	1.8	(265)
43	3.79	(0.587)					
			34	1.7	(3)	2.4	(345)
			3	0	(0)	- 2.9	(-422)
44	3.15	(0.489)					
			11	0.6	(1)	- 1.1	(-155)
45	3.15	(0.489)					
			19	1.1	(2)	1.5	(222)
46	3.15	(0.489)					
			27	1.1	(2)	4.3	(624)
47	3.15	(0.489)					
			35	1.7	(3)	4.6	(670)
			4	0	(0)	- 4.2	(-603)
48	2.52	(0.391)					
			12	0.6	(1)	- 3.6	(-516)
49	2.52	(0.391)					
			20	6.7	(12)	- 2.1	(-303)
50	2.52	(0.391)					
			28	27.8	(50)	- 4.2	(-608)
51	2.52	(0.391)					
			36	33.3	(60)	- 4.5	(-651)

BAR	AREA cm^2	AREA (in^2)	NODE	TEMPERATURE DIFFERENCE K	TEMPERATURE DIFFERENCE (°F)	LONGITUDINAL STRESS MPa	LONGITUDINAL STRESS (lbf/in^2)
			5	0	(0)	- 5.6	(-812)
52	2.52	(0.391)					
			13	0.6	(1)	- 7.1	(-1026)
53	2.52	(0.391)					
			21	27.8	(50)	-10.1	(-1471)
54	2.52	(0.391)					
			29	45.6	(82)	-11.3	(-1636)
55	2.52	(0.391)					
			37	52.8	(95)	-11.7	(-1691)
			6	0	(0)	- 6.7	(-972)
56	3.15	(0.489)					
			14	0.6	(1)	- 8.2	(-1187)
57	3.15	(0.489)					
			22	33.3	(60)	-11.5	(-1664)
58	3.15	(0.489)					
			30	52.8	(95)	-13.5	(-1953)
59	3.15	(0.489)					
			38	58.9	(106)	-14.0	(-2035)
			7	0	(0)	- 8.0	(-1155)
60	3.79	(0.587)					
			15	0.6	(1)	- 8.9	(-1285)
61	3.79	(0.587)					
			23	33.3	(60)	-10.1	(-1472)
62	3.79	(0.587)					
			31	52.8	(95)	-11.0	(-1592)
63	3.79	(0.587)					
			39	58.9	(106)	-11.3	(-1638)
			8	0	(0)	- 8.9	(-1297)
64	1.89	(0.293)					
			16	0.6	(1)	-11.0	(-1600)
65	1.89	(0.293)					
			24	33.3	(60)	- 8.3	(-1198)
66	1.89	(0.293)					
			32	52.8	(95)	- 6.5	(- 948)
67	1.89	(0.293)					
			40	58.9	(106)	- 6.0	(- 874)

FIGURE 90
TYPICAL LONGITUDINAL THERMAL STRESSES - THREE DIMENSIONAL HEATING

Concept	Design Cond.	Maximum Longitudinal Thermal Stresses					
		Due to Unsymmetric Heating Pattern	Due to Thermal Gradients		Total		
			Outer Skin	Tube	Outer Skin	Tube	
		MPa (lbf/in^2)	MPa (lbf/in^2)	MPa (lbf/in^2)	MPa (lbf/in^2)	MPa (lbf/in^2)	
FINNED TUBES	1	-4.9 (-705)	-11.1 (-1610)	12.2 (1770)	-16.0 (-2315)	7.3 (1065)	
FINNED TUBES	2	-9.3 (-1350)	-31.2 (-4530)	43.9 (6360)	-40.5 (-5880)	34.6 (5010)	
FINNED TUBES	3	-8.5 (-1240)	-47.3 (-6860)	67.5 (9790)	-55.8 (-8100)	59.0 (8550)	
MOD. BASELINE	1	-7.3 (-1065)	-19.3 (-2800)	30.8 (4460)	-26.6 (-3865)	23.5 (3395)	
MOD. BASELINE	2	-14.0 (-2035)	-33.4 (-4850)	48.6 (7050)	-47.4 (-6885)	34.6 (5015)	
INTER. MANIFOLD	1	-9.1 (-1320)	-11.8 (-1710)	14.1 (2050)	-20.9 (-3030)	5.0 (730)	
INTER. MANIFOLD	2	-14.4 (-2090)	-33.0 (-4780)	50.0 (7250)	-47.4 (-6870)	35.6 (5160)	
INSUL. PANEL	2	-16.0 (-2320)	-0.5 (-70)	-6.2 (-900)	-16.5 (-2390)	-22.2 (-3220)	
INSUL. PANEL	3	-14.6 (-2120)	-1.3 (-190)	-5.5 (-800)	-15.9 (-2310)	-20.1 (-2920)	
THICKENED SKIN	3	-12.6 (-1820)	-20.1 (-2910)	67.4 (9780)	-32.7 (-4730)	54.8 (7960)	

FIGURE 91
MAXIMUM LONGITUDINAL THERMAL STRESSES - THREE DIMENSIONAL CONCEPTS

total longitudinal thermal stresses were added, in turn, to the mechanical stresses to determine total stresses. As for the two dimensional heating studies, the thermal stresses were not critical. This was because the thermal stresses were compressive in the region of peak heating where the maximum mechanical stresses occur and the thermal stresses were of insufficient magnitude to cause the total compression stress to be more critical than the mechanical tension stresses. Similarly, the transverse thermal stresses were not sufficiently large to cause the total transverse thermal stresses to be critical. The transverse thermal stresses are the total stresses in that direction because mechanical stresses act in the longitudinal direction only.

It was concluded that the three dimensional heating patterns analyzed did not result in thermal stresses of sufficient magnitude to impact the mass of panels designed for two dimensional interference heating. The low thermal stresses are the result of the low maximum design temperature, 394 K (250°F), which limits the potential for significant thermal gradients. If the maximum allowable panel temperature were increased and/or the coolant temperature decreased it is possible that three dimensional heating could affect the panel mass significantly.

5.2 Panels Designed for Three Dimensional Heating

The study conducted to provide an insight into benefits that would be realized by designing a cooled panel specifically for a well defined three dimensional heating pattern made extensive use of previous results. These results indicated that no significant differences in structural mass would be realized. Therefore, it was necessary to determine only ACS component mass changes.

Of the concepts identified as leading contenders for regions exposed to interference heating, some were not suitable for this study. Since the Insulated Panel Concept ACS requirements are so small, the concept would be very insensitive to the modifications in the heating pattern and changes would not be readily identifiable. The Thickened Skin Concept would be competitive only at Design Condition 3 and varying skin thickness would cloud the results. Therefore, the choices for analysis were reduced to the Modified Baseline Panel, Finned Tubes, and Intermediate Manifold Concepts. Of these, the Modified Baseline Panel Concept at Design Condition 1 and the Finned Tubes Concept at Design Condition 2 were selected for preliminary analysis.

ACS component masses were determined for the three dimensional heating patterns based on the following assumptions:

a. The coolant flow per tube is that required to maintain a 394 K (250°F) maximum panel temperature. Therefore, coolant flow in one-third of the tubes is the same as for the panel designed for two dimensional interference heating, in another third of the tubes the flow is the same as that of the panel designed for uniform heating, and the flow per tube in the middle third of the panel varies between the two extremes.

b. Panel pressure drop and system operating pressure levels are dictated by the tubes that require maximum flow. As a result, the panel pressure requirements are the same for the three dimensional configurations as for two dimensional configurations.

Based on this approach, the major differences between panels designed for three dimensional rather than two dimensional heating are that the integrated panel flow requirements are reduced and the total heat absorbed is less. The study results are summarized in Figure 92.

ACS Component	Mass Reduction per 9.29 m^2(100 ft^2) Panel			
	Design Condition 1 (Modified Baseline Panel Concept)		Design Condition 2 (Finned Tube Concept)	
	kg	(lbm)	kg	(lbm)
Coolant in Lines	2.0	(4.3)	2.5	(5.6)
Coolant Distribution Lines	0.6	(1.4)	0.7	(1.6)
Heat Exchanger	0.1	(0.2)	0.4	(0.9)
Pumps	0.2	(0.4)	0.2	(0.5)
Pumping Power Penalty	0.6	(1.4)	0.7	(1.5)
Reservoir	0.1	(0.2)	0.2	(0.4)
Total	3.6	(7.9)	4.7	(10.5)

FIGURE 92
ACS COMPONENT MASS REDUCTIONS BY DESIGNING FOR THREE DIMENSIONAL HEATING

While these mass reductions are significant in terms of percent of ACS component mass, the reductions are small relative to total panel mass. Also, these reductions are optimistic in that they do not reflect a mass penalty for provisions necessary to provide individual coolant tube flow control. Another consideration is that very few panels per vehicle would have to be designed specifically for three dimensional heating patterns, so that the vehicle mass savings would be insignificant. In summary, it would not appear to be logical to increase design complexity by considering three dimensional heating patterns on a few individual panels as the potential advantages are negligible.

6. PARAMETRIC EVALUATION OF PANEL DESIGN TRENDS

A parametric evaluation was conducted to expand the usefulness of the derived information. The previously discussed analyses had addressed three specific design conditions in terms of uniform and peak heating rates as follows:

Design Condition	Uniform Heating Rate kW/m^2 (Btu/sec ft^2)	Peak Heating Rate kW/m^2 (Btu/sec ft^2)
1	22.7 (2)	45.4 (4)
2	22.7 (2)	113.5(10)
3	56.7 (5)	170.2(15)

For the parametric study, the range of uniform heating rates was expanded to include the range from 5.7 to 113.5 kW/m^2 (0.5 to 10 Btu/sec ft^2). Ratios of peak to uniform heating as high as 5 were considered to reflect interference heating. Previous results were reviewed to determine which design concepts merited consideration.

As summarized in Figure 84, a different concept was recommended for each of the three specified heating patterns studied: the Modified Baseline Panel Concept for Design Condition 1, the Finned Tubes Concept for Design Condition 2 and the Insulated Panel Concept for Design Condition 3. In addition, the Intermediate Manifold and Thickened Skin Concepts were considered to be reasonably competitive near certain design conditions. All five of these concepts were evaluated during the three dimensional heating pattern analysis, Section 5. However, during both the two and three dimensional pattern analyses there was no indication that the latter two concepts would provide any clear advantage over the recommended concepts regardless of the nature of the heating pattern. Therefore, they were not considered parametrically.

The approach used in the parametric evaluation was similar to that used in the two dimensional heating pattern analyses. Each concept was sized for the range of heating conditions over which it was reasonably competitive. When panel masses were established, a system ranking procedure like that discussed in Section 4.4 was used to derive an integrated score for comparative purposes. The mass grade for this evaluation was also determined in a manner similar to that described in Section 4.4. A single basic panel mass was used as the mass ratio denominator. This mass of 93.9 kg (207 lbm) was

established as the minimum 9.29 m^2 (100 ft^2) panel structural mass independent of ACS components mass. The producibility, reliability and inspectability/maintainability scores previously established for the subject concepts were not changed but were used in determining the integrated score for each concept over the extended range of design conditions.

The resulting integrated scores are presented in Figure 93. The more severe heating conditions resulted in lower scores. It is evident that the Modified Baseline Panel Concept is superior at the lower heating conditions, the Insulated Panel Concept is superior at the higher heating conditions and the Finned Tubes Concept is competitive between the extremes. The technique used to define the "cross-over" heating conditions was straight-forward. As shown in Figure 94, a curve was faired through the carpet plot data joining common points where the integrated scores are the same for two different concepts at identical values of $\dot{q}_{uniform}$ and $(\dot{q}_{peak}/\dot{q}_{uniform})$. Cross plotting of these loci of common points, presented in Figure 95, provided a clear division between the concepts and defined the regime of each concept's superiority. Figure 96 provides total panel masses. Given a set of defined interference heating conditions, Figure 95 can be used to select a panel design concept. The panel mass can then be obtained from Figure 96.

Figure 97 illustrates this procedure and reveals the significance of a singular design criterion - that of the maximum heating rate imposed on the panel ($\dot{q}$ peak) - in determining the panel mass. A number of peak heating rates, from 22.7 kW/m^2 (2 Btu/sec ft^2) to 227 kW/m^2 (20 Btu/sec ft^2), were considered. As indicated, the same peak heating rate can result as the product of various combinations of the uniform heating rate ($\dot{q}$ uniform) and the peak heating ratio ($\dot{q}$ peak/$\dot{q}$ uniform). The recommended panel design concept for each set of design conditions was obtained from Figure 95. Figure 96 was then used to find the appropriate panel mass.

At low peak heating conditions, below approximately 45.4 kW/m^2 (4 Btu/sec ft^2), where the Modified Baseline Panel Concept is recommended, the panel mass is found to be basically a function of the peak heating rate only. This trend is also evident at high peak heating conditions, above approximately 170.2 kW/m^2 (15 Btu/sec ft^2), where the Insulated Panel Concept is required.

Panel mass in the intermediate range of peak heating conditions is influenced by the relative magnitudes of $\dot{q}$ uniform and ($\dot{q}$ peak/$\dot{q}$ uniform). However, it can be noted that unless the peak heating rate is close to the

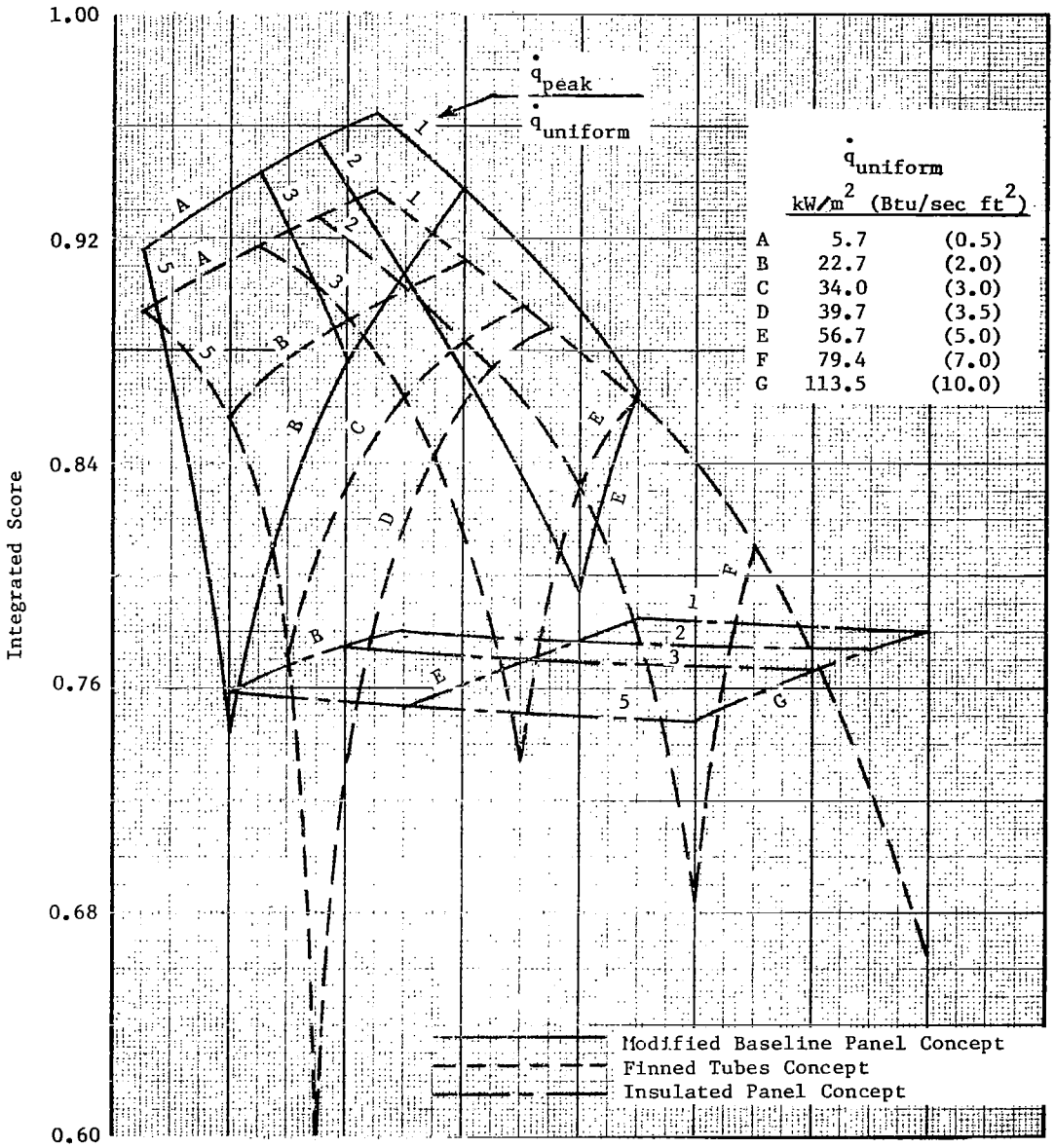

FIGURE 93
CONCEPT INTEGRATED SCORES - PARAMETRIC EVALUATION

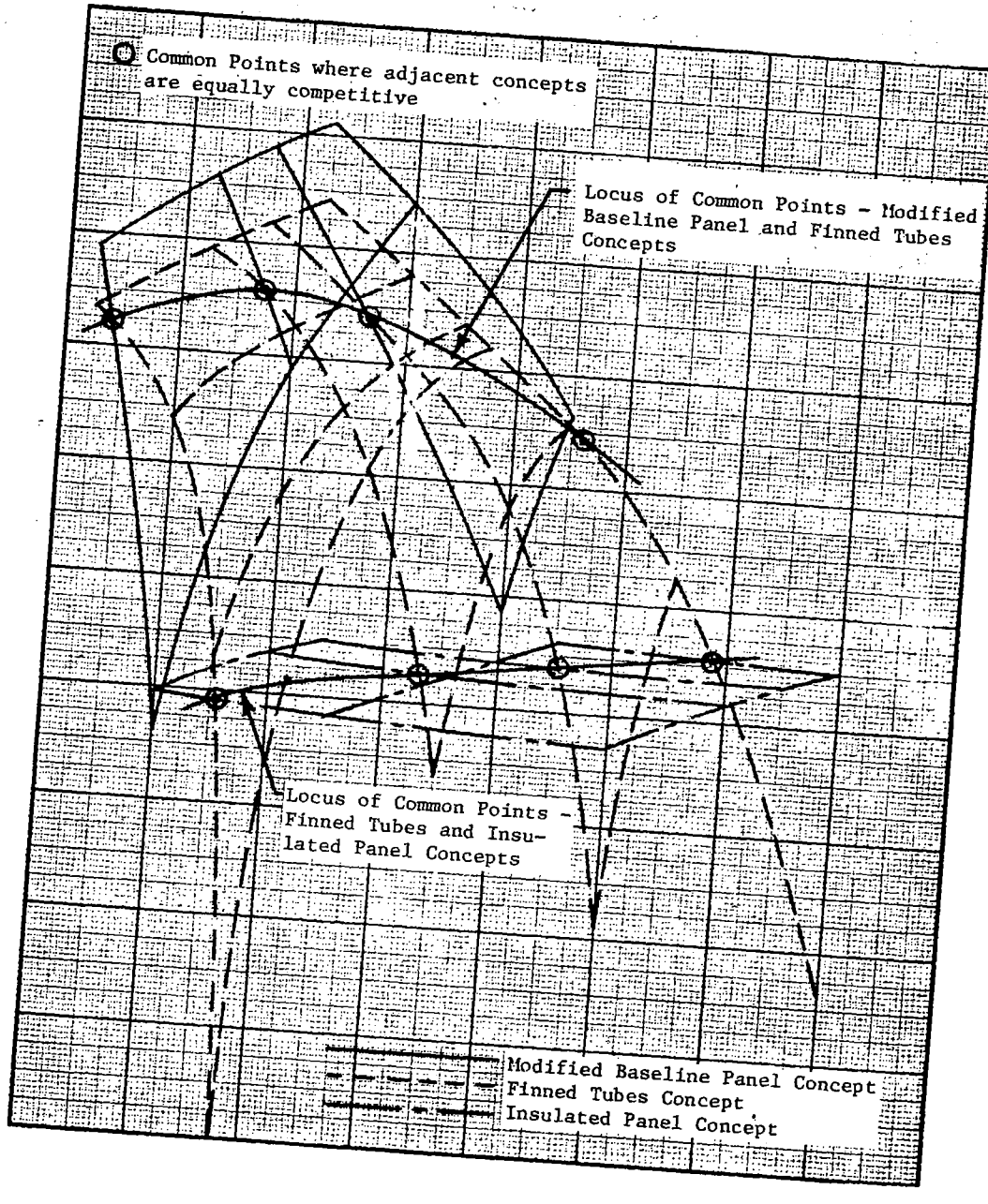

FIGURE 94
"CROSS-OVER" HEATING CONDITION DEFINITION TECHNIQUE

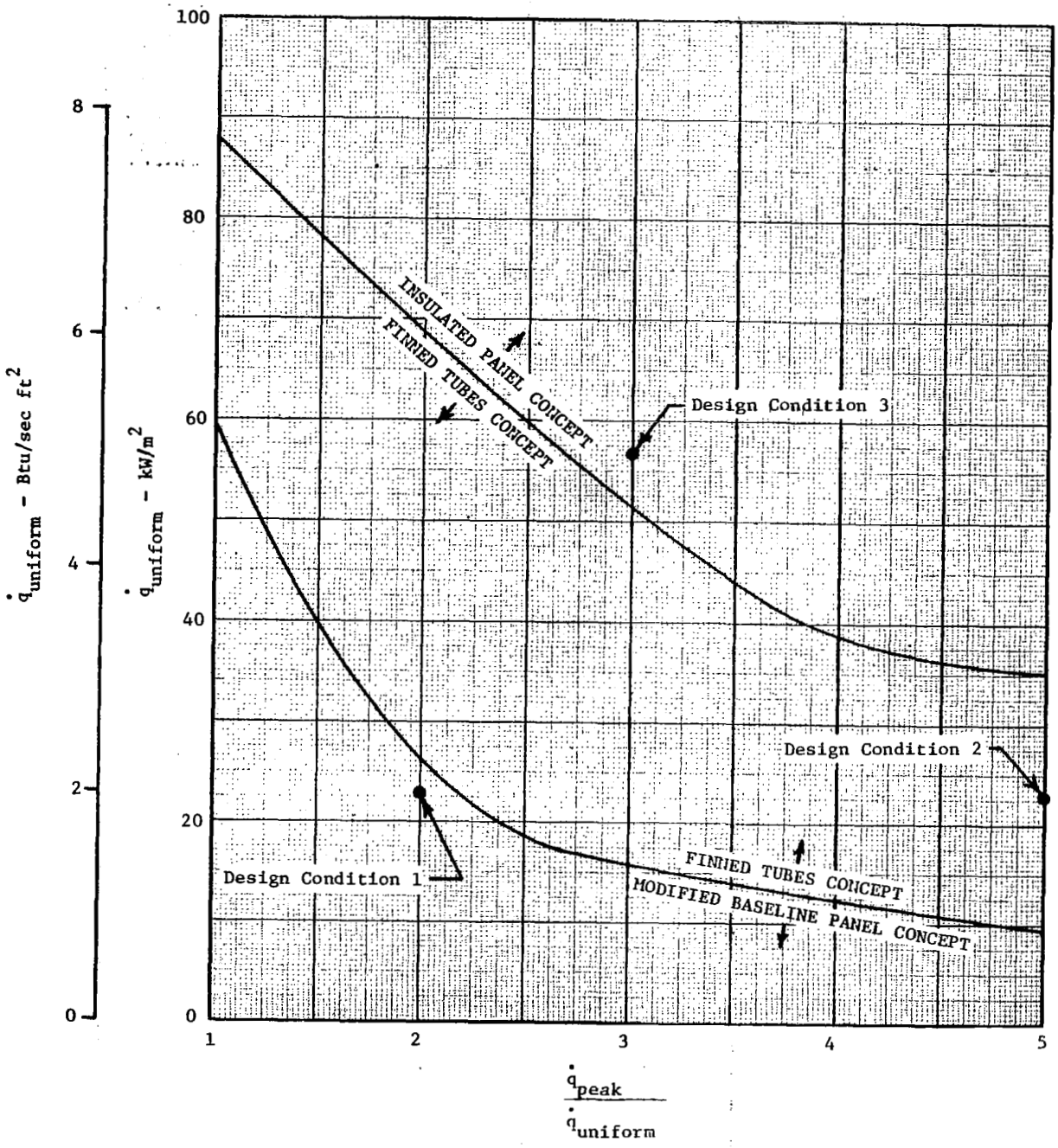

FIGURE 95
REGIMES OF APPLICABILITY - RECOMMENDED DESIGN CONCEPTS

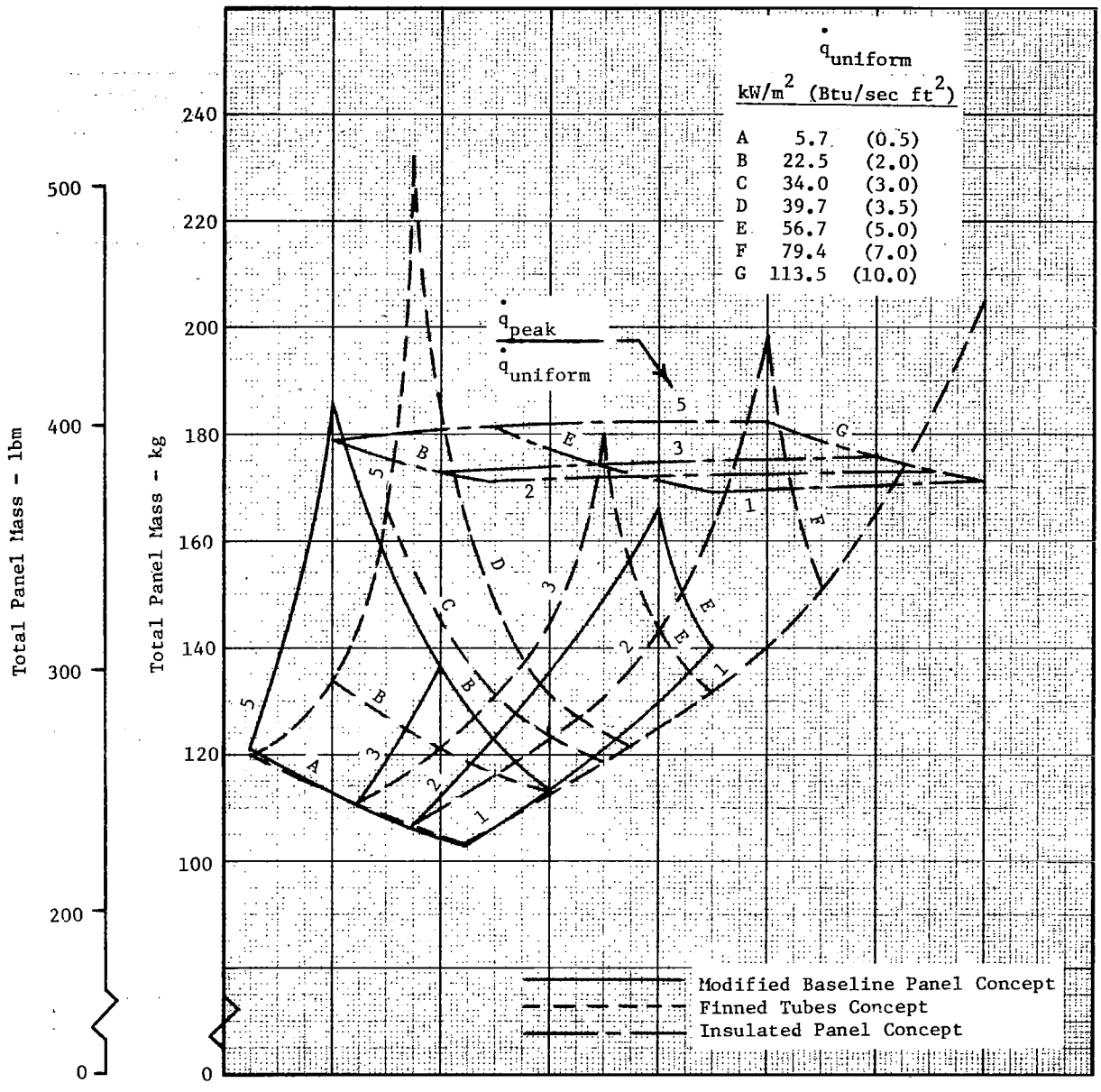

FIGURE 96
CONCEPT MASSES - PARAMETRIC EVALUATION

$\dot{q}$ peak kW/m^2 (Btu/sec ft^2)	$\dot{q}$ uniform kW/m^2 (Btu/sec ft^2)	$\frac{\dot{q}\ \text{peak}}{\dot{q}\ \text{uniform}}$	Panel Design Concept From Figure 95	Panel Mass kg (lbm)
22.7 (2)	22.7 (2)	1	Modified Baseline Panel	113 (249)
22.7 (2)	11.3 (1)	2	" " "	112 (247)
22.7 (2)	5.7 (0.5)	4	" " "	115 (254)
45.4 (4)	45.4 (4)	1	Modified Baseline Panel	130 (287)
45.4 (4)	22.7 (2)	2	" " "	124 (274)
45.4 (4)	11.3 (1)	4	" " "	127 (280)
45.4 (4)	9.1 (0.8)	5	" " "	131 (289)
68.1 (6)	68.1 (6)	1	Finned Tubes	140 (309)
68.1 (6)	45.4 (4)	1.5	" "	128 (282)
68.1 (6)	34.0 (3)	2	" "	123 (271)
68.1 (6)	22.7 (2)	3	" "	121 (267)
68.1 (6)	13.6 (1.2)	5	" "	125 (276)
90.8 (8)	90.8 (8)	1	Insulated Panel	170 (375)
90.8 (8)	60.5 (5.33)	1.5	Finned Tubes	141 (311)
90.8 (8)	45.4 (4)	2	" "	131 (289)
90.8 (8)	30.3 (2.67)	3	" "	128 (282)
90.8 (8)	22.7 (2)	4	" "	126 (278)
90.8 (8)	18.2 (1.6)	5	" "	128 (282)
113.5 (10)	113.5 (10)	1	Insulated Panel	171 (377)
113.5 (10)	75.7 (6.67)	1.5	Finned Tubes	162 (357)
113.5 (10)	56.7 (5)	2	" "	143 (315)
113.5 (10)	37.8 (3.33)	3	" "	135 (298)
113.5 (10)	28.4 (2.5)	4	" "	134 (295)
113.5 (10)	22.7 (2)	5	" "	134 (295)
170.2 (15)	113.5 (10)	1.5	Insulated Panel	172 (379)
170.2 (15)	56.7 (5)	3	" "	174 (384)
170.2 (15)	34.0 (3)	5	Finned Tubes	180 (397)
227.0 (20)	113.5 (10)	2	Insulated Panel	173 (381)
227.0 (20)	56.7 (5)	4	" "	181 (399)
227.0 (20)	45.4 (4)	5	" "	177 (390)

FIGURE 97
IMPORTANCE OF PEAK HEATING RATE AS DESIGN CRITERION

uniform heating rate, ($\dot{q}$ peak/$\dot{q}$ uniform) values less than 2, the panel mass is primarily dictated by the peak heating rate.

Structural analyses performed for the numerous panel concepts showed that thermal stresses did not significantly affect the panel mass. This result was due to the low magnitude of the thermal stresses, the longitudinal thermal stresses being tension in the tubes only (which had a higher allowable tension stress than the skins), and the allowable stresses of the skins being greater in compression than tension. To expedite the structural analyses to be considered in the parametric study, it was determined which cases, if any, would be impacted by thermal stresses. It was found that the thermal stresses had not significantly affected the structural mass unless the thermal tension stress in the tube had been sufficient to increase the total tube tension stress (in a panel sized for mechanical loads only) above the allowable tension stress. The mechanical tension stresses in the tube are limited by geometric considerations to less than 160.3 MPa(23250 lbf/in^2) ultimate (the allowable tension stress of the skins) although the allowable ultimate tension strength of the tubes is 237.9 MPa (34,500 lbf/in^2). Thermal tube tension stresses of less than the difference, 77.6 MPa (11,250 lbf/in^2), would not significantly affect the structural mass. It was also noted that the tube thermal tension stresses increased linearly with the difference between the maximum outer skin temperature and the minimum temperature in the adjacent tube. This is illustrated by Figure 98. This data was extrapolated to 366 K (200°F) as shown by the broken line to determine, for larger temperature differences, the approximate thermal tension stress in the tube. The effect of these higher thermal stresses on panel unit mass are shown in Figure 99. The unit masses were calculated by use of the ACPOP mechanical stress program considering combined stresses. Figure 99 illustrates the effect of temperature differences on panel mass. It shows that for temperature differences of less than about 89 K (160°F), panel mass penalties are not attributable to thermal stress. Since the maximum possible ΔT is less than 111 K (200°F) (with the specified maximum skin temperature of 394 K (250°F) and the coolant inlet temperature of 283 K (50°F)) temperature differences in excess of 89 K (160°F) have seldom been encountered. As a result, the effect of thermal stresses (in this study) were found to be minimal compared to other MCAIR studies which used higher (422 K (300°F)) allowable skin temperatures and/or lower coolant temperatures. Figure 99 also shows that, above the temperature differences where the effect on mass appears, the mass

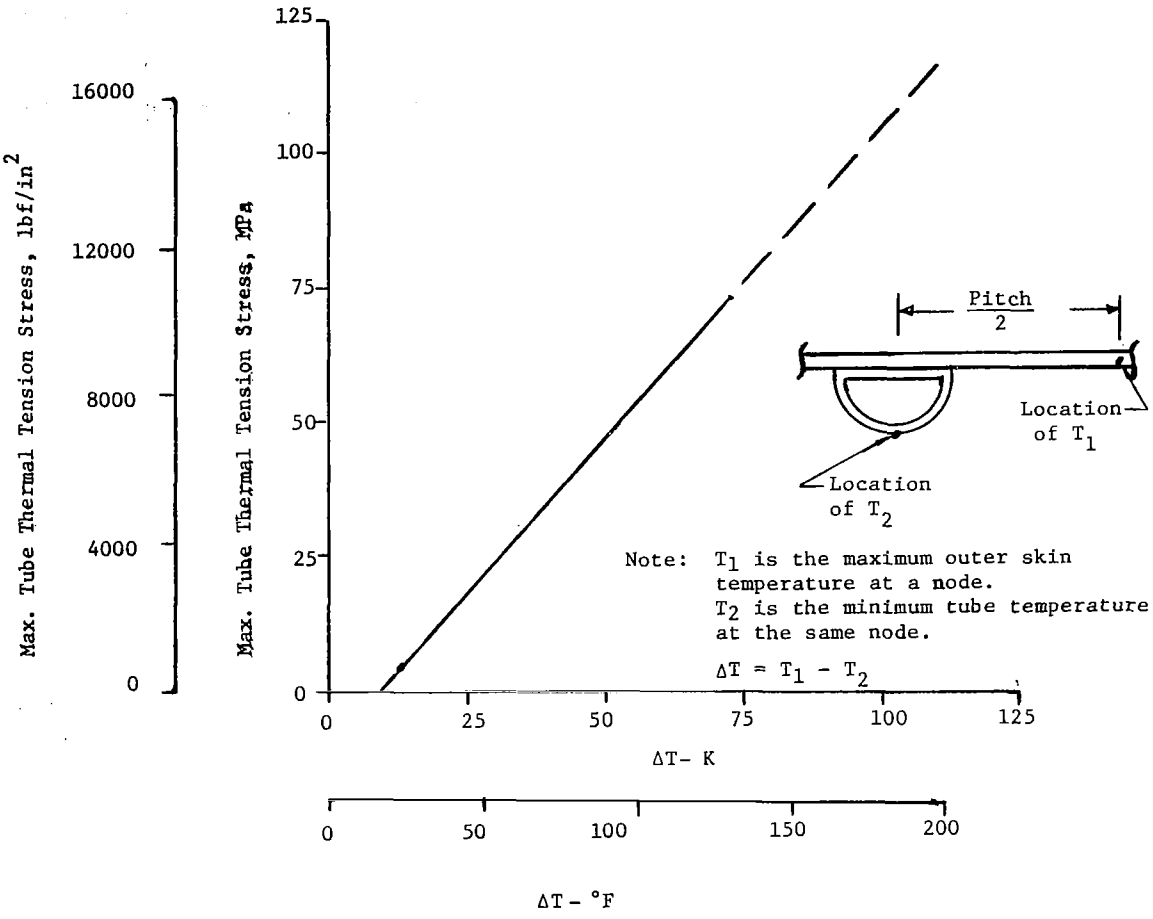

FIGURE 98
COOLANT TUBE THERMAL TENSION STRESS
SENSITIVITY TO STRUCTURAL TEMPERATURE DIFFERENCE

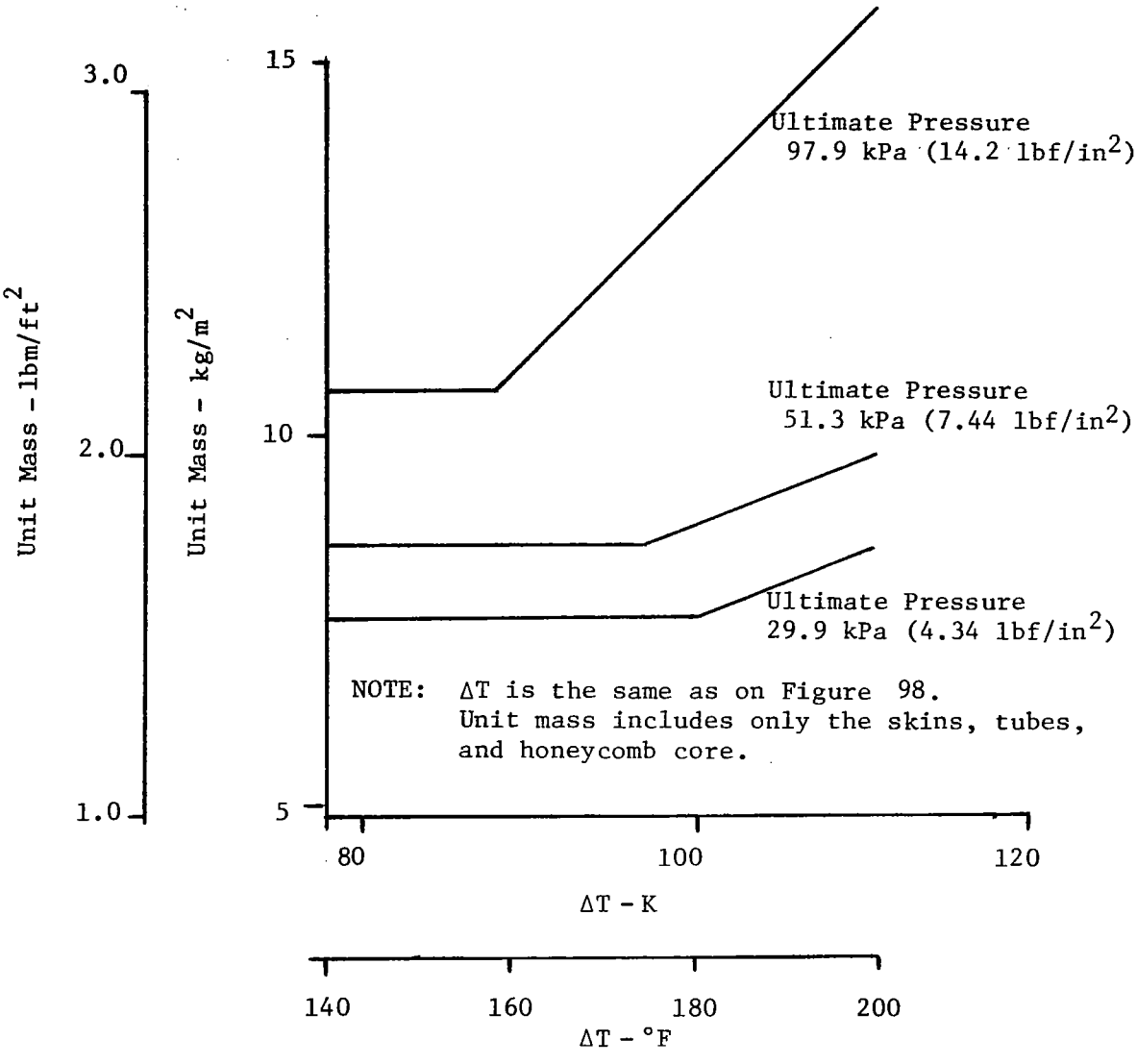

FIGURE 99
PANEL UNIT MASS SENSITIVITY TO STRUCTURAL TEMPERATURE DIFFERENCE

increases rapidly with increases in temperature differences. The mass increase was a result of reducing stress levels by means of increasing the panel height and inner skin thickness while maintaining a coolant tube wall thickness of 0.71 mm (.028 in). If the temperature differences, and the resulting thermal stresses, in this program had been of sufficient magnitude to result in the large mass penalties indicated in Figure 99, the lightest method of obtaining the required additional strength would have been determined. Because the higher thermal stresses are most critical on the tubes, it is anticipated that increasing the tube wall thickness would be beneficial. This would not only decrease the stress levels in the tube but would also increase the allowable tension stress of the tubes (based on crack growth rates).

7. CONCLUSIONS

In performing the study we selected three actively cooled panel designs that could be used in regions subject to interference heating. The regime of applicability was then defined in terms of design heating rate requirements, for each concept. These results are summarized below.

- o Modified Baseline Panel Concept - This concept is recommended for regions experiencing low uniform surface heating and low peak heating. This concept incorporates only minor changes, in the form of decreased tube spacing and increased coolant flow, compared to the basic actively cooled panel design.
- o Finned Tube Concept - This concept is recommended for regions experiencing moderate combined levels of uniform and peak heating rates. The only significant difference between this concept and the basic panel design is that specially configured coolant tubes would be employed in place of the smooth tubes normally used. These special tubes are internally finned to augment heat transfer and thus, reduce coolant flow requirements.
- o Insulated Panel Concept - This concept is recommended for regions experiencing severe uniform and peak design heating rates. This cooled panel would require only minor revisions to a basic panel in the form of provisions for a thermal protection system (TPS). The TPS, consisting of a superalloy shingle and a thin layer of insulation, would be installed on the panel's external surface. This arrangement would reduce the heat load that must be absorbed by the cooling system thus maintaining panel mass at reasonable levels.

Additional results were obtained and observations made during this study. These findings are as follows:

- o Location of the interference heating is not a driving factor - While it was shown that design requirements are more demanding when peak heating is located nearer the coolant exit rather than near the inlet of the panel, the resultant mass differences were small. Therefore, exact knowledge of heating pattern orientation and of its pattern shifting characteristics will not be required.

- Total panel mass is primarily dictated by peak surface heating rate - The total panel masses associated with the recommended concepts can be reasonably estimated using the singular criterion of peak heating rate. Unless this peak heating is near a uniform level over the entire panel, the ratio of peak to uniform heating is not of paramount importance. Thus, most panels designed for interference heating can be designed to satisfy a level of peak heating without imposing an undue mass penalty on the aircraft. This would alleviate some concern regarding the degree of accuracy required in analytically defining the details of interference heating patterns.
- Techniques that augment heat transfer in the coolant tubes reduce total panel mass - The advantages realized by increasing heat transfer through various augmentation techniques outweigh the disadvantages due to increased friction. The incorporation of internally finned coolant tubes proved to be attractive at all design conditions. Other techniques, such as forcing the flow to swirl within the tube or roughened tube internal surfaces also had advantages over smooth tube techniques. These advantages are realized largely due to the high Prandtl number characteristics of heat transfer fluids such as ethylene glycol/water.
- Mass charged to influences of thermal stresses can be minimized - Thermal stresses were found to impact only one concept; they affect the Thickened Skin Concept in terms of a structural mass requirement. Even this requirement was small compared to the ACS component mass variations. This was primarily due to the assumed maximum structural temperature, 394 K (250°F), and the coolant inlet temperature used, 283 K (50°F), which tended to minimize thermal stresses. Larger temperature gradients, with resulting higher thermal stresses, due to higher panel temperatures and/or lower coolant temperatures could increase the panel mass by a significant amount. Larger temperature gradients could result during transient heating conditions or if the assumption of a near adiabatic panel inner surface was not applicable.
- Designing for three dimensional, rather than two dimensional, heating patterns will not significantly impact total mass charged to a panel - The mass savings obtained with ACS components designed specifically for a three, rather than a two, dimensional heating pattern, for the range of peak heating rates investigated, were small. These mass savings

were not justifiable because of the uncertainties involved in predicting the exact shape, location, and magnitude of the three dimensional pattern. Thermal stress considerations are more complex for the three dimensional heating cases. However, for the panel concepts and heating patterns investigated, the influence of thermal stresses on panel structural mass was minimal.

- o Peak external normal pressures due to interference flow impact panel mass - The increase in local normal pressure within disturbed flow regions, for the range of conditions investigated, resulted in a greater impact on panel mass than the encountered thermal stresses. Thus, peak normal pressure, as well as peak surface heating rate, is important as a design parameter.
- o Producibility is not a driving factor in evaluating differences in actively cooled panel design - While widely different approaches to actively cooled panel design were evaluated, their producibility rankings were similar. This insensitivity is due to the high basic cost of fabricating any actively cooled panel. The design variations considered can be accommodated at a relatively small expense or, if amortized into an overall panel development program, would become insignificant.
- o Mass directly attributable to interference heating design requirements has small effect on aircraft performance - The mass increase per panel necessary to accommodate these requirements can be quite large. However, the number of panels, over an entire aircraft's surface, affected would be expected to be small. The Mach 6 hypersonic transport aircraft used as a basis for this study (and described in References 1 and 2) was examined to place a tangible value on these requirements. Shocks emanating from the wings and vertical tail and flow from the boundary layer diverter above the engine inlet duct were considered as sources producing interference heating. The number of cooled panels affected was estimated as 48 (compared to the total of approximately 400 panels over the entire vehicle). Uniform heating rates for these panels varied from 13.6 to 45.4 kW/m^2 (1.2 to 4.0 Btu/sec ft^2). Ratios of ($\dot{q}$ peak/$\dot{q}$ uniform) from 2 to 5 were assumed. The additional mass required (above that necessary for the uniform heating rate only) was determined to be 709 kg (1564 lbm). This mass is 0.2% of the basic aircraft takeoff gross weight. Range sensitivities developed for this aircraft during the Reference 1 study were also considered. This mass increase

would result in a 36.4 km (19.7 NM) range loss from the basic aircraft range capability of 9.20 Mm (4,968 NM).

- o Finned Tube Concept offers mass savings over wide range of potential design conditions - Based on the concept ranking system used, the Finned Tube Concept was found to be superior at many design conditions. In addition, if only the most important criterion, mass, was considered the concept's range of applicability would be expanded. Mass can be minimized with this concept unless design conditions that result in peak heating rates of 170.2 kW/m^2 (15 $Btu/sec\ ft^2$) or greater are encountered.

8. REFERENCES

1. C. J. Pirrello, A. H. Baker, and J. E. Stone, "A Fuselage/Tank Structure Study for Actively Cooled Hypersonic Cruise Vehicles - Summary," NASA CR-2651, February 1976.
2. C. J. Pirrello and R. L. Herring, "Study of a Fail-Safe Abort System for an Actively Cooled Hypersonic Aircraft - Technical Summary," NASA CR-2652, August 1976.
3. R. J. Nowak and H. N. Kelly, "Actively Cooled Airframe Structures for High-Speed Flight," Proceedings of 17th Structures, Structural Dynamics, and Materials Conference, AIAA/ASME/SAE, pp. 209-217, 1976.
4. SAE Aerospace Applied Thermodynamics Manual, Second Edition - October 1969.
5. R. G. Helenbrook and F. M. Anthony, "Design of a Convective Cooling System for a Mach 6 Hypersonic Transport Airframe," NASA CR-1918, December 1971.
6. E. G. Brogren, A. L. Brown, B. E. Clinger, V. Deringer, and C. L. Joeck, "Thermal - Structural Combined Loads Design Criteria Study," NASA CR-2102, October 1972.
7. S. P. Timoshenko and J. N. Goodier, "Theory of Elasticity," McGraw-Hill Book Company, Inc., 1951.
8. B. E. Gatewood, "Thermal Stresses," McGraw-Hill Book Co., Inc., 1957.
9. D. J. Thies, "Generalized Structural Optimization Computer Programs," McDonnell Douglas Corporation Report MDC A4205, 21 May 1976
10. Military Standardization Handbook," Structural Sandwich Composites," MIL-HDBK-23A, Department of Defense, December 1968.
11. Military Standardization Handbook," Metallic Materials and Elements for Aerospace Vehicle Structures," MIL-HDBK-5B, Department of Defense, August 1974.
12. "F-4 Fatigue and Damage Tolerant Assessment Program," McDonnell Douglas Corporation Report MDC A2883, Vol. I and II, 28 June 1974.
13. A. E. Bergles, "Survey and Evaluation of Techniques to Augment Convective Heat and Mass Transfer," Progress in Heat and Mass Transfer, Vol. 1, 1969, pp. 331-434.
14. A. E. Bergles, "Recent Developments in Convective Heat Transfer Augmentation," Applied Mechanics Reviews, Vol. 26, 1973, pp. 675-682.

15. D. F. Dipprey and R. H. Sabersky, "Heat and Momentum Transfer in Smooth and Rough Tubes at Various Prandtl Numbers," International Journal of Heat/Mass Transfer Series, Vol. 6, 1963, pp. 329-353.

16. J. W. Smith and R. A. Gowen, "Heat Transfer Efficiency in Rough Pipes at High Prandtl Number," A. I. Ch. E. Journal, Vol. 11, No. 5, 1965, pp. 941-943.

17. F. E. Megerlin, R. W. Murphy, and A. E. Bergles, "Augmentation of Heat Transfer in Tubes by Use of Mesh and Brush Inserts," Journal of Heat Transfer, Vol. 96, 1974, pp. 145-151.

18. E. Smithberg and F. Landis, "Friction and Forced Convection Heat Transfer Characteristics in Tubes with Twisted Tape Swirl Generations," Journal of Heat Transfer, Vol. 86, 1964, pp. 39-49.

19. R. F. Lopina and A. E. Bergles, "Heat Transfer and Pressure Drop in Tape-Generated Swirl Flow of Single-Phase Water," Journal of Heat Transfer, Vol. 91, 1969, pp. 434-442.

20. A. E. Bergles, R. A. Lee and B. B. Mikic, "Heat Transfer in Rough Tubes with Tape-Generated Swirl Flow," Journal of Heat Transfer, Vol. 91, 1969, pp. 443-445.

21. A. W. Date, "Prediction of Fully-Developed Flow in a Tube Containing a Twisted-Tape," International Journal of Heat and Mass Transfer, Vol. 17, 1974, pp. 845-859.

22. A. W. Date and J. R. Singham, "Numerical Prediction of Friction and Heat Transfer Characteristics of Fully-Developed Laminar Flow in Tubes Containing Twisted Tapes," ASME Paper 72-HT-17, 1972.

23. N. Hay and P. D. West, "Heat Transfer in Free Swirling Flow in a Pipe," Journal of Heat Transfer, Vol. 97, 1975, pp. 441-416.

24. S. W. Hong and A. E. Bergles, "Augmentation of Laminar Flow Heat Transfer in Tubes by Means of Twisted-Tape Inserts," ASME Paper 75-HT-44, 1975.

25. A. P. Watkinson, D. L. Miletti, and G. R. Kubanek, "Heat Transfer and Pressure Drop of Internally Finned Tubes in Laminar Oil Flow," ASME Paper 75-HT-41, 1975.

26. A. E. Bergles, G. S. Brown Jr., and W. D. Snider, "Heat Transfer Performance of Internally Finned Tubes," ASME Paper 71-HT-31, 1971.

27. W. M. Kays and A. L. London, "Compact Heat Exchangers," McGraw-Hill Book Co., Inc. 1958.

1. Report No.	2. Government Accession No.	3. Recipient's Catalog No.
NASA CR-2828		

4. Title and Subtitle	5. Report Date
THERMAL DESIGN FOR AREAS OF INTERFERENCE HEATING ON ACTIVELY COOLED HYPERSONIC AIRCRAFT	January 1978
	6. Performing Organization Code
7. Author(s)	8. Performing Organization Report No.
R. L. Herring and J. E. Stone	10. Work Unit No.
9. Performing Organization Name and Address McDonnell Douglas Corporation P.O. Box 516 St. Louis, MO 63166	11. Contract or Grant No. NAS1-14140
	13. Type of Report and Period Covered Contractor Report
12. Sponsoring Agency Name and Address National Aeronautics and Space Administration Washington, D.C. 20546	14. Sponsoring Agency Code

15. Supplementary Notes

Langley Technical Monitor: Charles B. Johnson
Final Report

16. Abstract

Numerous actively cooled panel design alternatives for application in regions on high speed aircraft that are subject to interference heating effects were studied. Candidate design concepts were evaluated using mass, producibility, reliability and inspectability/maintainability as figures of merit. Three design approaches were identified as superior within certain regimes of the matrix of design heating conditions considered. Only minor modifications to basic actively cooled panel design are required to withstand minor interference heating effects. Designs incorporating internally finned coolant tubes to augment heat transfer are recommended for moderate design heating conditions. At severe heating conditions, an insulated panel concept is required.

17. Key Words (Suggested by Author(s))	18. Distribution Statement
Hypersonic aircraft Actively cooled structure Thermal protection Interference heating	Unlimited - Unclassified Subject Category 05

19. Security Classif (of this report)	20. Security Classif (of this page)	21. No. of Pages	22. Price
Unclassified	Unclassified	173	$8.00

* For sale by the National Technical Information Service, Springfield, Virginia 22161

*U.S. GOVERNMENT PRINTING OFFICE: 1978 - 735-078/74